Department of
Industry and Resources

RECORD
2008/9

STRUCTURAL AND METAMORPHIC CONTROLS ON GOLD THROUGH TIME AND SPACE IN THE CENTRAL EASTERN GOLDFIELDS SUPERTERRANE — A FIELD GUIDE

by K Czarnota, RS Blewett, and B Goscombe

Geological Survey of Western Australia

Sponsors


AUSTRALIAN INSTITUTE OF GEOSCIENTISTS
Supporting Geoscientists


GEOLOGICAL SOCIETY OF AUSTRALIA
Incorporated


RioTinto


NORILSK NICKEL


CSIRO


integra
MINING Limited


THE UNIVERSITY OF WESTERN AUSTRALIA


INDEPENDENCE GROUP NL


ANGLOGOLD
ASHANTI


AUSTRALIAN JOURNAL OF
EARTH
SCIENCES


GEOCONFERENCES
(WA) INC.

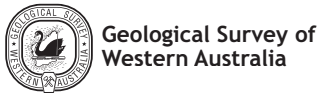
Geological Survey of
Western Australia


Chevron


riu
Resource Information
Unit

GEOLOGICAL SURVEY OF WESTERN AUSTRALIA

Record 2008/9
(Modified from GSWA Record 2007/19, Blewett and Czarnota, 2007a)

STRUCTURAL AND METAMORPHIC CONTROLS ON GOLD THROUGH TIME AND SPACE IN THE CENTRAL EASTERN GOLDFIELDS SUPERTERRANE — A FIELD GUIDE

by
K Czarnota[1], RS Blewett[1], and B Goscombe[2]

[1] **pmd*CRC, Onshore Energy and Minerals Division, Geoscience Australia, GPO Box 378, Canberra, ACT 2601**
[2] **pmd*CRC, Integrated Terrane Analysis Consultant (ITAC), 18 Cambridge Road, Aldgate, SA 5154**

Perth 2008

MINISTER FOR ENERGY; RESOURCES; INDUSTRY AND ENTERPRISE
Hon. Francis Logan MLA

ACTING DIRECTOR GENERAL, DEPARTMENT OF INDUSTRY AND RESOURCES
Stuart Smith

EXECUTIVE DIRECTOR, GEOLOGICAL SURVEY OF WESTERN AUSTRALIA
Tim Griffin

REFERENCE
The recommended reference for this publication is:
Czarnota, K, Blewett, RS, and Goscombe, B, 2008, Structural and metamorphic controls on gold through time and space in the central Eastern Goldfields Superterrane — a field guide: Geological Survey of Western Australia, Record 2008/9, 66p.

National Library of Australia Card Number and ISBN 978-1-74168-160-4 (PDF)

Grid references in this publication refer to the Geocentric Datum of Australia 1994 (GDA94). Locations mentioned in the text are referenced using Map Grid Australia (MGA) coordinates, Zone 51.

Cover image modified from Landsat data, courtesy of ACRES

Published 2008 by Geological Survey of Western Australia
This Record is published in digital format (PDF) and is available online at www.doir.wa.gov.au/GSWApublications.
Laser-printed copies can be ordered from the Information Centre for the cost of printing and binding.

Further details of geological publications and maps produced by the Geological Survey of Western Australia are available from:
Information Centre
Department of Industry and Resources
100 Plain Street
EAST PERTH, WESTERN AUSTRALIA 6004
Telephone: +61 8 9222 3459 Facsimile: +61 8 9222 3444
www.doir.wa.gov.au/GSWApublications

Contents

Figures

Structural and metamorphic controls on gold through time and space in the central Eastern Goldfields Superterrane —a field guide

by

K Czarnota[1], RS Blewett[1], and B Goscombe[2]

Introduction

This field guide accompanies a pre-conference excursion of the Geological Society of Australia (GSA) and the Australian Institute of Geoscientists (AIG) conference entitled 'Australian Earth Science Convention 2008 — New Generation Advances in Geoscience'.

*Most of the trip localities are in active tenements and permission from the respective tenement holders is required **before** the reader attempts to revisit the sites. Personal Protective Equipment (PPE) and inductions will also be a requirement and these may vary from site to site.*

The purpose of this excursion is to examine the diversity in the structural setting of gold deposits across the Eastern Goldfields Superterrane (EGST; Cassidy et al., 2006), and establish a regional deformation and metamorphic framework for the EGST (Fig. 1). The excursion will demonstrate that gold is hosted in a wide range of structures including reverse faults, both sinistral and dextral strike-slip faults, and extensional shear zones. The excursion will also highlight the range of host lithologies for gold, including sedimentary rocks, intrusive and extrusive ultramafic and mafic rocks, together with granitoids (syenite and porphyry). The excursion will traverse the Kalgoorlie and Kurnalpi Terranes of the EGST, with localities in the west at Leonora, through to the east around Laverton (Fig. 2). The excursion will attempt to place gold mineralization along with the host lithologies, controlling structures, and metamorphic grade within an integrated geodynamic framework (Fig. 3).

The science underpinning this excursion was developed during the Y1-P763 project of the Predictive Mineral Discovery Cooperative Research Centre (pmd*CRC) and Australian Mineral Industry Research Association (AMIRA) International Y1-P763 project and the Y4 pmd*CRC project. Module 3 of the Y1-P763 project forms the basis for the structural component of this field guide. This project involved a comprehensive structural study of 42 mines that was integrated with earlier work on 32 granite sites (Blewett et al., 2004a) and 3D regional map patterns (Henson et al., 2004a; Henson, 2006). A comprehensive database, atlas, series of posters, and a report were delivered to sponsors in November 2005. A public domain release of this document (Blewett and Czarnota, 2007b) is available at <http://www.ga.gov.au/minerals/research/pubspres.jsp#pub_2007>. The metamorphic component of this field trip results from Ben Goscombe's work in the Y4 project (Goscombe et al., 2007).

One of the science drivers behind the Y1-P763 and Y4 projects was to try to resolve the geodynamic evolution of the EGST. A range of competing models have been proposed, including:

- ensialic extensional rifts or basins (Archibald et al., 1978; Hallberg, 1985; Hammond and Nisbet, 1992; Williams and Whitaker, 1993; Passchier, 1994);
- convergent margin settings (Barley et al., 1989; Eisenlohr et al., 1989; Swager et al., 1992; Witt, 1994);
- accretionary models (Myers, 1995);
- strike-slip tectonics (Krapez et al., 2000);
- mantle plumes (Campbell and Hill, 1988).

The integration of a new structural and metamorphic framework together with previous studies of the stratigraphy, granite history, and gold mineralization in the EGST provides a more robust para-autochthonous plate tectonic geodynamic framework for the region.

This field guide is an extract of the final reports delivered to sponsors of the Y1-P763 and Y4 projects. The regional geology sections below are extracted from the pmd*CRC Y2 project report (see Cassidy, 2006). The sponsors of Y1-P763, Y2, and Y4 are acknowledged for permission to publish this guide.

[1] pmd*CRC, Onshore Energy and Minerals Division, Geoscience Australia, GPO Box 378, Canberra, ACT 2601

[2] pmd*CRC, Integrated Terrane Analysis Consultant (ITAC), 18 Cambridge Road, Aldgate, SA 5154

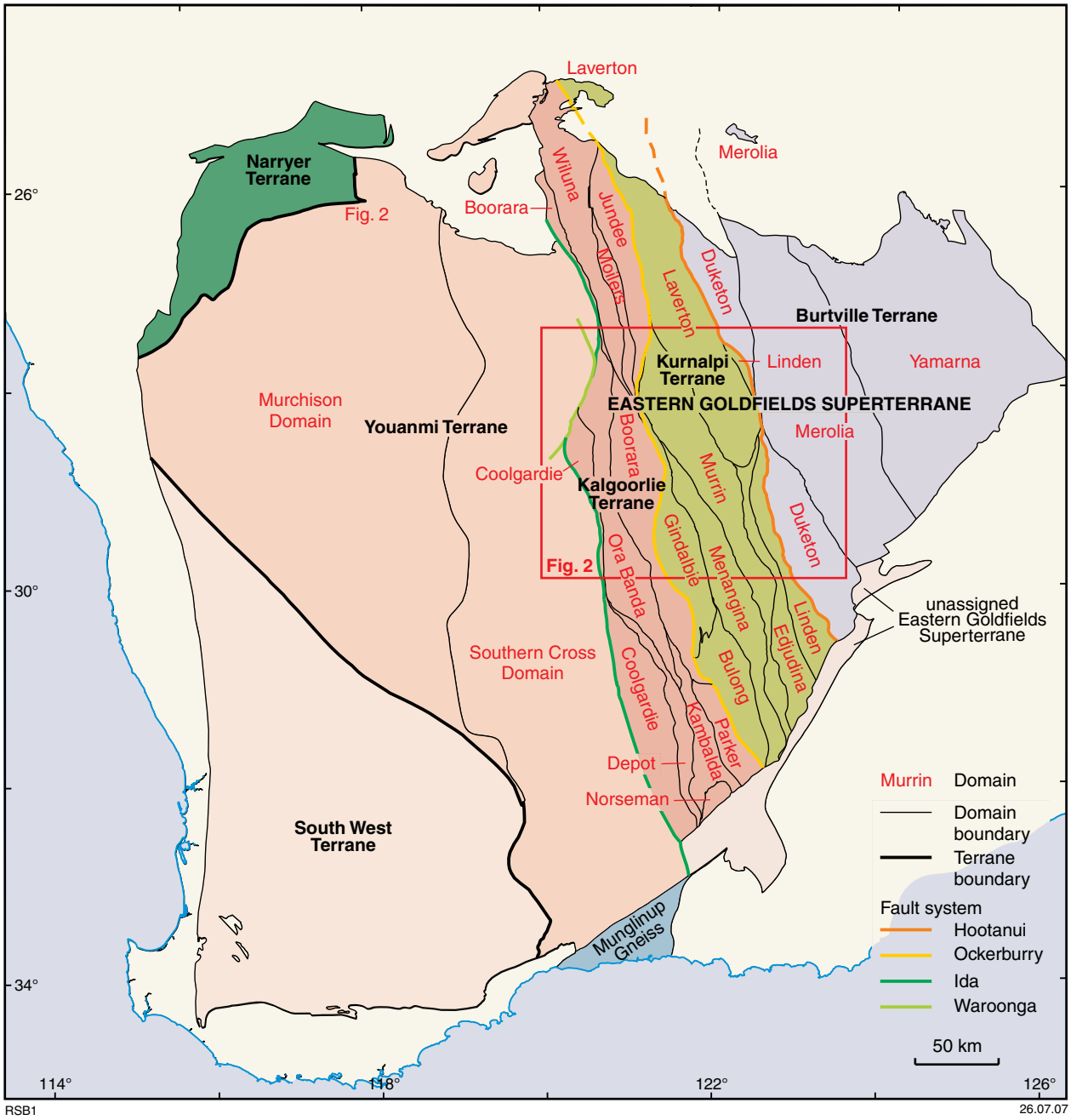

Figure 1. **Tectonic division of the Yilgarn Craton, showing subdivision into terranes and domains (after Cassidy et al., 2006). Note the north-northwesterly trending grain of the fault-bounded terranes and domains of the Eastern Goldfields Superterrane. The red box shows the location of Figure 2**

Regional geology terranes

The Yilgarn Craton has been recently subdivided by Cassidy et al. (2006) into six terranes, three of which constitute a superterrane (Fig. 1). In the west the Narryer Terrane and the South West Terrane are dominated by granite and granitic gneiss, whereas the central Youanmi Terrane and the Eastern Goldfields Superterrane are composed of north-trending greenstone belts separated by extensive granite and granitic gneiss.

The Narryer Terrane in the northwest part of the craton consists of c. 3.73 – 2.6 Ga high-grade gneiss, and supracrustal and granitic rocks. It is host to metasedimentary rocks famous for their greater-than-4.4 Ga detrital zircons (Wilde et al., 2001). The South West Terrane in the southwest part of the craton consists of greater-than-3.2 – 2.6 Ga high-grade gneiss, and supracrustal and granitic rocks. The Youanmi Terrane consists of c. 3.01 – 2.63 Ga greenstones and granitic rocks. It incorporates the 'Southern Cross and Murchison Provinces' of Gee et al. (1981), and includes the Cue Domain that may constitute a separate terrane.

The Eastern Goldfields Superterrane consists of three terranes. In the west the Kalgoorlie Terrane is made up of

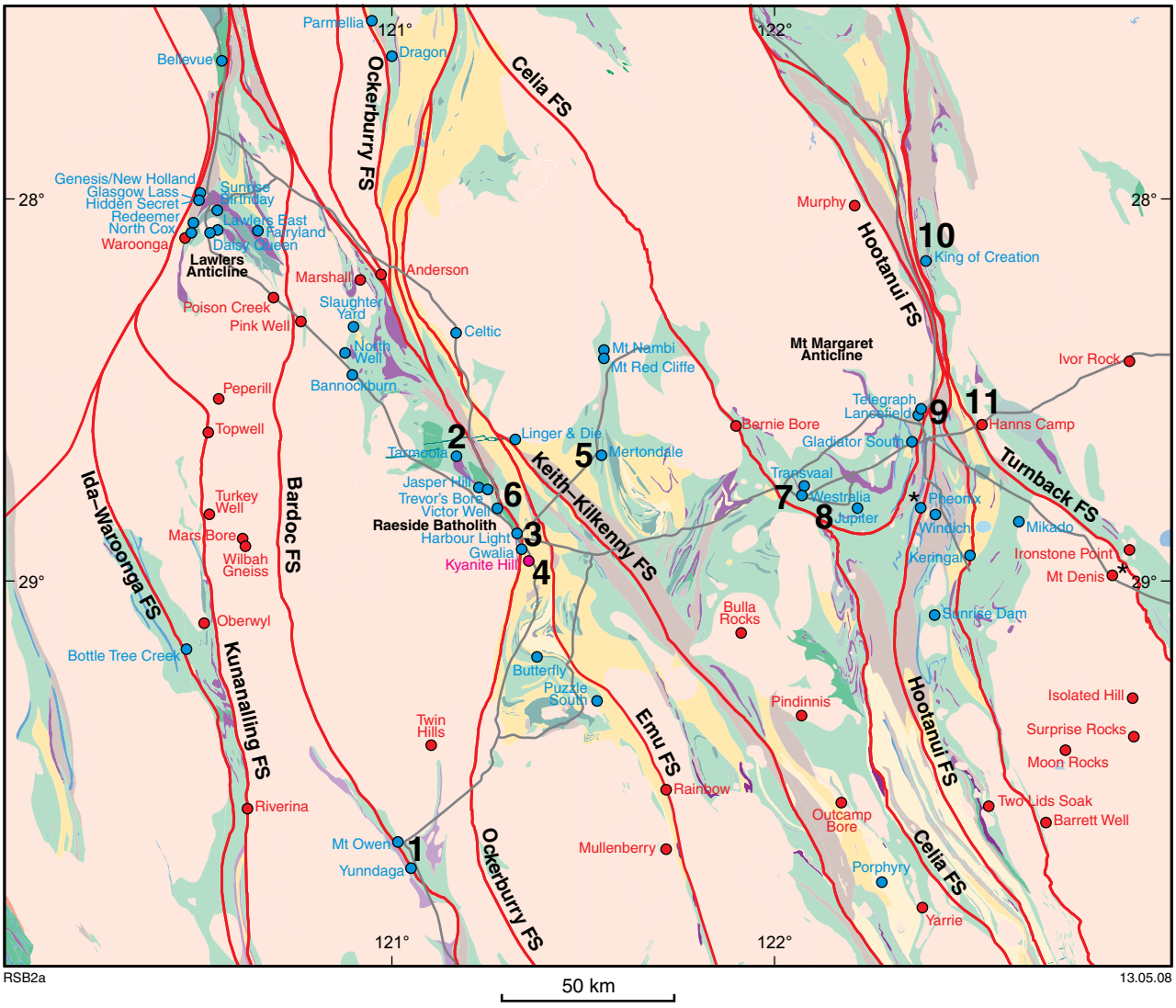

Figure 2. Map of the Eastern Goldfields Superterrane and sites of specific structural studies described (blue = mine sites; red = granite sites). The localities visited in this field guide are numbered. FS = fault system

a series of greater-than-2.76–2.63 Ga granite–greenstone domains that form part of the 'Eastern Goldfields Province' of Gee et al. (1981), and approximates the 'Kalgoorlie Terrane' of Myers (1997). The central Kurnalpi Terrane is a complex series of c. 2.95–2.63 Ga granite–greenstone domains that form part of the 'Eastern Goldfields Province' of Gee et al. (1981), and incorporates the 'Gindalbie, Kurnalpi, and Laverton Terranes' of Myers (1995, 1997). To the east is the Burtville Terrane, which is poorly defined by c. 2.95–2.63 Ga granite–greenstone domains, and forms part of the 'Eastern Goldfields Province' of Gee et al. (1981) and incorporates the 'Duketon Terrane' of Barley et al. (2002, 2003).

The terranes and domains in the EGST are bound by interconnected systems of faults (Swager et al., 1992, Swager, 1997; Liu et al., 2000) that have been defined as part of the pmd*CRC Y2 project (see Champion, 2006). From west to east, these terrane-bounding fault systems are the Ida, Ockerburry, and Hootanui Fault Systems (Figs 1 and 2).

Regional geology greenstones

Tholeiitic, komatiitic, and calc-alkaline volcanic and sedimentary rocks that developed dominantly between c. 2.72 and 2.66 Ga form the bulk of the successions in the EGST (Fig. 4). These sequences generally young towards the west, with the greenstone succession in the Kalgoorlie Terrane containing the youngest volcaniclastic units (Barley et al., 2002, 2003).

Kalgoorlie Terrane

The intensely mineralized Kalgoorlie Terrane is an amalgamation of young (<2.71 Ga) and fragments of old (>2.74 Ga) tectono-stratigraphic associations (Fig. 4). Enclaves or domains of older (>2.74 Ga) greenstone successions (Kambalda and Wiluna Domains, Leonora district in the Boorara Domain) are present in the

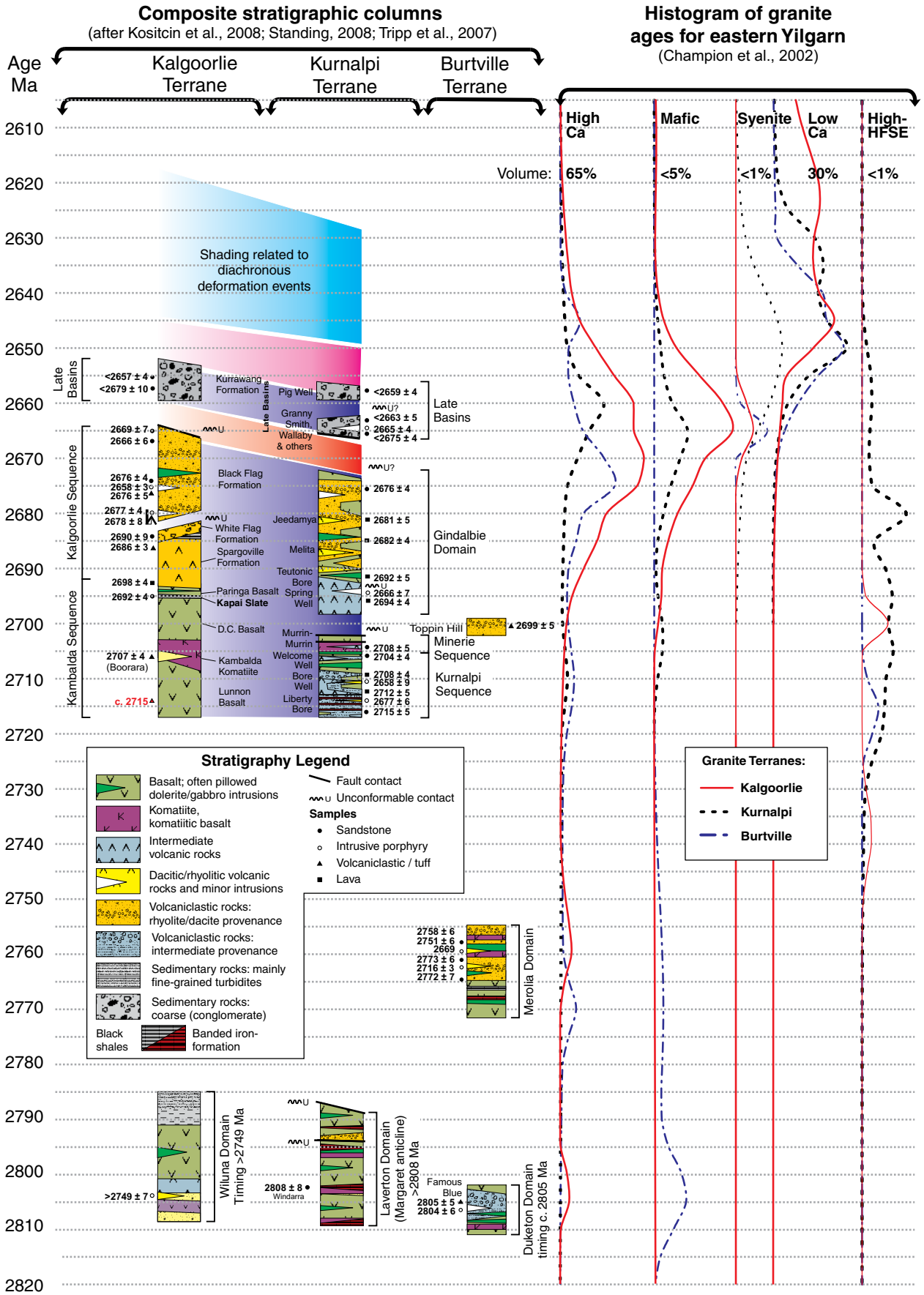

Figure 3. **Integrated time–space synthesis of greenstone stratigraphy, granite ages by type, structure, tectonic mode, metamorphism and gold mineralization ages for the Eastern Goldfields Superterrane (after Czarnota and Blewett, 2007)**

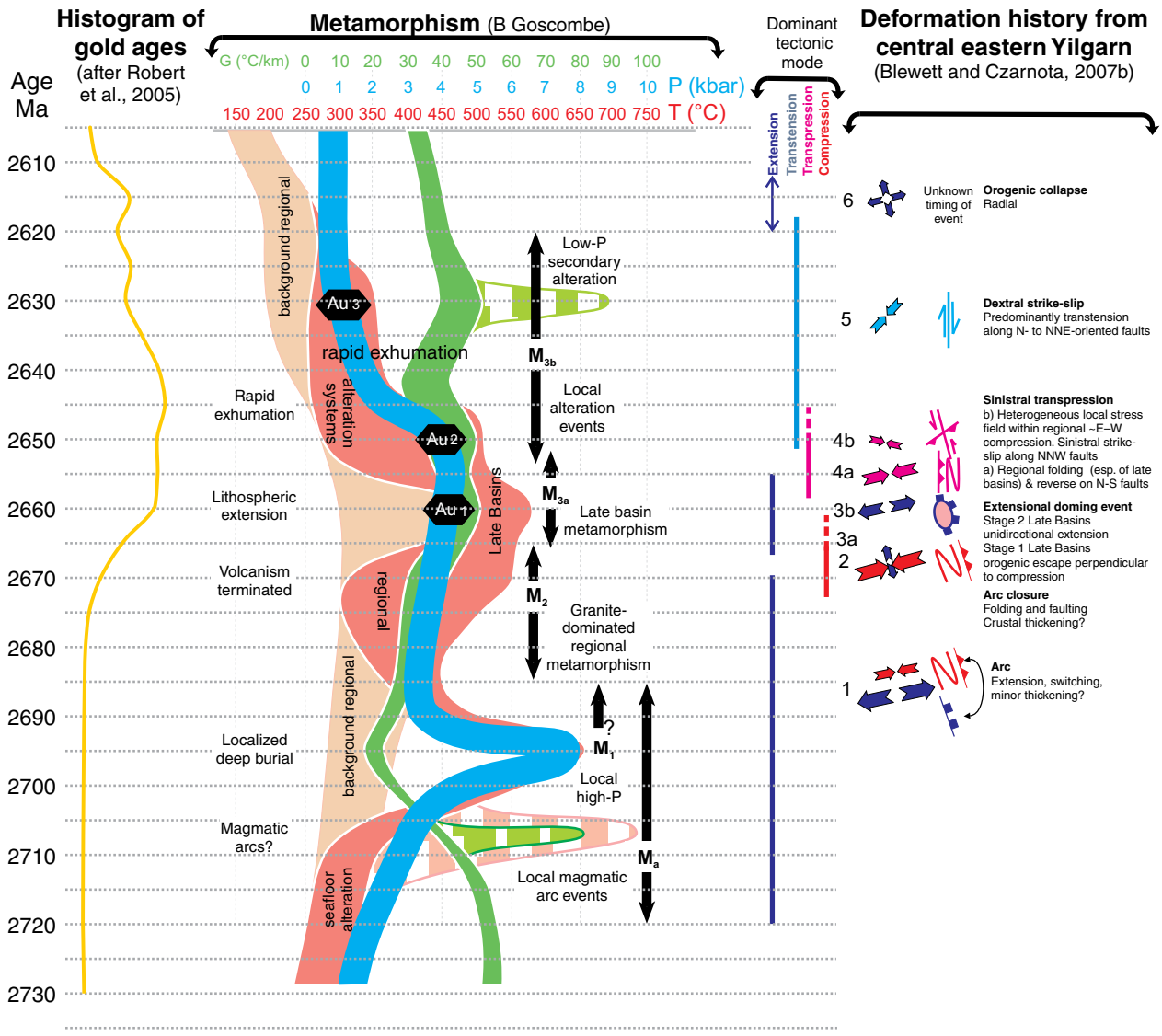

Metamorphic caveat

P–T–G evolution of the current exposure level of a hypothetical composite EYC that experienced all regionally extensive metamorphic events and most localized events. M_{3a} in post-volcanic Late Basins and M_1 high-P metamorphic events may be localized to some degree.

Evolution curves DO NOT track a single real location. Stripped bands highlight very localized metamorphic events.

There may be multiple M_1 and M_a metamorphic events and the M_{3b} period experienced many alteration events in different places (Goscombe et al., 2007).

Structure symbols:

- Extensional shear zones & normal faults
- Reverse shear zones and thrusts
- Upright compressional folds
- Extensional doming event
- Sinistral shear zones and faults
- Dextral shear zones and faults
- Extension and compression vectors, size indicates intensity of event

References

Blewett, and Czarnota (2007)
Blewett, et al. (2004c)
Champion et al. (2002)
Goscombe et al. (2007)
Kositcin et al. (2008)
Miller, (2006)
Mueller et al. (1988)
Nguyen (1997)
Standing (2008)
Swager (1997)
Robert et al. (2005)
Tripp et al. (2007)

Deformation correlation

Blewett and Czarnota (2007a)			Mueller et al. (1988)	Swager (1997)	Nguyen (1997)	Blewett et al. (2004)	Miller (2006)
Minor extension		D_6		Collapse		Late De	
Dextral strike-slip		D_5	D_3	D_4	D_4	D_3	D_4
Sinistral transpression	NW–SE local comp.	D_{4b}	D_2	D_3	D_3	D_3	D_3
	Late Basin upright folding	D_{4a}	D_1	D_2	D_2	D_{2b}	D_2
Extensional doming	Stage 2 Late Basins	D_{3b}		D_E	D_{e3}	D_{2e}	
	Stage 1 Late Basins	D_{3a}					D_1
Upright folding and reverse faulting		D_2		D_2		D_{2a}	
Extension with intermittent compression		D_1		D_E	D_{e1-2}	D_e	

RSB6a

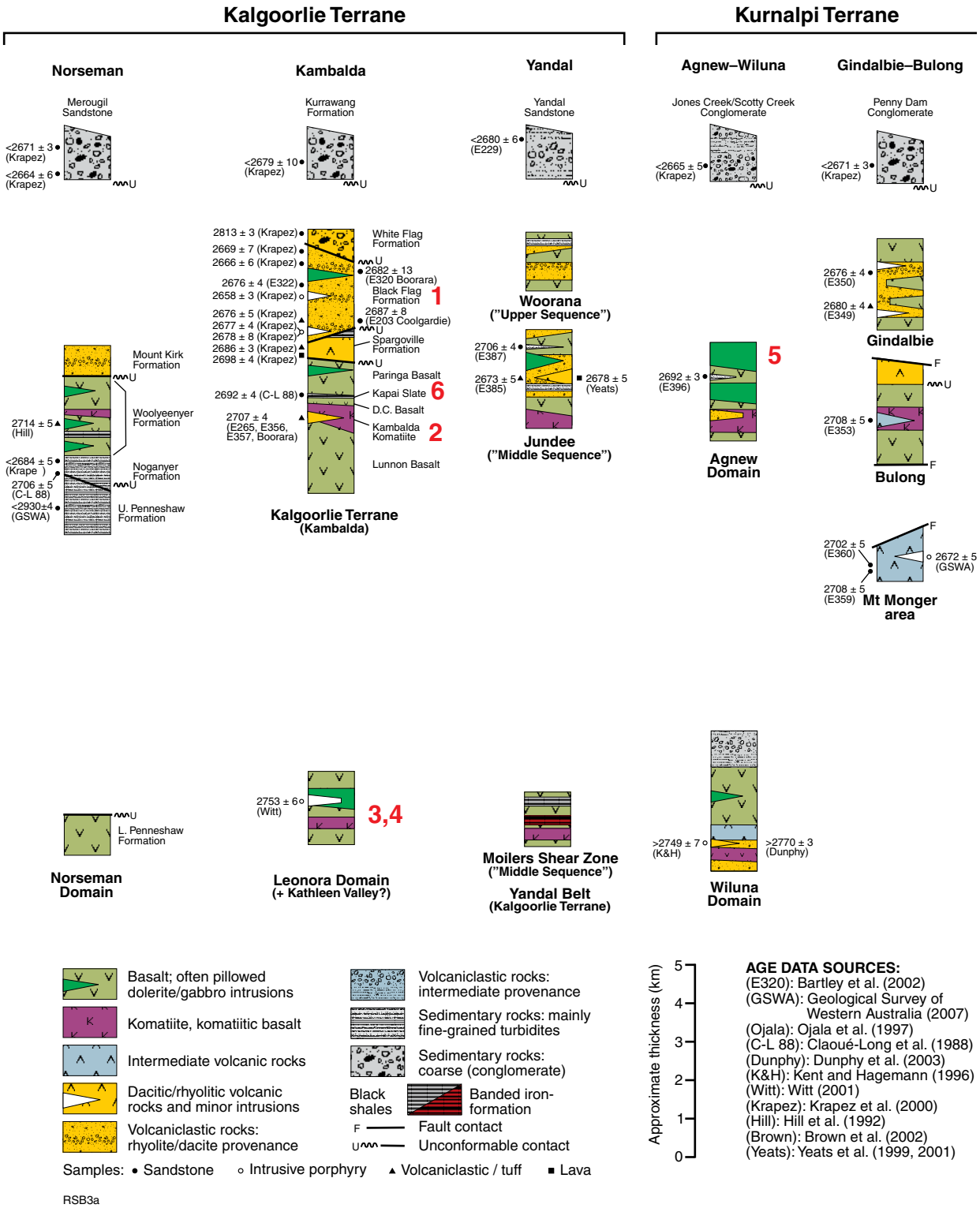

Figure 4. Greenstone stratigraphy of the Eastern Goldfields Superterrane (after Barley et al., 2002). Red numbers are the stratigraphic position of the locality stops in the field guide (except the two granite sites)

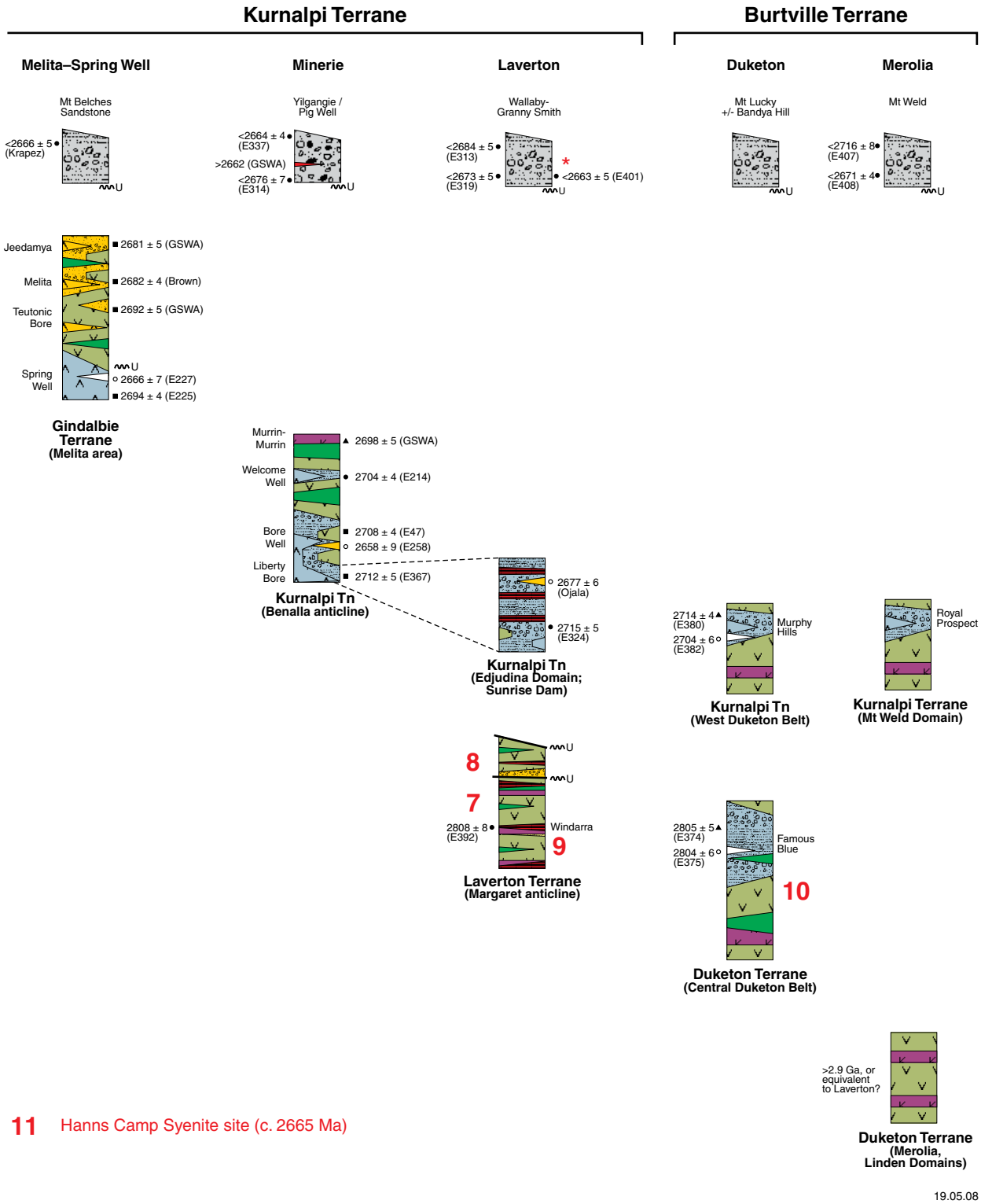
Kurnalpi Terrane
Burtville Terrane
Melita–Spring Well
Minerie
Laverton
Duketon
Merolia
Mt Belches Sandstone
<2666 ± 5 (Krapez)
U
Yilgangie / Pig Well
<2664 ± 4 (E337)
>2662 (GSWA)
<2676 ± 7 (E314)
U
Wallaby-Granny Smith
<2684 ± 5 (E313)
<2673 ± 5 (E319)
*
<2663 ± 5 (E401)
U
Mt Lucky +/- Bandya Hill
U
Mt Weld
<2716 ± 8 (E407)
<2671 ± 4 (E408)
U
Jeedamya
Melita
Teutonic Bore
Spring Well
2681 ± 5 (GSWA)
2682 ± 4 (Brown)
2692 ± 5 (GSWA)
U
2666 ± 7 (E227)
2694 ± 4 (E225)
Gindalbie Terrane (Melita area)
Murrin-Murrin
Welcome Well
Bore Well
Liberty Bore
2698 ± 5 (GSWA)
2704 ± 4 (E214)
2708 ± 4 (E47)
2658 ± 9 (E258)
2712 ± 5 (E367)
Kurnalpi Tn (Benalla anticline)
2677 ± 6 (Ojala)
2715 ± 5 (E324)
Kurnalpi Tn (Edjudina Domain; Sunrise Dam)
2714 ± 4 (E380)
2704 ± 6 (E382)
Murphy Hills
Kurnalpi Tn (West Duketon Belt)
Royal Prospect
Kurnalpi Terrane (Mt Weld Domain)
8
7
U
U
2808 ± 8 (E392)
Windarra
9
Laverton Terrane (Margaret anticline)
2805 ± 5 (E374)
2804 ± 6 (E375)
Famous Blue
10
Duketon Terrane (Central Duketon Belt)
>2.9 Ga, or equivalent to Laverton?
Duketon Terrane (Merolia, Linden Domains)
11 Hanns Camp Syenite site (c. 2665 Ma)
19.05.08

Kalgoorlie Terrane (Barley et al., 2002). It is possible that these older enclaves represent autochthonous fragments of Youanmi Terrane basement to the EGST younger rock units.

The less-than-2.71 Ga greenstone successions in the southern Kalgoorlie Terrane (especially the Kambalda Domain) are divided into the 2.71 – 2.69 Ga tholeiitic and komatiitic mafic–ultramafic (Kambalda sequence) and 2.69 – 2.66 Ga felsic volcaniclastic (Kalgoorlie sequence) sequences (Barley et al., 2002, 2003). The Kalgoorlie sequence (incorporating the Black Flag Group) is a tonalite–trondhjemite–granodiorite (TTG) volcaniclastic association restricted to the Kalgoorlie Terrane and was deposited in an extensional, deep-marine, ?intra-arc basin between 2.69 and 2.66 Ga. The Kalgoorlie Terrane includes similar greenstone successions in the Boorara and Yandal Domains (Fig. 4).

Kurnalpi Terrane

The Kurnalpi Terrane includes 2.715 – 2.705 Ga mafic volcanic rocks, intermediate calc-alkaline complexes, feldspathic sedimentary rocks, and mafic intrusive rocks, and 2.695 – 2.675 Ga bimodal high field strength element (HFSE)-enriched rhyolite–basalt and intermediate–felsic calc-alkaline complexes that extend along a linear belt (principally in the Gindalbie Domain) at the eastern edge of the Kalgoorlie Terrane (Fig. 4). The 2.71 – 2.715 Ga andesite-derived volcaniclastic rocks, and fine-grained sandstone–shale units ('BIF') in the eastern part of the Kurnalpi Terrane are separated out as the Edjudina Domain (Barley et al., 2002).

Despite now being juxtaposed, the felsic rocks in both the Kalgoorlie and Kurnalpi Terranes have distinct geochemistry at 2.715 – 2.66 Ga. Rocks of the c. 2.72 – 2.68 Ga Edjudina, Murrin, and Menangina Domains in the east Kurnalpi Terrane are interpreted as representing an arc basin. In contrast, the 2.69 – 2.68 Ga rocks of the Gindalbie Domain to the west are interpreted as a rifting phase of this Kurnalpi Terrane (or similar) arc (Barley et al., 2002, 2003).

The c. 2.81 Ga Laverton Domain includes less-than-2.8 Ga mafic and ultramafic volcanic rocks, BIF, fine-grained tuffaceous sediments, and possibly less-than-2.87 Ga mafic and ultramafic volcanic rocks and BIF of the Dingo Range greenstone belt (Barley et al., 2003). The Edjudina and Linden Domains may form subdomains above an unconformity-bound, not fault-bound, Laverton Domain basement to the younger rock units (Cassidy et al., 2006).

Burtville Terrane

The Duketon Domain in the Burtville Terrane (Fig. 1) includes c. 2805 Ma intermediate and felsic volcanic rocks and associated mafic(–ultramafic) rocks in the central and eastern parts of the Duketon greenstone belt, as well as greenstone assemblages dominated by mafic and ultramafic volcanic and fine-grained sedimentary rocks east of Laverton. The Merolia and Yamarna Domains contain poorly understood, variably deformed and metamorphosed mafic and felsic volcanic and sedimentary sequences.

Greenstones: tectonic implications and isotopes

Sensitive high-resolution ion microprobe (SHRIMP) U–Pb zircon data show three main peaks in age of the volcano-sedimentary sequences: 2.65 – 2.72, 2.81, and 2.95 – 3.05 Ga. Nd data suggest marginal arcs rather than purely oceanic arc systems, and recycling of crust (≥2.8 Ga) along a complex convergent margin, with the youngest crust represented by rocks of the Gindalbie Domain and some intermediate volcanic rocks from the Menangina and Murrin Domains of the Kurnalpi Terrane. Hf data suggest there were periods of addition of newly generated crust–lithosphere (+ve εHf) and that these episodes also reworked crust that originally formed at c. 3.05 Ga or earlier (Barley et al., 2003). Overall, there is a dominance of continental margin signatures as well as evidence of magmatic recycling of older arc-related crust. The terranes were possibly part of the same arc – back-arc system dismembered and then reassembled by accretionary tectonics.

Late basins

Late basins are coarse siliciclastic sequences that unconformably overlie, or are in fault contact with, the volcano-sedimentary successions. Based on intrusions by younger porphyries and syenites, or detrital zircon maximum-depositional ages, they were deposited after 2.665 Ga (Krapez et al., 2000; Barley et al., 2003; Rick Squire, unpublished data). Two facies types are recorded in the late basins — fluvial deposits and turbidites. Krapez et al. (2000) suggested that the fluvial facies are older than the turbidite facies, as the former have restricted provenance and the latter have a more diverse zircon population, reflecting a larger source area evolving through time.

SHRIMP dating of detrital zircons indicates multiple older sources corresponding to the ages of the greenstones and granites of the EGST (Barley et al., 2002, 2003). Some old populations however have no recognized source in the EGST. With the exception of some zircons from the Kurrawang and Jones Creek Conglomerates, the age and isotopic characteristics of these sources reflect major magmatic and crustal recycling.

The late basins lie with an angular unconformity on the older volcanic-dominated greenstone sequences (or granite basement), indicating that regional orogeny pre-dated the commencement of their deposition at c. 2.665 Ga (Blewett et al., 2004c). Their deposition was followed by the emplacement of low-Ca granites, syenites, lamprophyres and porphyries between c. 2.65 and 2.63 Ga, and various stages of the deformation cycle (see **Granites: tectonic implications and isotopes**).

Late basins: tectonic implications

The importance of the late basins is that they mark a fundamental change in geodynamics from volcanic-dominated sedimentation (the arcs shut off and mantle magmas appear) to clastic-dominated sedimentation with extensive recycling.

Presently, the late basins are preserved in structural basins mostly in the hangingwall of major terrane and domain-boundary faults. In a general pattern, these late basins fine upwards (conglomerates at the base and turbidites at the top). Although they are synorogenic, the late basins do not have the characteristic stacking pattern (coarsening upwards) of foreland or piggyback basins (DeCelles and Giles, 1996). Blewett et al. (2004c) interpreted these basins as 'surge basins' (a form of piggyback basins) and suggested that the fining-up record was a preservation anomaly and that the complete sediment cycle was missing. In contrast, Krapez et al. (2000) suggested that the late basins were developed in a strike-slip tectonic mode; however, most faults that are closely associated with these basins are rectilinear, with few localities for suitable releasing jogs and step-overs comparable to the dimensions of these basins.

Geometrically there are two types of late basins. The oldest (Stage 1) are arcuate and are preserved in the noses of major extensional granite domes (e.g. Wallaby and Kanowna Belle). The youngest (Stage 2) are elongate and linear, parallel to the main north-northwest–south-southeast tectonic grain. The arcuate Stage 1 late basins developed in the hangingwall of outward-facing extensional shear zones within the greenstone pile as these were shed off and away from rising and extruding granite domes. The Stage 2 late basins occur in the hangingwall of major north-northwesterly trending faults and are likely to have developed by down-to-the-east-northeast extension, reflecting the influence of the regional extensional-stress field.

Regional geology granites

Champion and Sheraton (1997) divided the granites of the Yilgarn Craton into five main classes or types (Fig. 5). These are in order of volumetric contribution: high-Ca (~60%), low-Ca (~25%), high-HFSE (~5%), mafic (~5%), and syenite (~1%). The evolution of granite magmatism, with the exception of the high-HFSE granites, is broadly similar across the EGST (Champion and Sheraton, 1997; Cassidy et al., 2002b; Champion, 2006). High-Ca, mafic and high-HFSE granites have equivalent timing and chemistry to specific volcanic associations in the greenstone belts. In contrast, the youngest magmatic rocks (low-Ca and syenitic granites) have no (preserved) extrusive equivalents in the EGST. All granite groups are present across the EGST (Fig. 5), with high-HFSE and syenitic granites mostly restricted to the western Kurnalpi Terrane (Champion, 2006).

Most magmatism occurred between c. 2.72 and 2.63 Ga (Figs 6 and 3). Remnants of older (>2.74 Ga) granites and older inherited zircons are most prevalent within the Kalgoorlie Terrane, and the Laverton, Linden and Duketon Domains. These are consistent with the Sm–Nd isotopic data (Fig. 7),which are indicative of older crust (Cassidy and Champion, 2004).

Although each granite/volcanic group was long lived (Fig. 6), there are distinct periods where particular groups are most common:

- 2.72 to 2.68 Ga was variably dominated by high-HFSE, high-Al TTG-type high-Ca and mafic magmatism;
- 2.675 to 2.655 Ga was dominated by transitional TTG-type high-Ca, with lesser mafic (sanukitoids) and syenitic magmatism;
- post-c. 2.655 Ga was dominated by low-Ca with lesser syenitic and minor mafic magmatism (Champion and Sheraton, 1997; Champion, 2006).

High-HFSE (and associated mafic) granites exhibit a broad decrease (diachroneity) in ages from east to west (Cassidy et al., 2002a). A similar decrease is evident in the geochronological data for felsic and intermediate volcanism in the Kurnalpi Terrane (Fig. 3).

The period c. 2.675 – 2.66 Ga is characterized by high-Ca and lesser mafic and syenitic magmatism across all the terranes within the EGST. High-Al TTG-type high-Ca and mafic granites that are geochemically similar to TTG-related volcaniclastic rocks that are confined to the Kalgoorlie sequence in the Kalgoorlie Terrane are present throughout the EGST, including intrusive dykes and plutons into older intermediate volcanic-dominated sequences in the Kurnalpi Terrane.

The switch in granite style from high-Ca and mafic granites to low-Ca-dominated magmatism at c. 2.655 Ga was preceded, and partly accompanied by, 'late' (2.66 to 2.65 Ga) high-Ca and mafic magmatism (Champion, 2006; Blewett et al., 2004b). This appears to be concentrated within the Kalgoorlie Terrane, suggesting that this region was the main locus of magmatism at this time (Fig. 3). Since these melts are associated with extension (Fig. 3) then it might suggest that the Kalgoorlie Terrane has seen more extension than the Kurnalpi Terrane. In support of this hypothesis is the greater preservation of younger and thicker stratigraphy in the Kalgoorlie Terrane. Furthermore, there are also large deposits associated with the extension in the Kalgoorlie Terrane (see **D_3: extensional granite doming, mafic granites and late basin formation**). Many of these 'late' granites are transitional TTG-type high-Ca and 'sanukitoid'-like mafic granites. This suggests that the switch in granite type from high-Ca mafic to low-Ca granites subsequent to c. 2.655 Ga accompanied availability of a metasomatized mantle source for the high-Ca mafic granites, at least in the Kalgoorlie Terrane, as well as a tectonic trigger to promote derivation of low-Ca granites through melting of older granitoid material within the crust.

Granites: tectonic implications and isotopes

The high-Ca, low-Ca, and high-HFSE granites have a clear crustal component involved partly or solely within their genesis (Champion and Sheraton, 1997). The Nd

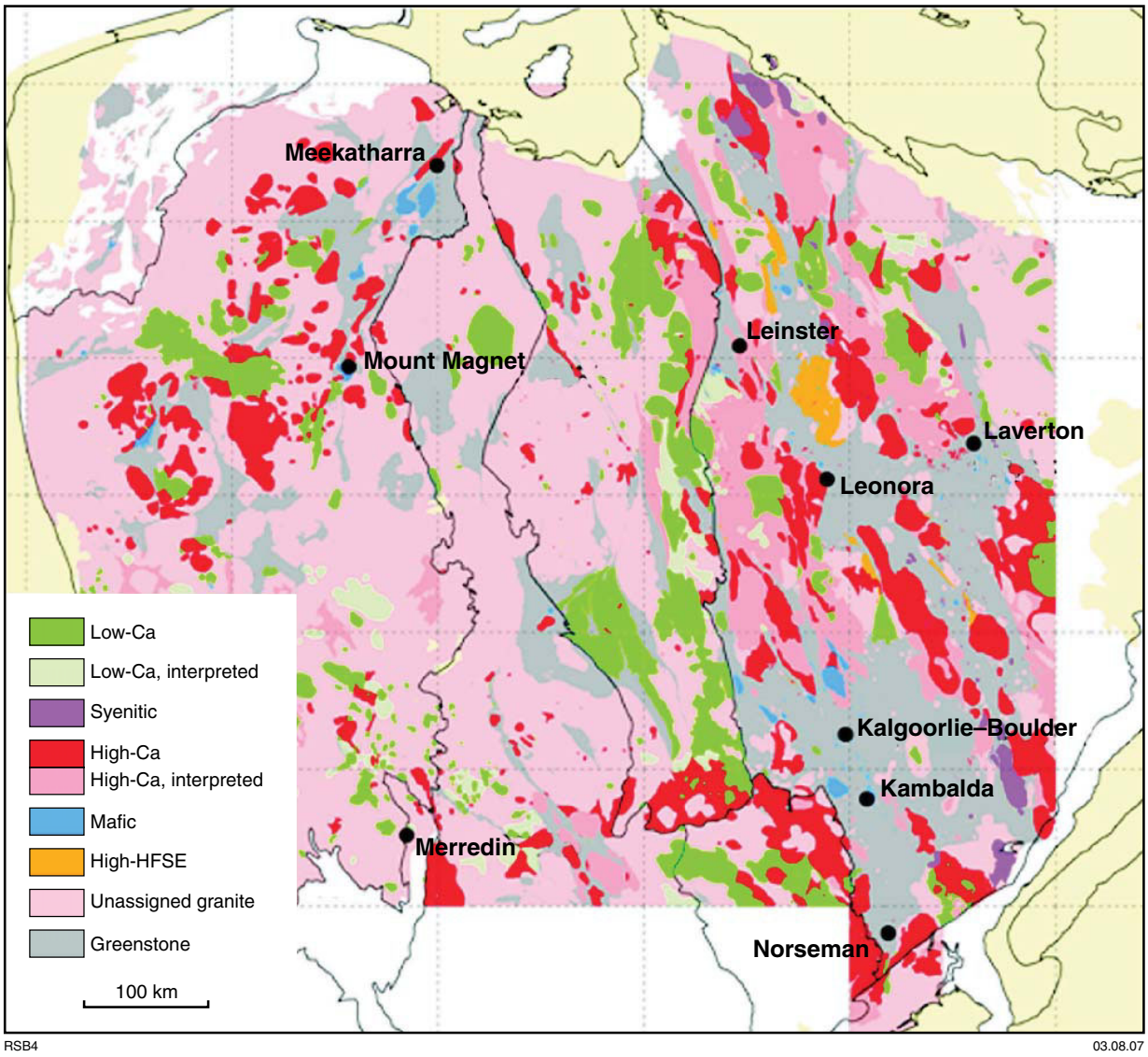

Figure 5. **Map of the five granite types of the Yilgarn Craton (after Cassidy and Champion, 2004). Note the large area of low-Ca granites (green) along the north–south strip to the west of Kalgoorlie**

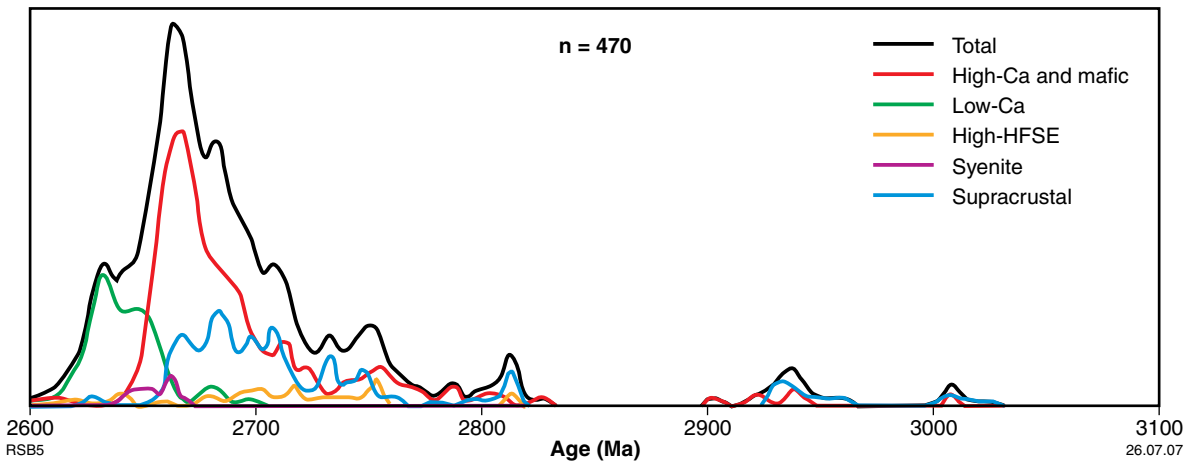

Figure 6. **Histogram of granite and greenstone ages for the Yilgarn Craton (after Cassidy and Champion, 2004). Note the peak in ages at around 2660 Ma, and the change from high-Ca magmatism to low-Ca magmatism**

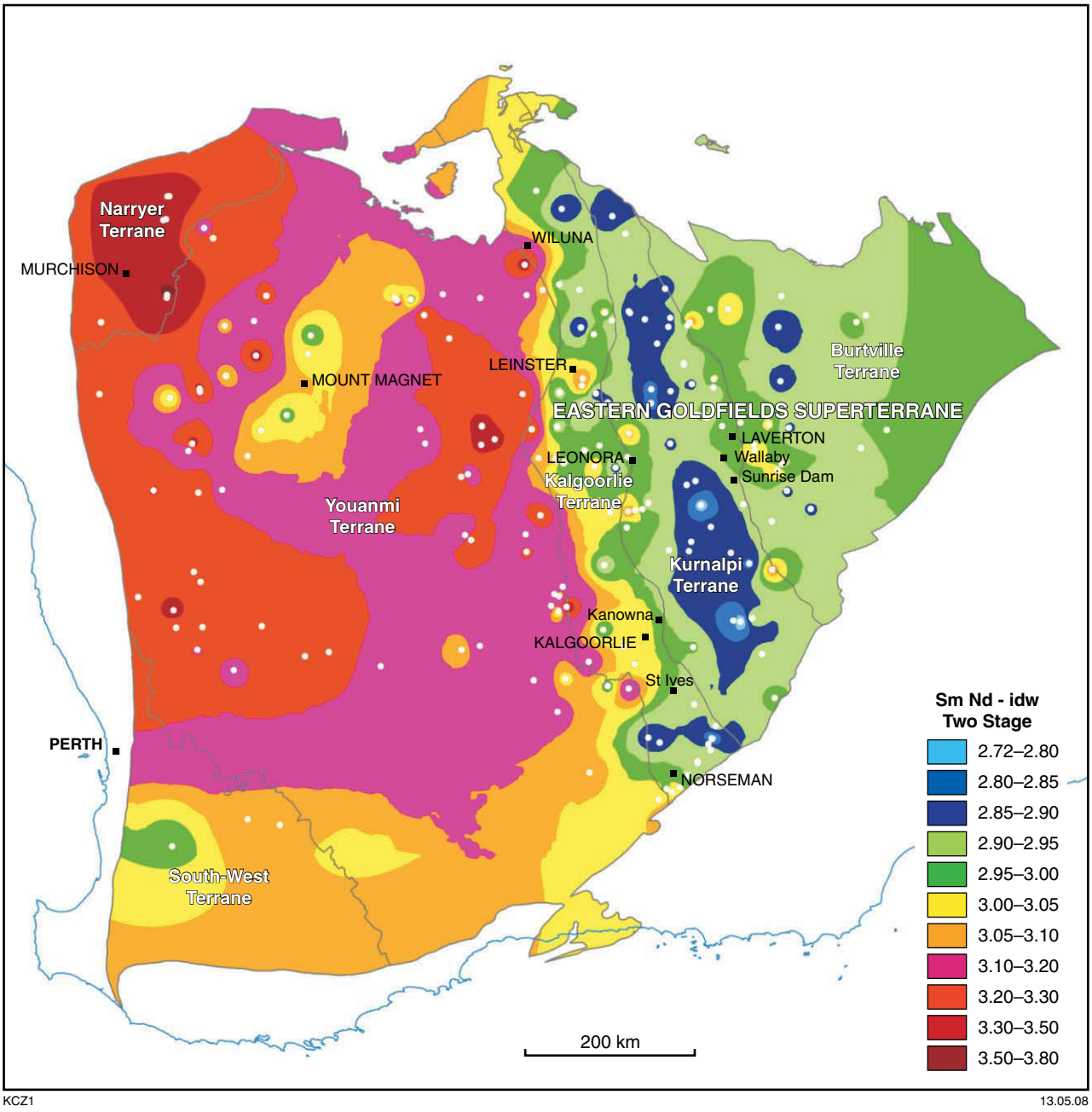

Figure 7. Fundamental architecture of the Eastern Goldfields Superterrane is revealed in the crustal residence ages (TDM). Note the north-northwesterly oriented grain marked by the Ida Fault System located around the orange–green colour change. 'Cooler' colours are younger TDM ages (after Cassidy and Champion, 2004)

model-age map of these granites (Fig. 7) shows that the crust within the EGST becomes older both east and west of a north-northwest zone approximating the western part of the Kurnalpi Terrane and its northern extension (Fig. 7). In addition, there is a clear isotopic change between the Kalgoorlie Terrane and the Youanmi Terrane that must represent a major crustal boundary (Fig. 7), i.e. the eastern Yilgarn crust represents younger crustal growth onto the pre-existing Youanmi 'proto-craton' (Cassidy and Champion, 2004).

Favoured tectonic models indicate a variety of arc environments before c. 2.655 Ga that maintain a pre-existing continental crust component with or without various rifting regimes (Cassidy, 2006). Earlier (>2.655 Ga) changes in the type of felsic magmatism are interpreted to represent variations within an overall subduction-related environment, with melts sourced directly off the descending slab. The change at c. 2.68 Ga, from high-Al TTG-type mafic and bimodal/high-HFSE to transitional TTG-type high-Ca-dominated, may relate to some form of terrane accretion at this time. In the EGST this change to mafic-type magmatism reflects access to the metasomatized mantle wedge, which has profound implications for a region's fertility and access to metal and sulfur sources. This change in magmatism is also observed

to the west, where widespread magmatism within the Youanmi Terrane effectively ceased at this time (Cassidy et al., 2002b).

The change at c. 2.655 Ga to widespread, continued, and voluminous low-Ca-dominated magmatism indicates a distinct change in the thermal regime of the crust and a similar process occurring craton-wide for the first time (Fig. 5). Low-Ca magmatism continued from 2.65 to c. 2.63 Ga across the entire craton and reflects low-pressure (crustal) melting (Cassidy and Champion, 2004). This period of change in granite magmatism is also marked by metamorphism and significant gold mineralization. Smithies and Champion (1999) suggested that these low-Ca melts were developed due to lower crustal delamination.

Previous structural frameworks

Because the gold deposits of the EGST are structurally controlled, structural geology and tectonics have been extensively studied in the region. This summary of previous work and the state of play prior to this study draws on the significant (regional) studies that describe more than an individual mine or map sheet.

Modern structural geology was not systematically applied to the eastern Yilgarn Craton until the studies of Platt et al. (1978), Archibald et al. (1978), and Swager (1989). These workers were the first to publish regional deformation-event histories that were subsequently adopted as a framework by later workers.

The pronounced north-northwesterly oriented structural trend of the EGST (the so-called 'D_2' trend) is defined by the regional fault pattern and elongate granitoid bodies (Gee, 1979). The regional-scale faults form an anastomosing network of high-strain zones that bound a number of terranes or structural domains (Swager et al., 1992; Myers, 1997) that are elongate or lensoid in map pattern, and separate different greenstone successions. The characteristic map pattern of the EGST was developed by a succession of compressional and extensional deformation events that have been interpreted as regional (province-wide) in extent. Swager (1997) summarized many of the interpretations of the regional deformation history, and it is this framework that has been further refined. Henson and Blewett (2006) produced a structural event history that honoured the 2D and 3D map patterns, and was built on the Swager (1997) and Blewett et al. (2004b) work. The map pattern analysis of Henson and Blewett (2006) defined the essential structural elements and their timing, and these are further refined and integrated in this study.

A nomenclature of 'D_1'* to 'D_{4+}' has been most widely used to describe the various deformation events of the EGST. Swager (1997) is the 'standard' terminology most workers have adopted (Fig. 7). Unfortunately most workers did not emphasize or enumerate the extensional deformation events (other than 'D_e' or 'D_E'). Swager's (1997) paper was a synthesis of over 10 years of research and extensive mapping, and he was also one of the few workers to attempt to integrate the rock record into the structural history. Swager (1997) also attempted to integrate the granites but, due to limited geochronology at the time, the result was not very reliable (see Weinberg et al., 2003).

Broadly, the recognized deformation (compressional history) involved early 'D_1' recumbent folding and thrusting during north–south shortening, followed by east–west shortening through large-scale upright 'D_2' folding and thrusting, and then a period of strike-slip 'D_3' faulting with associated folding that was followed by continued regional 'D_4' transpressive oblique and reverse faulting. Some authors have proposed early, intermediate, and late periods of extension throughout parts of this compressive history, although these are not enumerated as separate events.

The following section outlines the generally used structural framework (Fig. 8) and is mostly based on Swager (1997) and references therein.

D_E: early extension

A number of workers have suggested that early extension predated 'D_1' thrusting and may represent the last stages of development of the basin in which the greenstones accumulated (e.g. Williams et al., 1989; Hammond and Nisbet 1992, 1993; Williams, 1993). These workers argued that the external granites represent the substrate on which the greenstones were deposited, within an overall north–south-directed core-complex extensional setting. With recent advances in geochronology, the majority of these 'external' granites have been shown to be younger than the surrounding greenstones (Weinberg et al., 2003), thereby negating this model. SRK Consulting (2000) suggested that the core-complex model applied to the deposition of the Black Flag Group and younger sediments within an overall S-directed extensional model (Fig. 9). Detailed work in the Leonora area led Passchier (1994) to suggest that 'D_1' recumbent folds at Leonora may have formed in an extensional setting.

D_1: north–south contraction

Swager and Griffin (1990) suggested that the 'D_1' event involved large-scale stratigraphic repetition during north–south compression. For example, a regional-scale thrust duplex structure was interpreted to extend from Kambalda to Kalgoorlie and significantly duplicate stratigraphy. Regional 'D_1' in the EGST is thought by many to have developed roughly east–west-trending thrusts and folds as a result of north–south compression (e.g. Swager (1997) and references therein).

More recent interpretations of this map pattern suggest that these so-called 'D_1' thrusts are later than the first compressive event (Fig. 9). This new interpretation is

* Deformation in quotes are from other workers. The new deformation framework presented here is not placed in quotes.

Blewett and Czarnota (2007b)			Swager (1997)	Blewett et al. (2004b)	Miller (2006)
Minor contraction		D_7			
Minor extension		D_6	Collapse	Late DE	
Dextral transtension		D_5	D_4	D_3	D_4
Sinstral transpression		D_{4b}	D_3	D_3	D_3
		D_{4a}	D_2	D_{2b}	D_2
Extensional doming	Stage 2 Late Basins	D_{3b}	D_E	D_{2e}	
	Stage 1 Late Basins	D_{3a}			
Upright folding and reverse faulting		D_2	D_2	D_{2a}	D_1
Extension with intermittent compression		D_1	D_E	D_e, D_1, D_{1e}	

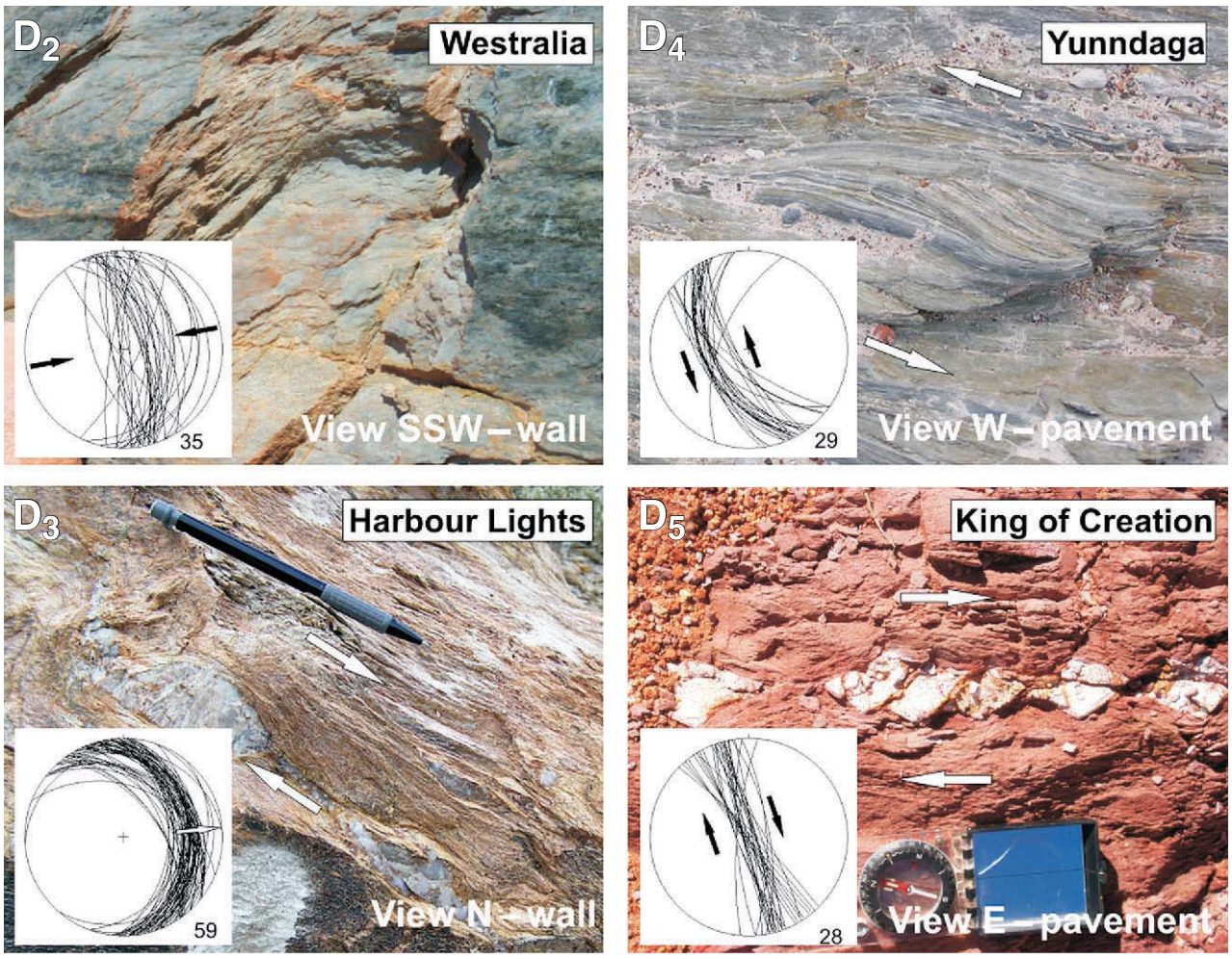

Figure 8. **Comparative deformation chronology of various workers in the Eastern Goldfields Superterrane and photos (as well as equal area lower hemisphere stereographic projections of foliation readings), showing various kinematics along the dominant north-northwest striking foliation of the EGST, indicating that the pervasive foliation without detailed kinematic analysis cannot be used as a means of structural correlation in the EGST**

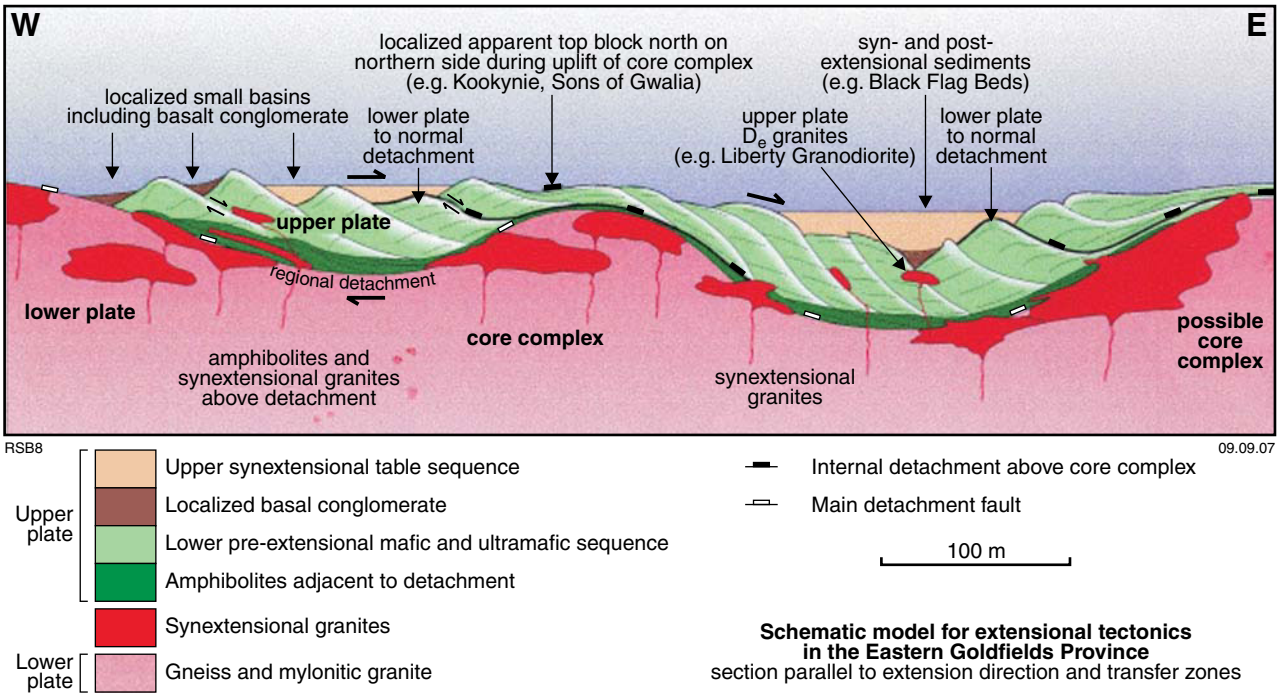

Figure 9. Schematic diagram from SRK Consulting (2000) illustrating the geometry of the extensional architecture of the system. The model has errors of fact such as assuming the late basins are the same age as the Kalgoorlie sequence (Black Flag Beds), but the overall picture is appealing. We have switched the view from one of east-northeast to one of north as we interpret the fundamental polarity of extension to be east–west not north-northwest–south-southeast

based on the observation that 'F_2' folds are transected by these so-called 'D_1' thrusts (Blewett, 2006). Recognition of 'D_1' north–south contraction has been a long-standing problem in the northern Goldfields (Wyche and Farrell, 2000; Beardsmore, 2002), and it was not observed in this study.

Late basins

Swager (1997) interpreted the late basins (Kurrawang, Penny Dam, etc) as being developed during extension after 'D_1' and before 'D_2' (Fig. 3), because they transect regional 'D_1' structures and they are deformed by 'D_2' (in his four-fold deformation chronology). This pre-'D_2' extensional phase was interpreted as oriented east–west and involving synclinal basins developed above rollover anticlines. Other workers have described these basins as 'compressional' basins that developed synchronous with 'D_2' (Liu and Chen, 1998). Krapez et al. (2000) and Weinberg et al. (2003) suggested that they were developed post-D_1 amalgamation in a strike-slip event (that is not enumerated by a separate event). However, it is difficult to reconcile how elongate north–south-trending terranes can be amalgamated by north–south contraction.

D_2: east–west contraction

The regional 'D_2' deformation was interpreted to have involved considerable east–west (east-northeast–west-southwest) crustal shortening, producing major regional-scale upright 'F_2' folds (seen as granite-cored domes), together with a pervasive metamorphic foliation (Swager, 1997). The subvertical penetrative foliation developed in all rock types and across a widespread region has been interpreted in most cases as a composite 'S_1–S_2' fabric. However, interpretation of the penetrative fabric across the EGST as pure-shear flattening has been shown by this study to be problematic. One of the main themes of this field trip is to demonstrate that not all north-northwesterly trending penetrative foliations are the 'main S_2' fabric and therefore this fabric can not be used as the sole means for structural correlation purposes.

The 'D_2' event has been attributed with the development of the major elements of the EGST architecture, including well-preserved regionally extensive 'F_2' granite-cored anticlines, commonly with doubly plunging to horizontal fold axes. The synclines are commonly more complex fault-related structures, with late basins locally defining the 'F_2' synclinal hinge zones (in most workers terminology). Hammond and Nisbet (1992) suggested that the regional antiforms represented hangingwall anticlines developed during west-directed thrusting, and this view was thought to be consistent with the seismic data from Kalgoorlie (Goleby et al., 1993; Drummond et al., 2000), and the seismic data and 3D model developed for the Leonora–Laverton area (Blewett et al., 2002a,b; Goleby et al., 2002). These workers suggested that the seismic data represent a classical fold-and-thrust belt such as the European Alps and North American Appalachians (Rodgers, 1995). This study suggests otherwise, and argues that the primary architecture map pattern and seismic architecture was developed during mostly east-northeasterly directed extension.

The regional 'D_2' event is considered by most workers to post-date the late basins. For example, the Kurrawang, Merougil, and Penny Dam Basins lie in regional 'D_2' synclines in the southern part of the EGST (Swager, 1997; Krapez et al., 2000; Weinberg et al., 2003). Similarly, in the Welcome Well area the Pig Well–Yilgangi Basin is folded by the northwest-trending Butcher Syncline (Gower, 1976) and is overprinted by a well-developed fabric interpreted as 'S_2' (Williams et al., 1989; Passchier, 1994; Liu and Chen, 1998; Stewart, 1998). Swager (1997) suggested 'D_2' was c. 2665 Ma, while Krapez et al. (2000) suggested that it was less than c. 2650 Ma*. Weinberg et al. (2003) stated that 'D_2' occurred after the deposition of the late basins and used Krapez et al.'s (2000) young age of about 2655 Ma for his 'D_2'.

Local extension

Interestingly, Swager (1997) outlined a series of extensional events between many of the contractional events, although he suggested that some of these were of local extent. Swager and Nelson (1997) noted local extension (after 'D_2') of the high-grade granite–gneiss domains into their final uplifted positions relative to the lower grade greenstone belts. They suggested that this extensional event was syn- to post-main granitoid emplacement at c. 2660 Ma. Wyche and Farrell (2000) described similar relationships along the Ockerburry Fault System in the northern Goldfields.

Most workers tended to focus on the contractional event history, and neglected the extensional part of the history. Davis and Maidens (2003) and Blewett et al. (2004b) have documented important extensional events during or just after the major 'D_2' contractional event. Blewett et al. (2004a) suggested that 'D_2' involved two contractional ('D_{2a}', 'D_{2b}') events separated by an extensional event ('D_{2e}') together with the deposition of the 'late basins', and that this more complex 'D_2' was diachronous (younging to the west or southwest). The timing (diachroneity) and relationship of the 'late basins' to a regional 'D_{2e}' extensional event was a significant departure from the established Swager (1997) framework (see Figs 3 and 8).

D_3: ongoing east–west contraction

Continued regional 'D_3' east–west shortening resulted in the development of north-northwesterly striking sinistral strike-slip faults and late-stage foliations (Swager, 1989). En echelon 'F_3' folds with very steep plunges developed as a consequence of sinistral strike-slip shearing along the already steeply tilted sequence. Hammond and Nisbet (1992) questioned the significance of the 'D_3' sinistral strike-slip event. They proposed that most of the so-called late movements were rotated north-directed 'D_1' thrusts that now recorded apparent sinistral kinematics.

* Krapez et al. (2000) interpreted the detrital zircon data to give a 10 m.y. younger maximum age for the late basins by using the youngest grain rather than the youngest statistical population.

Recent seismic imaging (Goleby et al., 2002), and work on the 3D geometry of the major shear zones in the Leonora–Laverton area (Fig. 1) has cast doubt as to the significance of steep strike-slip shearing in the EGST. The results of this work showed that most shear zones dip moderately to shallowly to the east (Blewett et al., 2002a,b), an **apparently** unlikely geometry for a significant strike-slip orogen. However, the limitation of seismic imaging is its inability to directly image steeply dipping features. Detailed analysis of reflector truncations is required to pick steep structures. With continental seismic work this often proves to be a challenge. However Henson and Blewett (2006) were able to resolve the steeply dipping Hootanui Shear Zone (or Far Eastern Shear Zone) at Laverton in their more detailed 3D model of Laverton.

D_4: late contraction

Post-'D_3' compressional structures ('D_4') have been described as variably oriented kink bands and crenulation cleavages, as well as oblique-slip sinistral and dextral faults (Swager, 1997; Vearncombe, 1998; Chen et al., 2001). The northeast-trending faults are mostly dextral, and the east- to east-southeasterly trending faults are mostly sinistral, suggesting renewed east–west compression. However, Mueller et al. (1988), attributed this change in tectonism to a small anticlockwise rotation in the main shortening direction. Swager (1997) considered the 'D_4' structures to be c. 2620–2600 Ma.

Structure in granites

Another feature of most structural studies in the eastern Yilgarn Craton was the emphasis on the greenstone sequences. Many of the granites of the central-eastern Yilgarn Craton are well exposed, with granite pavements providing unique lateral continuity to map structures. This good exposure, coupled with recent high-resolution geochronology (Cassidy et al., 2002a; Black et al., Geoscience Australia unpublished data), allowed Blewett et al. (2004a) to erect a new event history that was better constrained in time. The granites were also useful as they are now exposed at a range of crustal levels and in a range of regions in terms of the distribution of regional strain.

Late extension

Late-stage crustal-scale extensional faulting is recognized on the Ida Fault (Fig. 1) by an abrupt eastward change in metamorphic grade, with exhumed higher grade rocks in the footwall to the west (Swager, 1997). Seismic reflection data reveal that about 5 km of downthrow to the east occurred across the fault (Goleby et al., 1993). The orientation of the Ida Fault, parallel to the 'D_2' 'compressional' structures, might infer extension or post-orogenic collapse following 'D_2–D_3' shortening.

Blewett et al. (2002a,b) and Goleby et al. (2002) noted a similar east-block-down sense of extensional movement on domain-bounding faults in the Leonora–Laverton area seismic reflection data. The extensional movement

on the Ida Fault is constrained as older than the stitching Clarke Well Monzogranite (2640 ± 8 Ma: Nelson, 1997). This extensional movement was younger than peak metamorphism (Swager, 1997), and corresponded with a change in granitoid magmatism to the low-Ca suite below the base of the greenstone sequences (Champion and Sheraton, 1997).

Previous metamorphic framework

Peak metamorphic (low- to intermediate-pressure) conditions are considered to be related to late 'D_2/D_3' deformation (Swager et al., 1992). Binns et al. (1976) recognized both static and dynamic (shear zone) styles of metamorphism. The regional patterns they mapped (supported by Hallberg, 1985) show lowest grades (greenschist and lower) in the internal and thickest parts of the greenstone belts, furthest from the external granites. Metamorphic temperature increases towards the margins of the greenstone belts, towards the external granites. These regional patterns transect the domain boundaries (Fig. 3), illustrating relatively late or long-lived metamorphic event(s). More recently, Mikucki and Roberts (2003) reported two metamorphic events, with a low-pressure event associated with the late-stage low-Ca granites.

New structural framework

Strain was heterogeneously partitioned across the EGST. The preservation of vast areas of relatively intact greenstone stratigraphy that envelope and young away from broad elongate, gently north-northwest – south-southeasterly plunging granite domes, contrast with localized (up to 5 km wide) highly deformed zones (of intense shear foliation) with steeply dipping stratigraphy (and steeply plunging folds). These high-strain zones are commonly areas of significant reworking and were subject to intense east-down extension (D_3*) and subsequent various contractional events with σ_1 oriented from east-northeast (D_{4a}) through east-southeast (D_{4b}-sinistral) to northeast (D_5-dextral). These four events developed most of the foliations in the region, but there are many areas where these fabrics are weakly developed.

Most mineral deposits of the Eastern Goldfields Superterrane are structurally controlled, so knowledge of their structure and tectonics is critical to understanding the region's endowment and to predicting new resources. A nomenclature of 'D_1'† to 'D_{4+}' has been most widely used to describe the various deformation events of the EGST. Many workers adopted the Swager (1997) terminology which is: 1) early 'D_1' recumbent folding and thrusting during north–south shortening, followed by; 2) east–west shortening through large-scale upright 'D_2' folding and thrusting, then; 3) sinistral strike-slip 'D_3' faulting along north-northwesterly oriented structures with associated folding, followed by; 4) continued regional 'D_4' transpressive dextral oblique and reverse faulting along north to north-northeasterly oriented faults. Some authors have proposed extension throughout parts of this compressive history, although these are not enumerated as separate events (other than D_e or D_E). Swager's (1997) paper was a synthesis of over 10 years of research and extensive mapping; he was also one of the few workers to attempt to integrate the rock record into the structural history.

Building on the work of Swager (1997) and references therein, we present a new integrated tectonic framework for the EGST that incorporates a decade of new geochronology, geochemistry, isotopes, stratigraphy, deep seismic profiles, 3D models, and structural mapping from various Geoscience Australia (GA), Geological Survey of Western Australia (GSWA), Australian Mineral Industries Research Association Limited (AMIRA) and pmd*CRC projects. This new framework (Fig. 3) integrates the greenstone stratigraphy, granite evolution, structure, tectonic mode, and mineralization into a coherent history in time and 3D space.

A new integrated tectonic framework

The tectonic grain of the EGST was established as a result of predominantly east-northeasterly directed extension (D_1 and D_3) and predominately east (east-northeast)–west (west-southwest) (D_2, D_4) to northeast–southwest (D_5) compression. The result has been a succession of north-northwesterly striking coplanar, but temporally discrete, fabric elements that can be difficult to reliably interpret at any single location. Past workers have incorrectly interpreted the nature of the north-northwesterly striking penetrative fabric (usually termed 'S_2'), and used the interpretation as a basis for correlating structural events across the region (Fig. 8). However, this fabric can not be used as the sole correlation marker (Czarnota and Blewett, 2005, 2007). We present a new seven-fold (D_1 to D_7) deformation nomenclature based on kinematic analysis and crosscutting relationships (Fig. 10), with the main areas of advancement from Swager (1997) outlined as follows:

- Extension, and transtension/transpression, characterized by extensional and strike-slip shear zones, are considered the dominant tectonic mode (not thrusting cf. Drummond et al. 2000). This mode is reflected in 3D map patterns, stratigraphic considerations, and important deep seismic-reflection imaging.
- The EGST essentially faced east-northeast and inherited this grain during D_1 extension ('D_E' in Swager, 1997), which caused the deposition of most of the EGST greenstone stratigraphy on the eastern margin of the Younami Terrane. All subsequent events reused and modified this initial architecture.
- Many areas with intense D_3 extension do not record a significant contractional overprint, despite them being favourably oriented (e.g. the north–south-striking margin of the Raeside Batholith at Leonora).

* D_3 is separated into D_{3a} and D_{3b} stages in detail, but when described collectively it is referred to as simply D_3.

† Deformation in quotes are from other workers. The new deformation framework presented here is not placed in quotes.

- Late basins were developed in a complex extensional-tectonic mode (D_3) following the first contraction (D_2), which resulted in arc accretion and termination of volcanism. This D_2 contraction did not develop significant foliation. Granite doming and late basin sedimentation are linked by a common process of D_3 extension.
- **Major** crustal thickening did not occur and the contractional events largely inverted a previously extended architecture.
- Upright folding (D_{4a}) and sinistral strike-slip shearing (D_{4b}) overprinted all greenstones and all but the low-Ca granites.
- The first north–south contraction (Swager 'D_1') is older than the late basins, is now considered regional D_{4b}, and was developed during sinistral strike-slip transpression with regional σ_1 oriented east-southeast – west-northwest.
- Low-Ca granites are associated with D_5 dextral strike-slip tectonics, which was long-lived and was a result of an inclined σ_1 that plunged southwest.
- Gold is associated with all events, with D_3 to D_5 being the most productive.
- Late extension (D_6) may not have occurred at the same time everywhere, and its intensity is variable.

D_1: long-lived extension and granite–greenstone formation

The D_1 event was extensional, with a dominantly east-northeasterly directed polarity, and was likely to be the result of east-northeasterly directed rollback of a subduction zone(s). Evidence of D_1 extension is preserved in the broadly north-northeasterly trending distribution of the greenstone stratigraphy (Swager, 1997); the north-northwest trends in the granites, εNd model-age map (Cassidy and Champion, 2004); the subduction signature of the high-Ca granites (Champion and Sheraton, 1997); metamorphic patterns (Goscombe et al., 2005, 2007); the presence of unconformities and the excision of stratigraphy in the greenstone sequence (Swager, 1997; Krapez et al., 2000); and mesoscale structures in gneisses and older greenstone fragments (Blewett et al., 2004a; Blewett and Czarnota, 2007b).

D_1 extension in the EGST was active from the earliest greenstone rock record (c. 2720 Ma and probably earlier) through to the onset of the first significant contraction at around 2665 Ma. Relicts of the older basement (maybe Youanmi Terrane) are preserved as the small slivers of greater than 2750 Ma greenstones at Leonora, Duketon, Dingo Range, and Laverton (Figs 3 and 4). These may represent the rifted remnants of the older Youanmi Terrane. The voluminous high-Ca plutonism that occurred during this period (Fig. 3) is likely to have initiated early elongate domes — 'sowing the seeds' of the domal architecture seen today (Henson et al., 2005).

D_2: termination of an arc and east-northeast – west-southwest contraction

The first significant contraction (D_2) occurred around 2670–2665 Ma, terminating volcanism in the greenstones (Fig. 3). During this time interval disparate associations (in chemistry and age distribution) were juxtaposed at a time when the late arcs shut off in the Kalgoorlie Terrane (Fig. 4).

In general, D_2 developed without significant regional foliation development. Although in areas away from late basins and D_3 extension, structures here correlated with D_4 may well be associated with D_2 (as D_2 and D_4 are coplanar and may lack overprinting relationships). D_2 macroscopic structures indicate that shortening was oriented east-northeast – west-southwest, perpendicular to the grain of the D_1 extensional orogen. Accretion of an external body (an oceanic plateau) into the receding subduction zone is interpreted to have terminated volcanism and sent a wave of D_2 contraction across the orogen.

Blewett et al. (2004b) described two examples of regional macroscale F_2 folds. The first, in the Kalgoorlie Terrane, was the S-plunging regional anticline–syncline pair at Ora Banda, which is overlain by the Kurrawang Basin. The second, in the western Kurnalpi Terrane, was the S-plunging upright Corkscrew Anticline at Welcome Well, which is overlain by the Pig Well Basin. At both these examples Stage 2 late basins lie across folded greenstone sequences, providing an age constraint of greater than 2660 Ma for the development of these folds (Blewett et al., 2004b). These authors described the regional folds as 'D_{2a}'.

To the east in the Kurnalpi Terrane, the map patterns of the Mount Margaret Anticline around Laverton also show that old greenstone sequences are folded more tightly than the upper surface of the domal batholith and the base of the folded Stage 1 (2665 ± 5 Ma) Wallaby late basin. This relationship suggests that east-northeasterly oriented shortening had at least commenced before the Stage 1 late basins were initiated. In the southern EGST, the east-northeasterly directed Foster Thrust at Kambalda is interpreted as a D_2 structure.

D_3: extensional granite doming, mafic granites, and late basin formation

The D_2 contraction was followed by a dramatic change in tectonic mode, as well as greenstone and granite type. The D_3 extensional event was associated with significant granite doming (Henson et al., 2005), a peak in high-Ca granite emplacement, late basin formation, and deformation (Fig. 3). The event is characterized by extensional high-strain shear zones that wrap around major granite-dome margins.

Late basins (Krapez et al., 2000) display two geometrical forms (and ages). Stage 1 late basins are arcuate and located in the hangingwall of extensional shear zones along the south-southeast margins of some major granite domes. The polarity of D_{3a} extension of the Stage 1 basins is orthogonal to, and within the strain shadow of, the east-northeast – west-southwesterly directed regional D_2 contraction. This D_2 contraction has been estimated to have occurred at around 2665 Ma, which is within error of the formation of the Stage 1 Wallaby Basin (c. 2665 Ma), but on geometrical arguments (above) is likely to have initiated

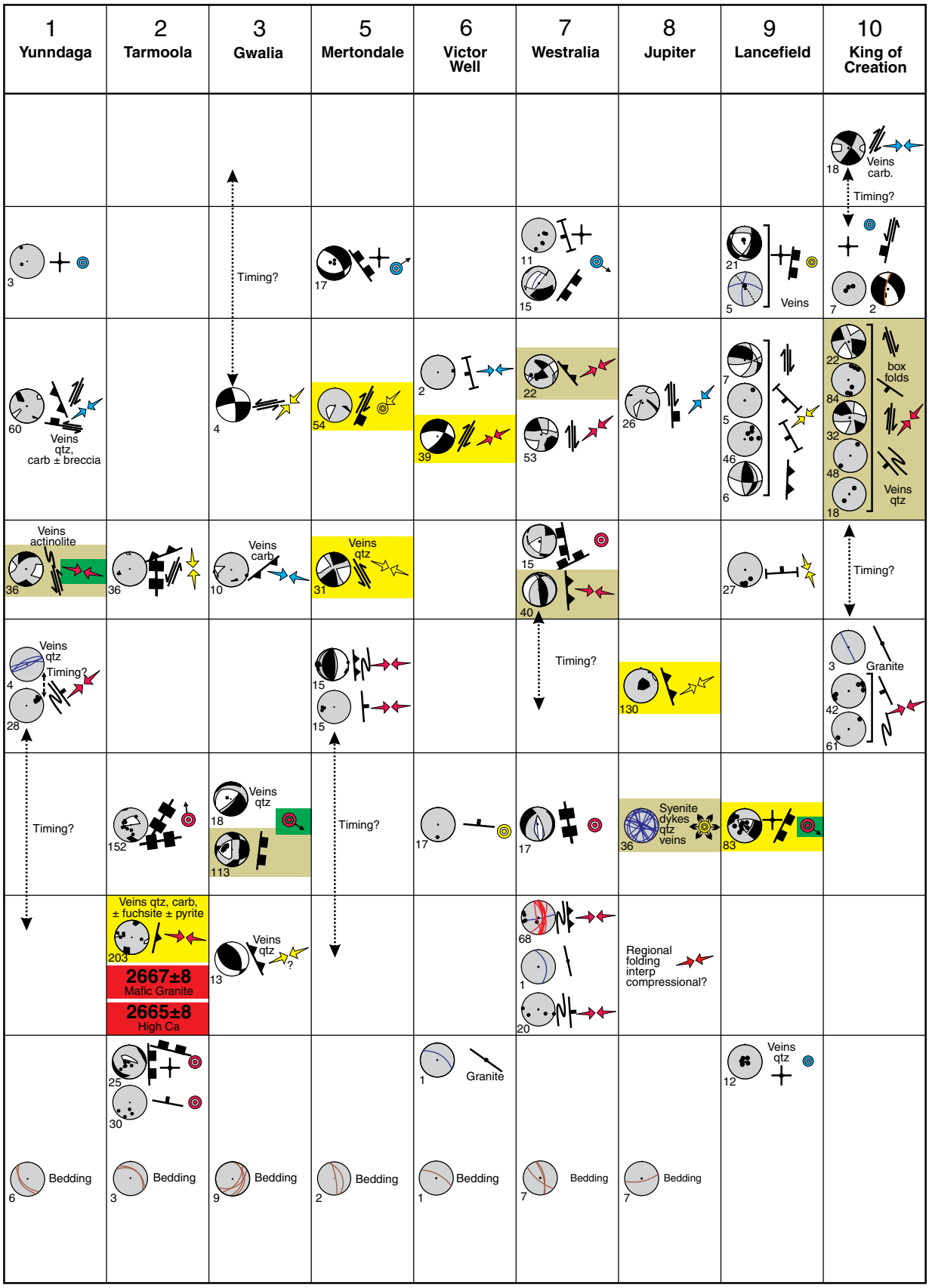

Figure 10. **Synthesis structural-event chart of the localities visited in this field guide (adapted from Blewett and Czarnota, 2007b). Stereonets are lower hemisphere projections of P–T (compression–tension) dihedra and their associated structures. See Angelier (1984) and Blewett and Czarnota (2007a) for a description of the method. The white sectors in the stereonets show the 3D region of possible σ_1 and the black sectors show the 3D region of possible σ_3. These dihedra are analogous to fault-plane solutions used in seismology**

11 **Hanns Camp**	* Phoenix	* Mt Denis	*Brief description of events* **New nomen-clature** **Swager (1997)** **Average orientation of σ_1** **Age of events in Ma**
			~E-W striking brittle faults cross cutting major shear zones **7**
	Veins 30		*Regional orogenic collapse* **6**
	63 21	**2645±3** Low-Ca	*Dextral strike-slip along N to NE striking faults, locally intense* **5** **D_4** <2638±2 start to c. 2650
	21	granite granite	*Sinistral wrenching along NNW striking faults, Reverse on N-S striking structures* **4b** **D_3** c. 2645 to c. 2655
		3 phases of granite	*Upright folding of late basins and greenstone sequence* **4a** **D_2**
2664±2 Syenite	Bedding 5 **<2663±5** Granny Smith Late Basin	Timing?	*Late basins forming event. Granite doming and core complex formation* **3** **D_{E3}** c. 2655 to c. 2665
			Upright folding of greenstones and dextral shearing in external granites **2** c. 2668
		Subhoriz foln and N-plunge lineation Granite sheets & dykes **2670±4** High Ca	*Earliest extension related to:* *1. mafic–ultramafic sequence deposition* *2. voluminous granite emplacement and doming initiation* **1** **D_{E2}** **D_1** **D_E**

04.06.08

Dihedra representing possible areas of: σ_1—white, σ_3—black

Pole to foliation or axial plane of fold. Approximate orientation of σ_1 if pure shear or in conjugate faults

Simplified representation of horizontal compression i.e. σ_1. Fill colour represents intensity of deformation: red—high (high-strain ductile shear zone), yellow—medium (structures with moderate strain), cyan—low (brittle faults & minor crenulations)

Simplified vertical orientation of σ_1 i.e. horizontal extension, arrow in extension direction

Foliation

Horizontal foliation

Crenulation

Thrust/reverse fault/shear

Normal/extensional fault/shear

Shearing

Open folding

Tight folding

Dyke

Sinistral fault/shear

Dextral fault/shear

Recumbent folding

Horizontal foliation

Uncertainty in timing of event, arrows point to possible correlations

Indicates structure is amphibolite grade otherwise assume greenschist-facies condition.

2645±3 Low-Ca granite age (Ma)

2665±3 High-Ca/mafic granite age (Ma)

2665±3 Syenite/HHFSE granite age (Ma)

<2662±5 Maximum age of metasediments (Ma)

Gold event

Inferred gold event

late- to post-D_2 contraction (Fig. 3). In contrast, Stage 2 late basins are north-northwesterly trending elongate 'rifts', interpreted here to have developed as a result of D_{3b} unidirectional east-northeast-down, asymmetric extension (inversion of ?D_2 thrusts). The formation of the Stage 2 late basins equates to the 'D_{2e}' extension of Blewett et al. (2004b).

The D_3 event is associated with the introduction of mafic-type granite magmatism across the EGST (Fig. 3). These magmas, with sanukitoid affinity, were derived from a metasomatized mantle source (a good source for gold and sulfur). Earlier high-Ca magmas (peaking around c. 2670 Ma) are of the high-Al type, whereas after this they change to a more transitional type (Cassidy and Champion, 2004). Syenite magmatism (mantle sourced) commenced in the Kurnalpi and Burtville Terranes at this time (Fig. 3). This dramatic change in felsic magmatism suggests that a fundamental geodynamic adjustment occurred, rather than the system returning to the previous D_1 extensional setting. Beakhouse (2007) attributed the equivalent change from slab melting (TTG) to metasomatized mantle melting (sanukitoid) in the Archean Superior Province of Canada to be a function of slab detachment following collision.

Major granite domes controlled the locus of this D_3 extension, with a strong meso- and macroscale record of extension at Lawlers, Leonora, and Mount Margaret. The accumulation/preservation boundaries of the main greenstone belts also record greenstone-down extension along the Ida Fault to the west and the Pinjin shear zone to the east (Swager and Nelson, 1997). At Leonora on the eastern margin of the large Raeside Batholith, extensional S–C–C' shear zone fabrics are well developed at the mesoscale, and at the macroscale in seismic reflection images (Czarnota and Blewett, 2007). Furthermore, large metamorphic-grade jumps consistent with excision of stratigraphy have also been documented across extensional shear zones at Leonora (Williams and Currie, 1993). All scales infer granite-up and greenstone-down sense of movement (down to the east), with Stage 2 late basins (Pig Well <2665 Ma) developed further east in the hangingwall to extensional shear zones.

A working model is therefore proposed where the D_3 extension, and its associated rock record in the EGST (Fig. 3), were the result of detachment (or delamination) of the D_1 slab following D_2 collision. This detachment provided drivers, pathways, and access to fertile sources for subsequent heat, gold-bearing fluids, and magmas. The gross architecture of the EGST is therefore attributed to have being developed during the D_1 and D_3 phases of extension as opposed to during contraction as suggested by Drummond et al. (2000).

D_4: sinistral transpression

D_4 was a progressive sinistral transpressional event recorded across the terranes of the EGST, both within the granites and the greenstones. It has been subdivided into two distinct stages (Fig. 3) as follows:

- The first stage (D_{4a}) involved horizontal compression with σ_1 just north of east–west and a vertical σ_3 (coplanar to the D_2 stress field). D_{4a} is characterized by pure shear (significant flattening), late-basin inversion, north-northwesterly striking upright folding and associated cleavage formation, reverse faulting, and tightening of earlier domes and D_2–D_3 folds. The geometrical result was the rotation and steepening of stratigraphy (including late basins) along the margins of east-facing granite domes (e.g. the Bardoc Tectonic Zone north of Kalgoorlie, Scotty Creek Basin at Lawlers, and the Mount Varden area north of Laverton). This event was termed 'D_2' by Swager (1997) and 'D_{2b}' by Blewett et al. (2004b) since it overprints the late basins.
- The second stage (D_{4b}) involved the development of north-northwesterly striking, steeply dipping, ductile sinistral shear zones associated with a slight clockwise rotation of σ_1 to east-southeast – west-northwest and a horizontal σ_3 (see also Weinberg et al., 2003). Sinistral strike-slip shear zones have been best developed in regions with steep-dipping stratigraphy (where thrusting and flattening ceased to be effective in dissipating the stress) and within the internal granites. This D_{4b} event equates to the 'D_3' deformation of Swager (1997).

Low-strain structures associated with the D_{4b} event resolve a locally highly variable stress field with σ_1 ranging from east-southeast – west-northwest to north–south in orientation (e.g. the main gold event at Wallaby; Miller, 2006). This large variation in the local stress field is inferred to be a direct consequence of the development of sinistral strike-slip shear zones on a pre-existing highly anisotropic architecture, primarily composed of doubly plunging granite domes overlain by folded greenstones.

In a significant change from the Swager (1997) framework, the south-over-north thrusts from the Kambalda and Kanowna areas (such as Tramways, Republican, and Fitzroy), described as 'D_1' (Swager, 1997), are reassigned to D_{4b}. This is based on regional map-pattern superposition relationships where the 'D_1' thrusts overprint north-northwesterly trending upright 'F_2' folds (see Henson et al., 2004b). An analogy of how north-directed thrusts developed at a high angle to north-northwesterly trending D_{4b} sinistral strike-slip faults exists in the eastern Gobi–Alty region of Mongolia (Bayasgalan et al., 1999). Thrusts in this example develop at the terminations of major strike-slip faults, acting as accommodation structures to rotational strain, and at restraining step-overs where they accommodate displacement between parallel strands of a strike-slip fault system. Locally σ_1 was oriented northwest- to north-striking across these transfer structures and restraining bends despite the regional stress field being oriented east-southeast – west-southwest (Fig. 3).

D_5: dextral transtension and crustal melting

The D_5 event was developed in an overall dextral transtensional-tectonic mode accompanying the emplacement of low-Ca granites and characterized by brittle–ductile north- to north-northeasterly striking dextral strike/oblique-slip faults. This D_5 event equates to the 'D_4' event of Swager (1997). Many past workers

have suggested that it was a progressive event from earlier 'D_2' (Weinberg et al., 2003 and references therein). However, this study has shown that a significant rotation of the paleostress field (~60°) occurred between the D_{4b} sinistral (σ_1 east-southeast – west-northwest) and the D_5 dextral (σ_1 northeast–southwest) events, so the transition was not progressive, but probably marked a major plate reconfiguration such as occurred in the Pacific Plate at 38 Ma.

This event is remarkably consistent across the EGST and thereby forms a good marker for structural correlation across the region. D_5 ductile high strain and locally transpressional shear zones occur along the most significant terrane boundaries such as the western and eastern margin of the Kalgoorlie Terrane (Ida – Waroonga Fault System and the Ockerburry Fault System respectively) and the eastern margin of the Kurnalpi Terrane (Hootanui Fault System). Distant from these terrane boundaries, the D_5 event is expressed as brittle faults with very well-developed quartz–carbonate slicken lines (e.g. Wiluna, Mertondale, and Jupiter). The development of local transpressional–transtensional structures is controlled by pre-existing fault strike and the geometry of adjacent granite batholiths within a system where σ_1 was inclined towards the southwest (Blewett and Czarnota, 2007b).

D_5 was a long-lived event and was associated with a significant change in magmatism to low-Ca granites (Fig. 1). These are significant because low-Ca granites are high-temperature crustal melts emplaced late in the evolution of the Yilgarn Craton (<2655–2630 Ma), marking a fundamental change in the thermal regime of the crust. These granites make up 20% of the exposed area of granites and so are likely to be volumetrically significant (Fig. 5). These magmas were intruded into granite domes below the greenstone base (Henson et al., 2005, 2007), indicating the doming and uplift continued throughout D_5.

D_6: low-strain extension

The last event inferred to be part of the EGST tectonic cycle (cratonization of the Yilgarn) is systemic extension. This event is characterized by mostly low-strain crenulations, with subhorizontal axial planes at a range of amplitudes from millimetres to metres. The fold hinges plunge variably. The structural style is brittle to locally brittle–ductile normal faulting. No specific vector of extension has been defined; and the driver for this extension may have been a readjustment of localized topographic highs from earlier events rather than a regional or far-field control. Structures ascribed to this event have been noted previously by Swager (1997), Davis and Maidens (2003), and Weinberg et al. (2003).

D_7: Proterozoic contractional events

The D_7 event occurred across the EGST and was associated with minor east-northeasterly oriented contraction and the emplacement of dolerite dyke swarms and minor east–west sinistral strike-slip faults. Numerous small displacement faults occur in the granite pavements of the external granites (Blewett et al., 2004a). Swager (1997) also described similar structures. These are all likely to be Proterozoic in age and may reflect events at the craton margin (e.g. the Albany–Fraser and Capricorn Orogenies).

Timing constraints of deformation

The best dataset available for constraining the ages of the deformation framework is available for the granites (Blewett et al., 2004a). This work was based on the geochronological framework established by many workers, but in particular Nelson (1996, 1997), Fletcher et al., (2001), Cassidy et al. (2002a), Dunphy et al. (2003), and Black et al. (Geoscience Australia unpublished data). The EGST was deformed by a series of what appear to be long-lived extensional stages associated with granite emplacement, interspersed with short-lived contractional stages (Fig. 3).

A graphical representation of the timing constraints on deformation is presented in Figure 3 and a comparison with the deformation framework of Swager (1997) is presented in Figure 8. The classical 'D_1' north–south contractional event of Swager (1997) appears to be absent.

D_1 constraints

The D_1 period is interpreted as long-lived extension, with the space creation and formation of the rock record itself as the best evidence. A question remains as to whether the extension was episodic or continuous. The Kambalda Komatiite is dated around 2705 Ma (Nelson, 1997), and the Upper Basalt is younger than the Kapai Slate, which is dated at around 2692 ± 4 Ma (Claoué-Long, et al., 1988). The Kalgoorlie sequence (Black Flag Formation) has age ranges from 2690 to c. 2665 Ma (Krapez et al., 2000). The Kalgoorlie sequence has a number of unconformities, with one at around 2675 Ma (Fig. 4). At the same time in the 'external' granites, a major melting and exhumation event occurred. The ages of the gneissic fabrics are in the range of 2672 ± 2 Ma (Two Lids Soak); 2675 ± 2 Ma (Barrett Well); 2670 ± 10 Ma (Ivor Rocks); 2681 ± 4 Ma (Isolated Hill), and 2674 ± 3 Ma (Wilbah; ages reported in Cassidy, 2006). Such consistent data, across regionally separate sites (similar ages are reported from Duketon: Champion, D, 2005, written comm.), indicate a maximum age for metamorphism and D_1 extension of around 2672 Ma.

D_2 constraints

The first contractional event, D_2, has a maximum age range constrained by the dates of deformed granites and a minimum age range from crosscutting granites. Direct age constraints for D_2 were only available in the study of Blewett and Czarnota (2007a) from the Burtville and Kurnalpi Terranes. In the Burtville Terrane, D_2 is constrained by being younger than the 2668 ± 4 Ma granites at Ironstone Point and older than the 2664 ± 2 Ma syenites at Hanns Camp. In the Kurnalpi Terrane, D_2

was younger than the 2667 ± 4 Ma granite at Pindinnis, the 2665 ± 4 Ma granite at Granny Smith mine, and the 2667 ± 5 Ma granite at the Porphyry mine, and was older than the 2660 ± 5 Ma granite at Bulla Rocks (ages reported in Cassidy, 2006).

D_3 constraints

D_3 is a strong extensional event associated with the development of late basins and the commencement of the emplacement of the mafic and syenitic granites. The syenite and mafic granite types are generally regarded as reflecting regional extension, as these rock have 'seen' the mantle (Champion and Sheraton, 1997). A maximum age for D_3 can be inferred from the overprinting extensional fabric on granites such as the 2664 ± 2 Ma Hanns Camp Syenite and 2660 ± 5 Ma Bulla Rocks Monzogranite. If the mineralization at Sunrise Dam is related to the D_3 extension, then the overlap in Au mineralization ages at Sunrise Dam can be used to constrain the timing of D_3 to 2658 ± 4 Ma (ages reported by Miller, 2006). The maximum depositional ages of the late basins provide constraints on the age of D_3 basin formation, their initial burial, and deformation. Late basin ages include 2662 ± 5 Ma (Scotty Creek: Dunphy et al., 2003); 2665 ± 5 Ma (Jones Creek: Krapez et al., 2000); 2657 ± 4 Ma (Kurrawang: Fletcher et al., 2001); 2664 ± 6 Ma (Merougil: Krapez et al., 2000); 2666 ± 5 Ma (Mount Belches: Krapez et al., 2000); 2664 ± 4 Ma (Pig Well – Yilgangi: Barley et al., 2002); and 2663 ± 5 Ma (Granny Smith: Barley et al., 2002) These ages around 2665–2660 Ma (reported in Cassidy, 2006) are consistent with regional extension post-dating the D_2 contraction and final closure of the arc(s).

D_4 constraints

The age of D_4 can only be inferred from crosscutting relationships. It is obviously younger than the 2665–2660 Ma D_3 extension. The D_{4a} event was previously known as 'D_2' (Swager, 1997) and is the first contraction inverting the late basins. A maximum age for D_{4a} is obtained from the youngest phases of the D_{4a}-deformed Kanowna Belle Batholith and associated porphyries in the Kanowna Belle gold mine. These felsic rocks have U–Pb SHRIMP ages of 2655 ± 6 Ma (Ross et al., 2004). The D_{4b} east-southeast – west-northwest sinistral transpressional stage occurred prior to any low-Ca granite-type magmatism that is present across all terranes (and the Yilgarn Craton as a whole). The low-Ca granite-type granites were emplaced following a switch in paleostress to southwest-directed transtension (D_5).

D_5 constraints

The low-Ca granites provide a maximum age for D_5 of less than 2652 ± 5 Ma (Pink Well), less than 2650 ± 8 Ma (Mount Denis), and less than 2645 ± 6 Ma (Surprise Rocks). At Mars Bore, a dyke of low-Ca type granite with an age of 2647 ± 3 Ma overprints D_5 dextral shear zones and is overprinted by further developed D_5 dextral shear zones (demonstrating the syntectonic nature of these magmas). A minimum age for D_5 (ages reported in Cassidy, 2006) was obtained from low-Ca granite-type dykes that overprint D_5 fabric elements of 2638 ± 2 Ma (Ironstone Point). The D_5 event is likely to have developed after about 2650–2645 Ma.

Post-D_5 and younger event age constraints

The ages of post-D_5 events are poorly constrained. The D_6 event is a late phase of extension and may not have occurred at the same time throughout the whole region. 'Young' ages of about 2600 Ma from various isotopic systems may reflect these late events in the final cratonization of the Yilgarn Craton. Significant east-northeasterly trending Proterozoic mafic dykes transect the Yilgarn Craton, and these are interpreted to be associated with the D_7 contraction. Blewett et al. (2004a) described a number of poorly constrained very minor deformation events in the granites. These were interpreted by these authors as Proterozoic in age and related to distant reworking events on the margins of the craton (e.g. Capricon Orogen in the northwest and the Albany–Fraser Orogen in the southeast).

New metamorphic framework

In the pmd*CRC Y4 project a metamorphic database covering the entire eastern Yilgarn Craton has been compiled from pre-existing mapping, 14 500 sites with qualitative metamorphic information, and 470 key sites with detailed quantitative metamorphic data including P, T, average thermal gradient and P–T paths. The derived temporal and spatial patterns contrast with previous tectonic models based on an invariant crustal depth with a single prograde metamorphic event. In particular, there are large variations in peak metamorphic crustal depths (12.3 to 30.5 km), and five metamorphic events can be recognized:

- **M_a**: very localized, low-P granulite of high average thermal gradient (>50°C/km).
- **M_1**: high-P (6–8.7 kb), low average thermal gradient (≤20°C/km) assemblages localized to major shear zones with clockwise isothermal decompression P–T paths.
- **M_2**: regional matrix parageneses with T ranging 300–550°C across greenstone belts and elevated average thermal gradients of 30–40°C/km throughout. Tight clockwise paths evolved through maximum prograde pressures of 6 kb and peak metamorphic pressures of 3.5 – 5.0 kb.
- **M_{3a}**: an extension related thermal pulse localized on the Ockerburry Fault and post-volcanic late basins. Anticlockwise paths to peak conditions of 500–580°C and 4.0 kb, define moderately high average thermal gradients of 40–50°C/km.
- **M_{3b}**: multiple localized hydrothermal alteration events during a period of exhumation from 4 to 1 kb.

Metamorphic patterns during each event have been temporally and spatially integrated with the new deformation framework (Blewett and Czarnota, 2007a,

GA Record 2007/15) by a process of metamorphic domain analysis and using metamorphic field gradients.

Implications for predictive gold discovery

Gold is associated with all of the events throughout the geodynamic history of the EGST; however, significant gold mineralization did not occur until the D_3 extension event (Fig. 3). The genetic link between D_3 extension and late basin formation provides insight into the empirical observation that large gold deposits occur in proximity to late basins (Hall, 2007). This is because late basin distribution is associated with crustal-penetrating shear zones developed during D_3 extension. These shear zones are necessary to tap deep fluids and metals (from the mantle). The emplacement of mantle-derived mafic and syenitic granites into the upper crust during D_3 extension reflects this deep connection. Furthermore, extension is an efficient way to draw fluids down shear zones to facilitate fluid mixing (Sheldon et al., 2007). Significant gold mineralization is hosted in high-strain, extensional ductile shear zones at Gwalia, Lancefield, and the Lawlers camp. Extensional shear zones occur in other areas of the Yilgarn Craton, so there is significant potential for finding Sons of Gwalia-like ore deposits. The D_3 extension is also responsible for setting up the domal architecture of the EGST that is critical for fluid focusing during subsequent events.

The D_4 sinistral transpression event was imposed on the highly anisotropic architecture developed largely during D_3. This resulted in the creation of numerous depositional sites with significant structural complexity, and the development of locally variable and complex stress fields as the anisotropy in the orogen was being 'ironed out'. Gold is associated with brittle–ductile sinistral strike-slip shear zones at deposits such as Wallaby and Sunrise Dam, St Ives camp, Kalgoorlie, Kanowna Belle, Lawlers, and Wiluna (Swager, 1997; Weinberg et al., 2003; Miller, 2006 and references therein).

The final gold event was associated with D_5 dextral shearing (brittle transtension), with deposits including Sunrise Dam and Wallaby, Transvaal, Wiluna camp, New Holland, Golden Mile, St Ives camp, and Kundana being examples. In contrast to the earlier gold-dominated events ($D_{3–4}$), the mineralogy associated with D_5 included base metals and tellurides and may reflect the influence of basinal fluids (Goscombe et al., 2007).

Excursion localities — Menzies to Leonora

Day 1

We are driving from Kalgoorlie northwards to Leonora (approximately 220 km) and will be traversing through the Kalgoorlie sequence up the Bardoc Shear Zone, which is a narrow zone of reverse shearing and sinistral strike-slip deformation between the Mount Pleasant and Kanowna Batholiths (west and east respectively). We will pass the KCGM smelter and historical mines such as Paddington, Goongarrie, and Sand Queen en route to the Menzies township and Yunndaga.

Locality 1: Yunndaga — a sinistral shear-hosted gold deposit (MGA 311580E 6707563N)

The purpose of visiting Yunndaga is to illustrate gold mineralization in metasedimentary rocks with dolerite intrusions providing a local competency contrast and the classical 'D_2–D_4' deformation framework of Swager (1997). The main foliation is associated with the initial development of upright folds and subsequent bedding-parallel sinistral strike-slip shearing. This foliation will be contrasted with superficially similar (in intensity, strike, and metamorphic grade — but not kinematics and timing?) foliations throughout the EGST.

The Yunndaga gold deposit is located approximately 6 km south of Menzies along the northern part of the Bardoc tectonic zone (Fig. 2). Yunndaga yielded approximately 8.75 t (approx. 31 000 ounces) of gold between 1897 and 1935 (Witt, 1992). Recent openpit operations (1995–98) have produced approximately 2.02 t of gold (Evans, 2003). The deposit is hosted by clastic sedimentary rocks and carbonaceous shale, along with a central dolerite–gabbro dyke, which locally is a chlorite schist.

Morey (2007) reported that gold mineralization is associated with a strike-parallel laminated vein located at the contact between the western margin of the dolerite and the quartz-rich sedimentary units (Fig. 11). Wallrock alteration is characterized by quartz–carbonate–biotite–chlorite–arsenopyrite–pyrrhotite–gold assemblages. Gold is associated with fine fractures within the arsenopyrite.

Two progressive major contractional events (D_{4a} and D_{4b}) and a late transtensional event (D_5) deformed the area (Figs 11 and 12). Gold was probably associated with the D_4 events. The main fabric elements (D_{4a}) were developed under a horizontal east-northeast – west-southwest contraction, and associated with upright tight to isoclinal folding of the sedimentary sequence and axial planar cleavage. Evidence of this folding is clearly displayed in the northeastern wall of the pit (best viewed from the southern end of the pit) and as upright outcrop mesoscale folds in the pavement (Fig. 13a). Most authors would equate these D_{4a} structures with the classical 'D_2' event of Swager (1997).

The upright folds (Fig. 13d) are overprinted by D_{4b} north-northwesterly striking sinistral strike-slip shearing associated with a clockwise rotation of σ_1 to an east-southeast – west-northwest orientation (Fig. 12). This event is responsible for the majority of the structures that can be observed in the pavement of the Yunndaga ramp, including boudinage of gold-bearing quartz veins (Fig. 13b,e); typically approximately 20°S-plunging stretching lineations on the main bedding-parallel foliation (Fig. 13c); and drag folds with near vertically plunging fold axes (Fig. 13f). Clear S–C' structures associated with sinistral strike-slip deformation (Fig. 13b,e,f) are developed within the less competent units within the sedimentary rocks. East-northeasterly striking dextral quartz veins with actinolite wallrock alteration developed late during this event (Fig. 14a,b). These veins are best exposed along the northeastern wall of the pit.

Structural elements of the D_{4b} event are overprinted by a series of D_5 brittle faults. The most notable of these is the east-northeasterly striking sinistral fault associated with a large quartz vein at the northern end of the pit. Outcrop along the northeastern wall of the pit shows a series of what appear to be normal shear veins; however, in detail they are sinistral normal most likely associated with the larger sinistral fault (Fig. 14c,d). P–T (comPression–Tension) dihedra analysis of these structures indicates that these structures (like the rest of the D_5 structures) formed under a southwesterly inclined σ_1. Traditionally these structures would be associated with Swager's (1997) 'D_4' event.

The last event, D_6, is associated with the development of horizontal crenulations that can be observed on D_5 fault surfaces. This event is interpreted to represent the phase of the EGST tectonic system.

Locality 2: Tarmoola — contractional gold with an extensional overprint (MGA 320753E 6827328N)

Leave Yunndaga and drive north through the historical town of Menzies (once a bustling centre) to Leonora. We will travel across the Ockerburry Fault System into the Kurnalpi Terrane and greenstones of the Melita belt, which hosts small mines around Kookynie (a popular prospecting location). After crossing Lake Raeside we pass back into the Kalgoorlie Terrane and a narrow sliver of greenstones on the eastern margin of the Raeside Batholith. Keep travelling through Leonora for 31 km to the Tarmoola sign. A locked gate secures the access road to the mine.

The Tarmoola goldmine is an example of the role of competency contrasts (granite–greenstone) in localizing structures and hence permeability, fluid flow, and ultimately mineralization. The purpose of visiting Tarmoola is to illustrate the relationship between contractional gold and later overprinting by extensional shearing, inferred to be related to doming and the development of the late basins. A more extreme version of this extension is found in Gwalia (Locality 3).

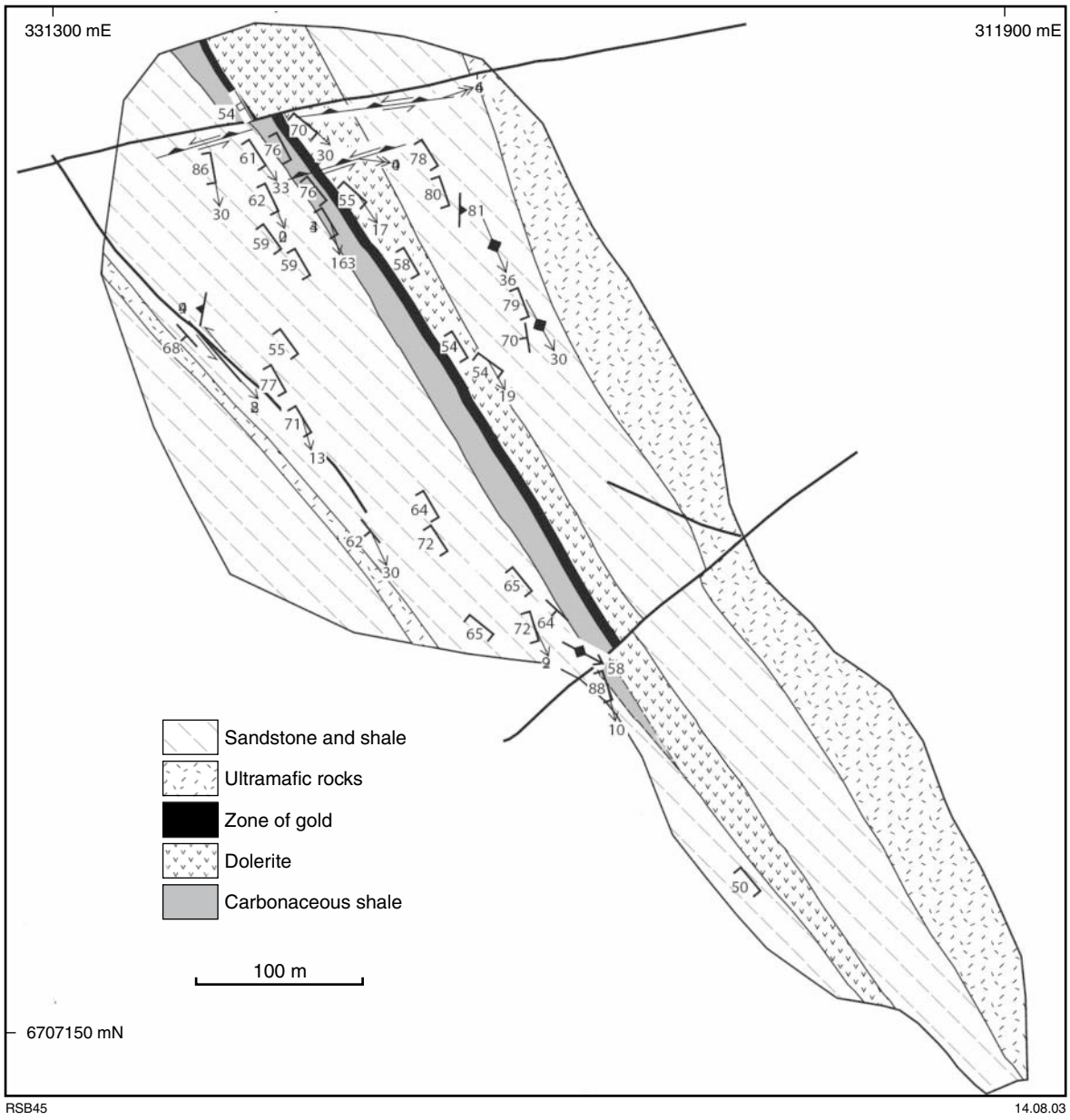

Figure 11. Simplified geological map of the Yunndaga pit near Menzies (after Morey, 2007)

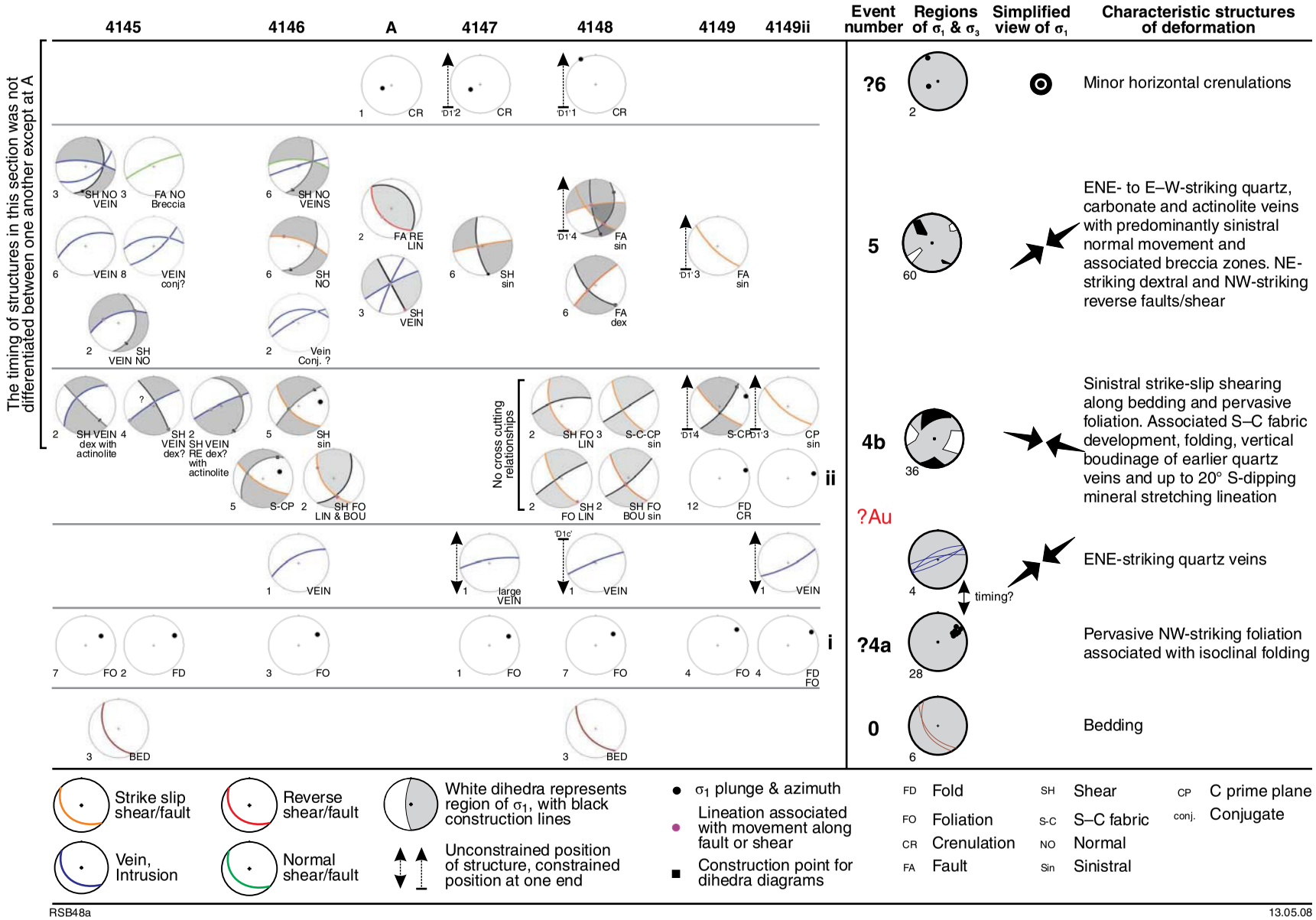

Figure 12. Stereographic compilation of structural elements into discrete events at the Yunndaga deposit

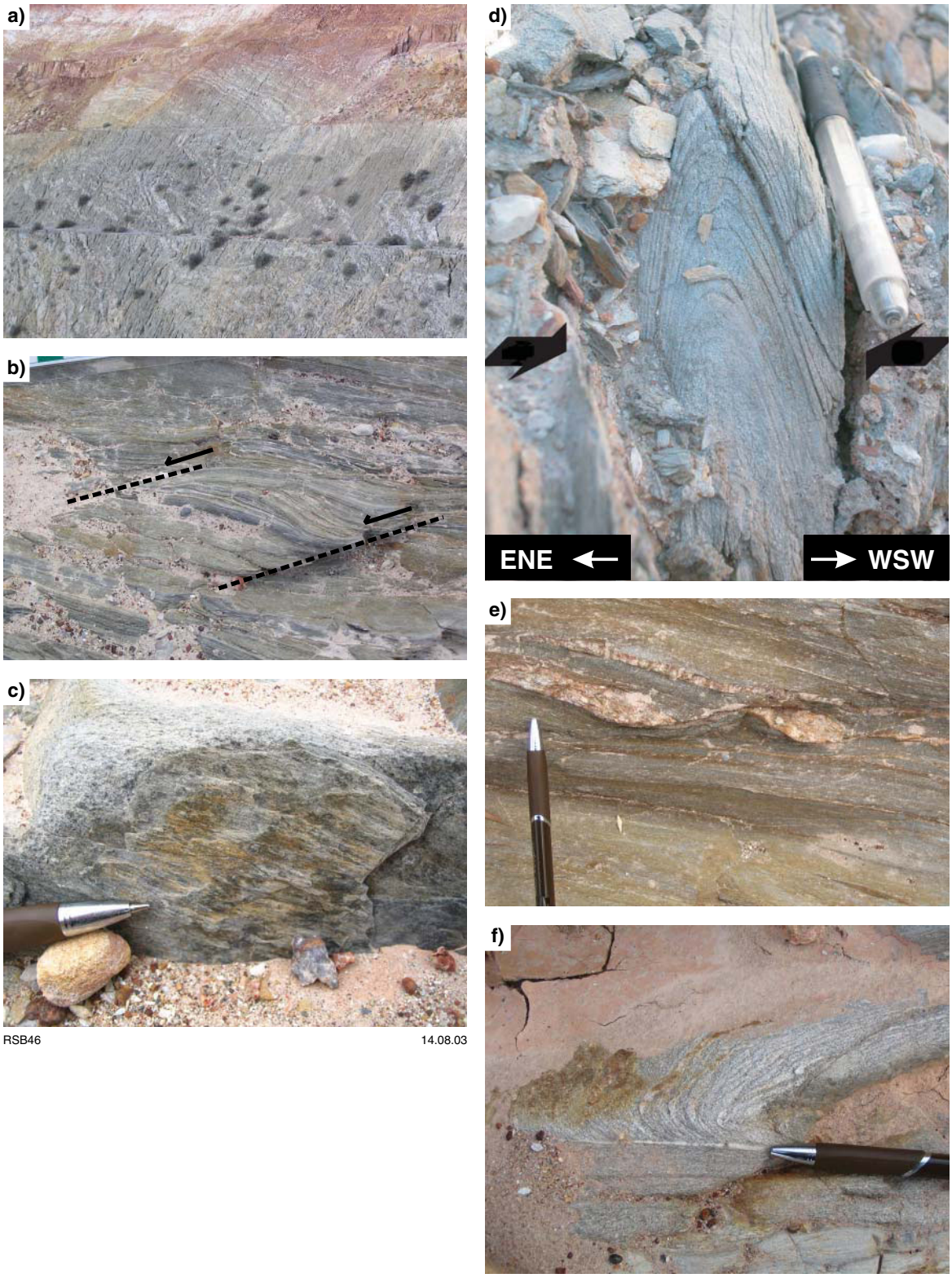

Figure 13. Compilation of photographs from the Yunndaga pit: a) F_4 folds in the east wall of the pit (view northeast); b) D_{4b} sinistral C' planes in metasedimentary rocks in the western access ramp (view west onto pavement); c) oblique-slip L_{4b} lineations associated with north-northwesterly oriented sinistral shearing (view west); d) upright tight gently north-northwesterly plunging F_{4a} fold of bedding and laminae (after Morey, 2007); e) D_{4b} sinistral C' planes in metasedimentary rocks cutting boudinaged quartz veins (view west onto pavement); and f) D_{4b} drag fold with steep plunge consistent with strike-slip shearing (view west onto pavement)

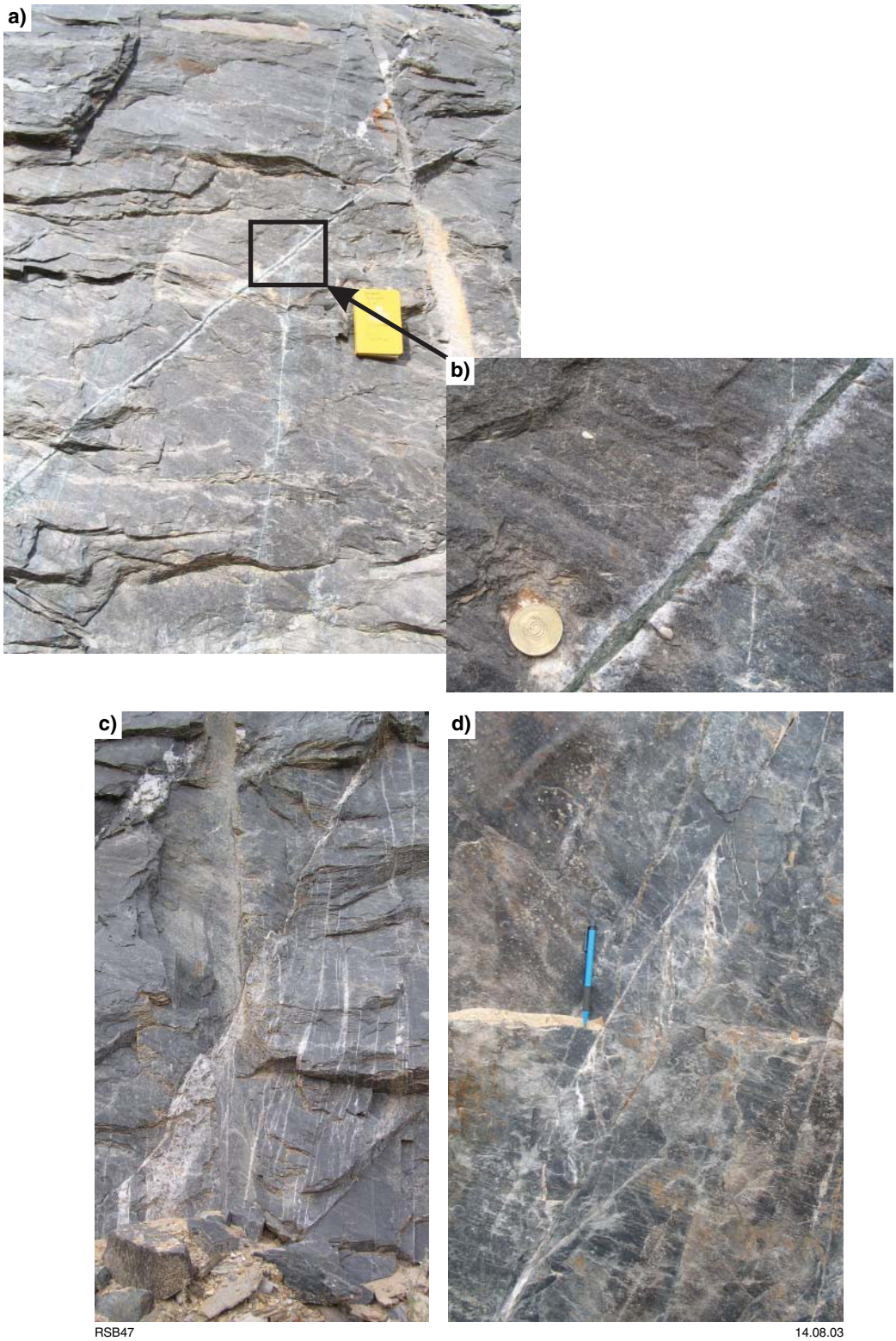

Figure 14. Compilation of photographs from the Yunndaga pit: a) D_4 quartz–carbonate–actinolite veins in chlorite schist (view west onto steeply dipping wall); b) detail of carbonate alteration of dolerite host rock adjacent to the amphibole veins (view east onto steeply dipping wall); c) sinistral normal quartz–carbonate veins associated with D_5 southwest-inclined σ_1 (view east onto steeply dipping wall); and e) sinistral normal quartz–carbonate shear and extension veins associated with D_5 southwest-inclined σ_1 (view east)

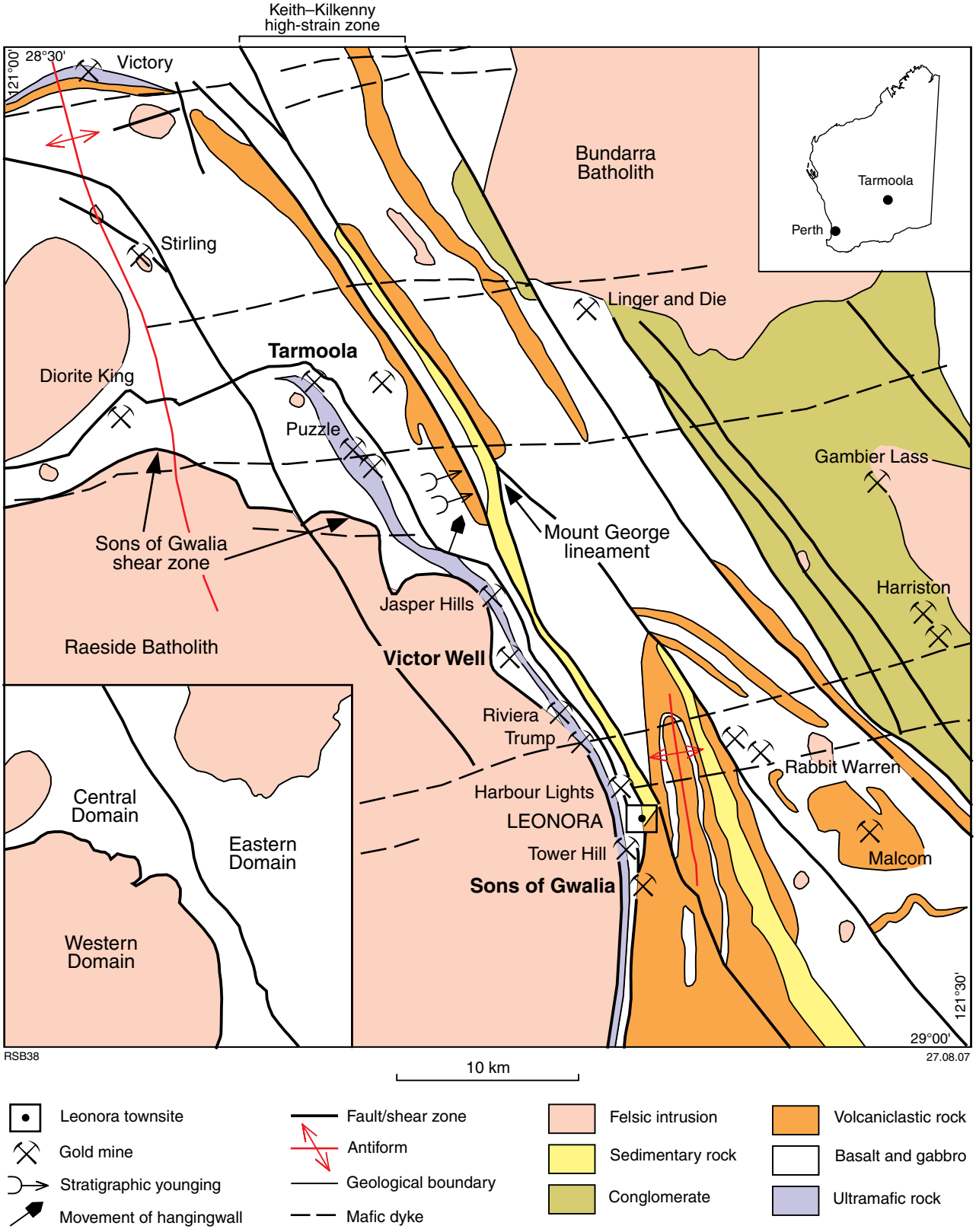

Figure 15. Simplified geological map of the Leonora district with the Tarmoola (Locality 2), Sons of Gwalia (Locality 3), and Victor Well (Locality 6) sites shown. Note the large granite batholith (Raeside) in the southwest of the map and the enveloping shear zones (extensional; after Duuring et al., 2002) that mantle the granite–greenstone contact

The Tarmoola gold deposit is located approximately 30 km north of Leonora, on the northern end of the Raeside Batholith (Figs 2 and 15). The deposit is 'cored' by a trondhjemite with diorite dykes dated at 2667 ± 8 Ma (Lance Black, unpublished Geoscience Australia data). This current study has elucidated five phases of deformation, and as with other deposits in the area, has a significant component of extensional deformation (Swarnecki, 1988; Vearncombe, 1992).

The greenstone stratigraphy is upward facing, based on numerous pillow lavas. The first fabric(s) is developed in the greenschist-facies mafic and ultramafic rocks that are intruded by the trondhjemite. The fabric is patchy in distribution and preserved as a steeply dipping, east–west striking, penetrative foliation. The kinematics on this fabric are uncertain. It is a hard event to correlate across the Tarmoola pit and the significance of this fabric with respect to regional deformation events is unclear. It is interpreted as part of the long-lived D_1 extensional event (Fig. 16).

The second event involved the development of an extensional S–C' shear fabric that is especially well developed in the talc schists. Sigma 1 was subvertical during D_1, with extension off to the northeast and southwest (Fig. 16).

Gold is hosted in spectacular D_2 quartz–carbonate (–fuchsite) veins related to dextral strike-slip shearing along the northeast-striking east edge of the Tarmoola trondhjemite. The dominant dextral shear planes are expressed as continuous sheeted quartz veins along the southeast wall of the south pit. Associated with these dominant shear veins are synthetic (dominant set) and antithetic en echelon quartz–carbonate(–fuchsite) veins (Fig. 17a–d). Brecciation occurs at many of the intersections of the synthetic and antithetic shear-vein sets, with fuchsite-altered wallrock incorporated into a 'blow out' of quartz–carbonate veins (Fig. 17c).

The above veins cut an associated north- to north-northeasterly striking S_2 foliation associated with the dominant shear veins. Mohr circle analysis by Duuring et al. (2001) showed that the presence of this pre-existing foliation would preferentially localize shear failure along the eastern edge of the trondhjemite. The D_2 contraction is well constrained, with σ_1 oriented just south of east and σ_3 oriented horizontally orthogonal to this with some local heterogeneity in the vicinity of the saddle pit (Fig. 18).

Some gold veins were deformed by a second extensional event, most notable in the saddle pit. This D_3 extensional event involved mostly down-to-the-north transport, with σ_1 again vertical (Fig. 17d). The final event was the development of D_{4b} north-over-south thrusts (Fig. 17e–f) and shear veins, together with more steeply dipping sinistral faults and approximately north-trending normal faults.

Locality 2a: Mineralized greenstone with steep contact with trondhjemite

This locality is at the southeastern part of the south pit and shows the steep contact with the main trondhjemite body and mafic schists (Fig. 19). The trondhjemite is

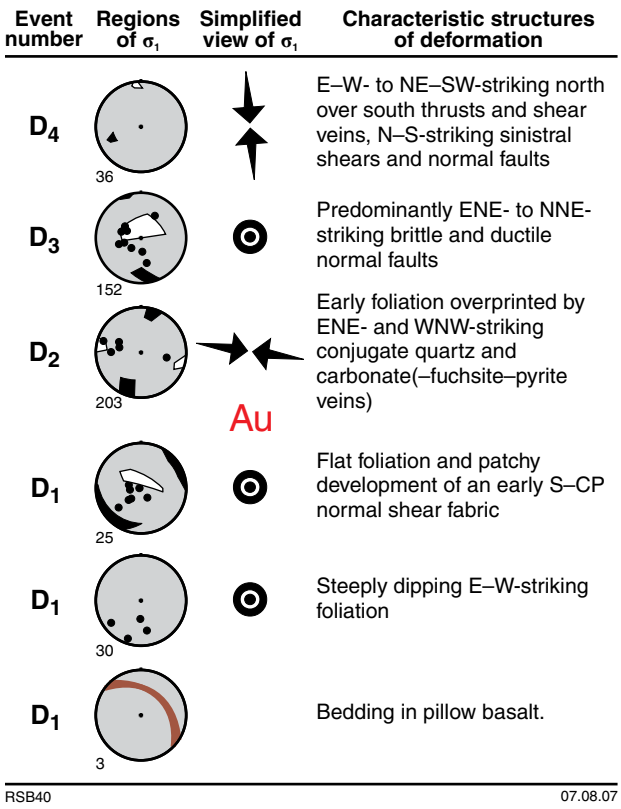

Figure 16. Stereographic compilation of structural elements into discrete events at the Tarmoola deposit. Tarmoola is an example of D_2 gold. Note how more than 200 structural readings resolve a very small S_1 sector to be just south of east–west and an orthogonal S_3 that is subhorizontal. It is likely that this subhorizontal S_3 reflects the overall transpression associated with D_2 contraction (as recorded in the granites), or the geometry of the trondhjemite contact with the greenstones

largely unfoliated, and irregular apophyses of granite project outwards into the greenstone country rock. Sets of en echelon D_2 quartz–carbonate (gold-bearing) veins cut both the granite and greenstone. The dominant vein sets are dextral. The smaller synthetic and antithetic shear-vein sets display sinistral and dextral kinematics. An analysis of all the vein sets across the deposit resolves a maximum compression direction of approximately east–west. At the trondhjemite contact with the greenstones, notice the east-northeasterly striking brittle sinistral-normal quartz shear veins in the trondhjemite. These veins are consistent with formation during dextral movement along the main dextral sheeted veins under approximately east–west compression (Fig. 16).

All quartz vein sets overprint an earlier foliation (S_2) in the greenstone. Walk the section up the ramp and note the large steeply east-dipping 'wall' of quartz with extension veins (sinistral and dextral en echelon sets) striking at acute angles to this main vein (Fig. 17c). Notice the horizontal lineation on the main quartz vein, consistent with dextral strike-slip shearing along this vein (Fig. 17b). The large veins that appear in the walls above are further examples of this vein set and the view is onto their dip

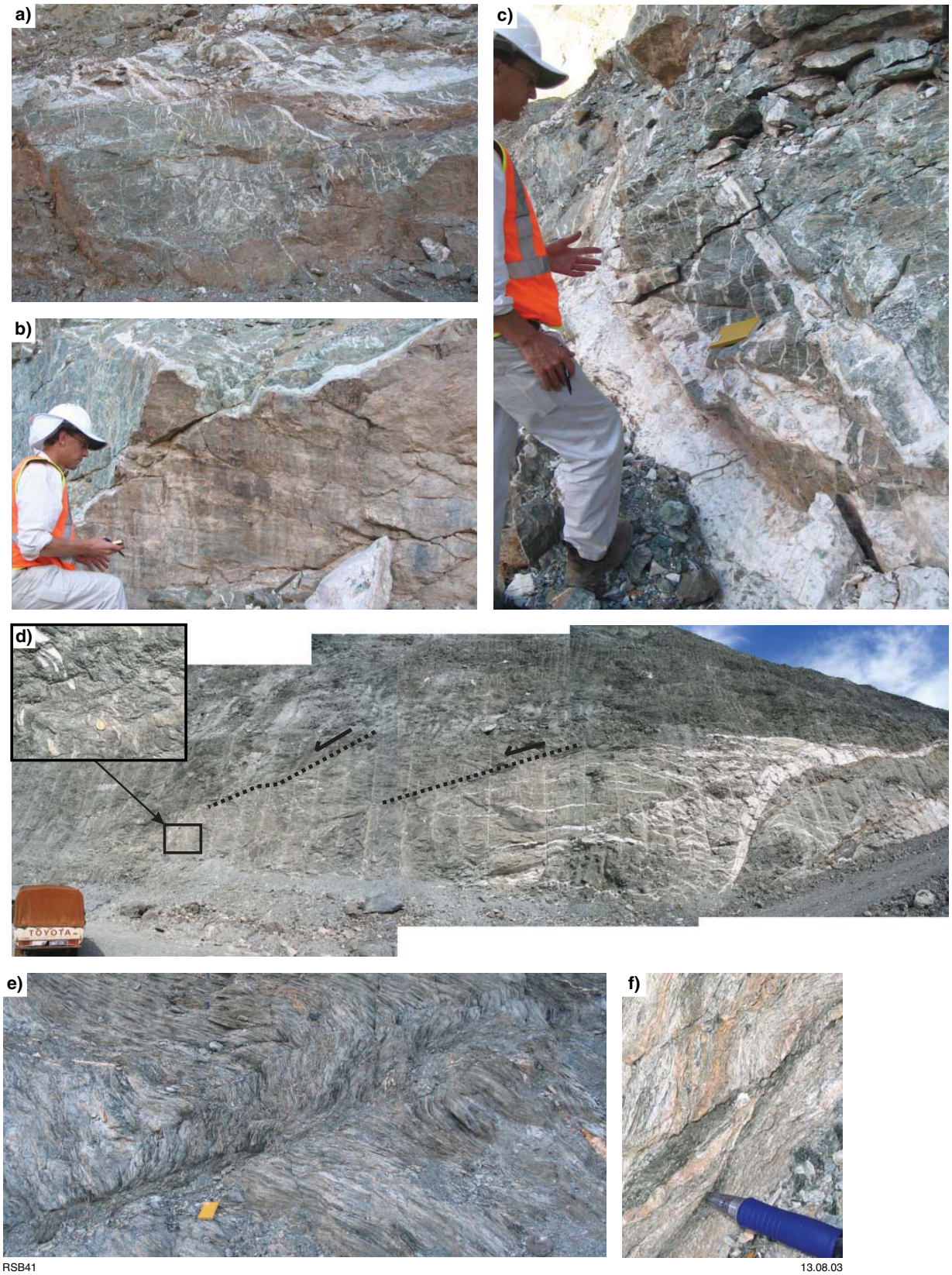

Figure 17. Compilation of photographs from Tarmoola: a) en echelon sinistral and dextral shear-vein arrays splaying from the main dextral fault (view southeast); b) dextral strike-slip fault strikes northeast–southwest and mirrors the margin of the trondhjemite (view southeast); c) detail of vein arrays and brecciation and fuchsite alteration associated with D_2 dextral shearing (view northeast); d) compilation of D_2 dextral strike-slip fault and spectacular wing-crack veins overprinted by normal (extensional) shearing during D_3. Inset shows detail of S_3 extensional crenulations (view southeast); e) top to the northeast D_5 thrusting overprints S_3 extensional crenulations in ultramafic schist (view northwest); and f) detail of D_5 thrusts (view northwest)

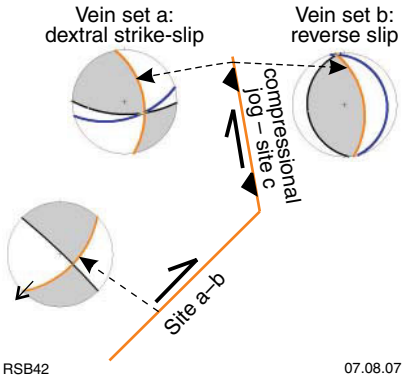

Figure 18. Schematic diagram illustrating how the geometry of faults (caused by a heterogenous body like a granitoid) influences the structures observed at each location. Note how the structures change from reverse faults and veins to strike-slip under the same regional east–west contractional stress regime

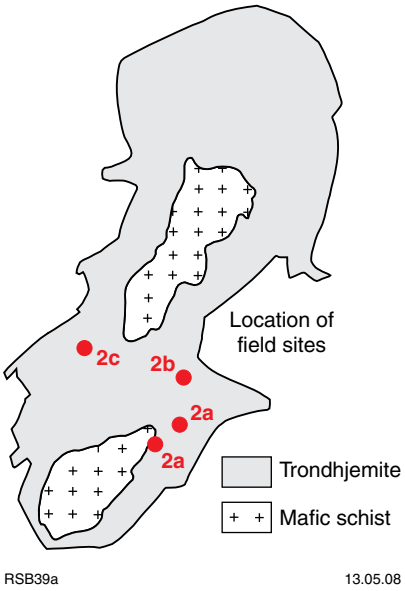

Figure 19. Location of field sites in the Tarmoola pit

direction so that they appear subhorizontal in this section provided by the openpit.

Warren Potma from the computational geoscience group at CSIRO funded by St Barbara Limited conducted deformation driven fluid flow modelling of the Tarmoola deposit (Potma et al., 2007). Using detailed mine data around Tarmoola the geometry of the trondhjemite intrusion was determined and used as an input into the numerical modelling. Modelling of variable paleostress directions indicated that the results from models under east–west contraction resulted in the best fit between regions of known mineralization (Fig. 20a,d) and regions of greatest dilation and fluid flux in the model (Fig. 20b,c,e). These results agree with the paleostress direction determined for this event in this study (Fig. 16), illustrating that the numerical model is consistent with field observations. Based on the veracity of the modelling results in regions of known mineralization Warren was able to predict a down-dip extension of mineralization at the Tarmoola deposit (Fig. 20b,c) and three new mineralization targets around the Tarmoola trondhjemite (Fig. 20f).

Locality 2b: Extensional overprint of contractional gold

A spectacular east-dipping dextral D_2 vein with associated wing-crack veins is exposed in the west wall of the small saddle pit at the edge of the trondhjemite (Fig. 17d). This large vein is interpreted to be of the same set as the most prominent veins at Locality 2a (but in this case strikes north-northeast). There are three minor vein sets associated with this vein, indicating a dextral and reverse-slip component of shear along the main vein. Using the P–T dihedra, the stress direction resolves as northeast–southwest compression (Fig. 16). This local variation in the stress field is due to a strike change of the greenstone–trondhjemite contact and the establishment of a restraining jog along the trondhjemite contact (Fig. 18). This feature is analogous to the north-northwest – south-southeast compression observed along some structures related to the regional sinistral strike-slip event. That is, the resolved stress field at a location may be influenced more by the fault orientation than the regional stress direction.

To the north (down the ramp), the wing-crack veins are overprinted by increasingly intense extensional shear zones and vertically flattened folds and crenulations (D_3). In the highest strain domains, the original vein geometry is largely obliterated by the extensional shearing (Fig. 17d inset). Analogies with the high strains at Gwalia are thus drawn. The extension is down to the north and is interpreted to be related to doming from the Raeside Batholith and development of the late basins.

Locality 2c: Late thrust overprinting extension

On the decline leaving the pit, a series of D_3 extensional shears are developed in talc–chlorite schists. These extensional shears are overprinted by D_{4b} thrusts with top-to-the-northwest shear (Fig. 17e,f).

We are staying two nights at Morapoi Station near Kookine. For those that are interested we will hold evening talks in the conference room starting at 8 pm.

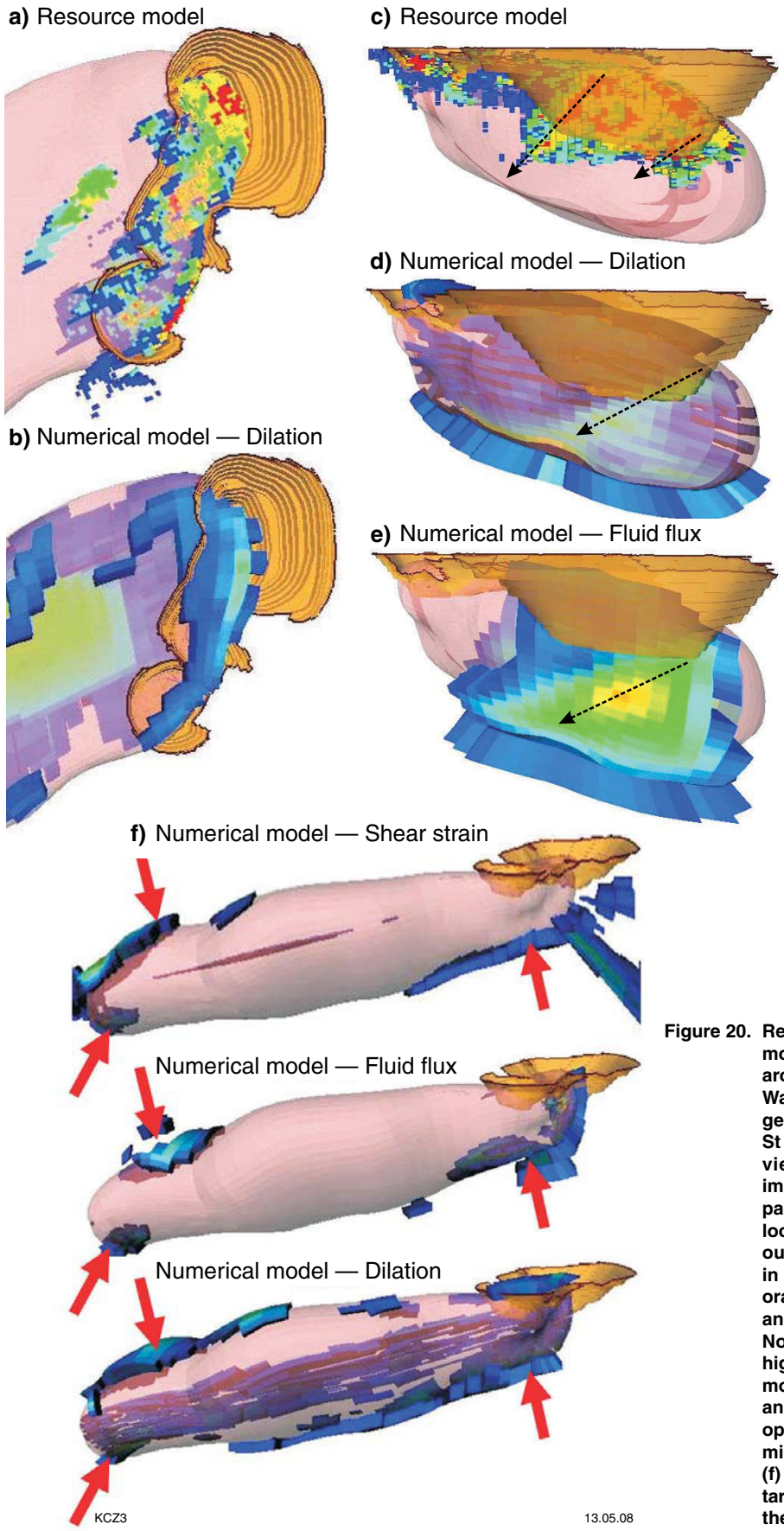

Figure 20. **Results of deformation-driven fluid flow modelling under east–west contraction around the Tarmoola trondhjemite by Warren Potma from the computational geoscience group at CSIRO funded by St Barbara Ltd: a–c) are cross section views looking west; d–e) are plan images with north at the top of the page; f) displays cross section views looking north. Each figure shows the outline of the Tarmoola trondhjemite in pink and the Tarmoola openpit in orange; warm colours in the resource and numerical models indicate highs. Notice the replication of the plunging high-grade ore shoots from the resource model (a) in the numerical model (b–c) and the localization of dilation in the openpit (e) which corresponds to known mineralization in the resource model (d); (f) shows the location of three new gold targets (red arrows) in regions away from the mine**

Excursion localities — Leonora area

Day 2

Locality 3: Sons of Gwalia mine — gold in extension during formation of the late basins (MGA 337665E 6800124N)

Leave Morapoi Station and travel back to Leonora. Veer left just south of Leonora, around Mount Leonora (Locality 4) to the St Barbara Ltd's Gwalia mine main office and we will be escorted in their transport down the openpit to the entrance to the underground portal.

The Sons of Gwalia mine is an excellent example of an extensional shear zone developed in greenstones of the Kalgoorlie Terrane that are exposed as a narrow (<10 km) sliver adjacent to a major granite batholith (Raeside). The granite margin, like the adjacent greenstones, is sheared with extensional kinematics (Williams et al., 1989). The shear zone 'faces' the dominant contractional vector that has been traditionally assigned to 'D_2' (Swager, 1997). In this example, the dominant ductile fabric is an extensional schistosity to mylonite in places, which dips moderately to gently to the east. It is not a contractional 'S_2' fabric, illustrating the contention here that foliation intensity and orientation makes an unreliable marker for correlating structural events.

Sons of Gwalia is the third-largest gold deposit in the Eastern Goldfields Superterrane. It is the southernmost deposit in the Leonora camp (Fig. 15), and is located 3 km south of the township along the Sons of Gwalia shear zone (SGSZ). Parallel shear zones host the other major gold deposits in the camp, namely Tower Hill and Harbour Lights (Figs 15 and 21a). The deposit is hosted in a sequence of tholeiitic pillow basalts and minor interflow sedimentary rocks (Fig. 22a); which are intruded by dolerite sills. The greenstones of the Leonora camp are thought to be older than 2750 Ma, based on a Re–Os age on molybdenite at Tower Hill (Witt, 2001). The Raeside Batholith is a high-Ca granite-dominated batholith with intrusions ranging in age from 2760 ± 4 to 2669 ± 7 Ma (Cassidy, 2006). The youngest of these intrusions display the extensional kinematics observed at the Gwalia deposit and hence date the extension and associated Au mineralization to less than 2670 Ma.

Williams et al. (1989) identified the main tectonic mode in the camp as extensional, with high strains being accommodated along east-dipping shear zones that juxtaposed amphibolite- and greenschist-facies rocks. Using P–T estimates of rocks in a deep diamond drillhole through the Gwalia shear zone, Williams and Currie (1993) estimated around 3 kb of pressure and greater than 200°C temperature differences (extensional excision) had occurred across this shear zone. Work by Blewett and Czarnota (2007b) also confirmed that the dominant tectonic mode was extensional ductile shearing with downthrows towards the east for the entire camp district.

The Gwalia orebody (three vertically stacked en echelon lenses) lies within the pervasive S_3 foliation in a chlorite–sericite schist with numerous quartz–carbonate veinlets (Coates, 1993) and plunges within the SGSZ down to the southeast, parallel to the stretching lineation (Fig. 21a). The extreme linear-aspect ratio of the orebodies and the parallelism of the stretching lineation indicates that extension was the principal control on the formation of this gold deposit.

Locality 3a: View north of the Sons of Gwalia openpit

Views to the north show the main fabric elements consisting of the stratigraphy, lodes, and pervasive foliation, all of which dip around 35° to the east (Fig. 23a,b). The western lode is exposed just west of the portal and the main lode is characterized as a distinct bleached and brown layer east of the portal, halfway towards the eastern edge of the pit.

The dip of the pervasive fabric is consistent with the dip of reflectors imaged on the east–west NY1 seismic line across the Sons of Gwalia deposit (Fig. 23d). The strong reflectors define a 5 km-wide zone parallel to the Raeside granite batholith margin. Through extrapolation of the kinematics from the Sons of Gwalia line of deposits we infer this zone to be a 5 km-wide extensional shear zone. This interpretation is consistent with the geometry outline in the seismic data. In the hangingwall to this shear zone, the youngest part of the Yilgarn Craton stratigraphy (late basin) is preserved, consistent with extensional tectonics (Fig. 23c). A similar relationship occurs with respect to the Pig Well late basin, although the granite batholith controlling the localization of the shear zone does not outcrop but is imaged at 3 km depth. The reflectors related to the SGSZ roll into a detachment above a granite dome displaying an open concave geometry consistent with development in an extensional tectonic mode (Fig. 23d). Compare this seismic section with the cartoon sketch of core complexes (Fig. 9).

Locality 3b: Extensional kinematics of the Sons of Gwalia shear zone

The SGSZ is expressed as a pervasive foliation (D_3) within the pit (Fig. 22a–f). The pervasive fabric overprints an earlier set of quartz veins and foliation that appear locally to be early reverse shear veins (Fig. 22b,f). These veins may represent evidence for an earlier phase of contraction before the dominant extensional fabric-forming event (cf. Tarmoola). While most asymmetric folds indicate extensional tectonics, some folded veins have conflicting senses of vergence, indicating that the axial-plane foliation contains a strong flattening component of strain. These folded veins are likely to be the result of the particular angle between one conjugate vein set and the later extensional shearing (Fig. 22c). However, some quartz veins appear to have been formed during the extensional

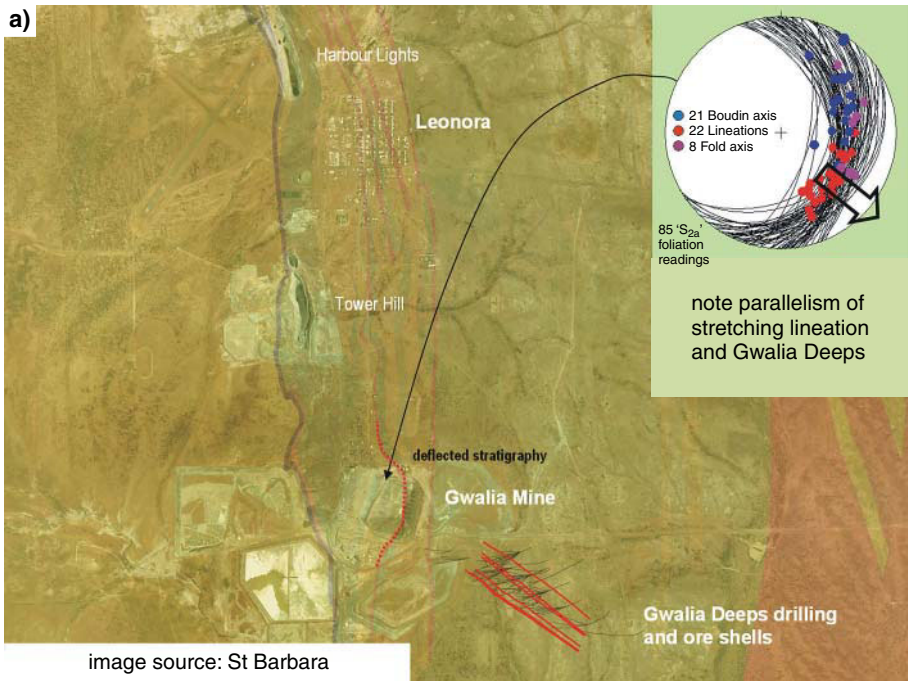

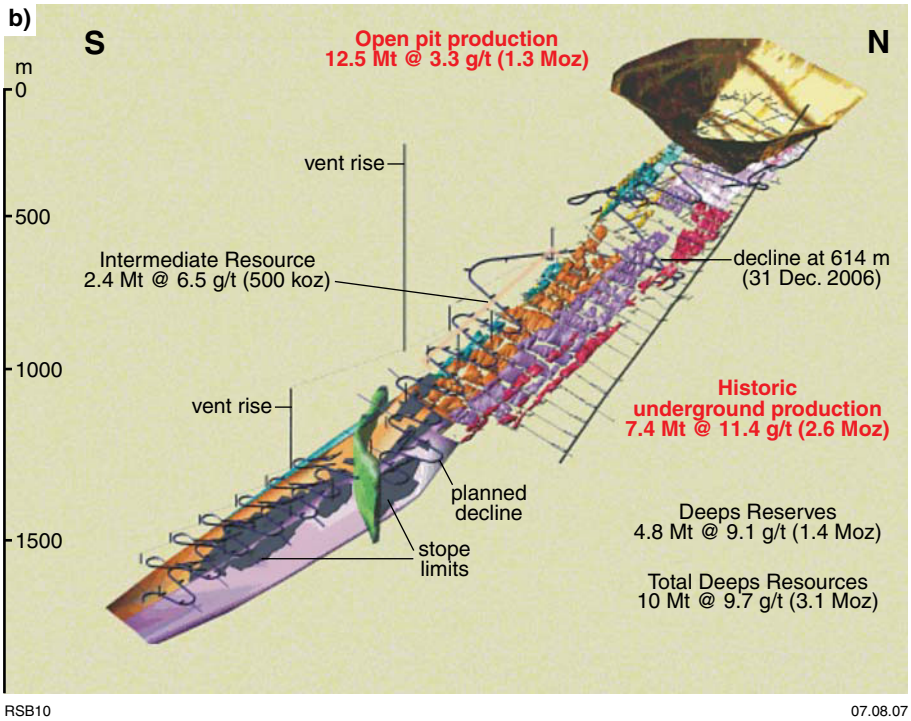

Figure 21. a) Orthophotograph of the Leonora area showing the location of the Gwalia mine and the 'deeps' to the southeast of the openpit and parallel to the stretching lineation (courtesy St Barbara Mines); b) geometry of the Gwalia openpit and associated Gwalia deeps. Note the extremely attenuated aspect ratio of the ore zone, despite the host lithologies and shear zones extending north and south of the mine (courtesy St Barbara Mines)

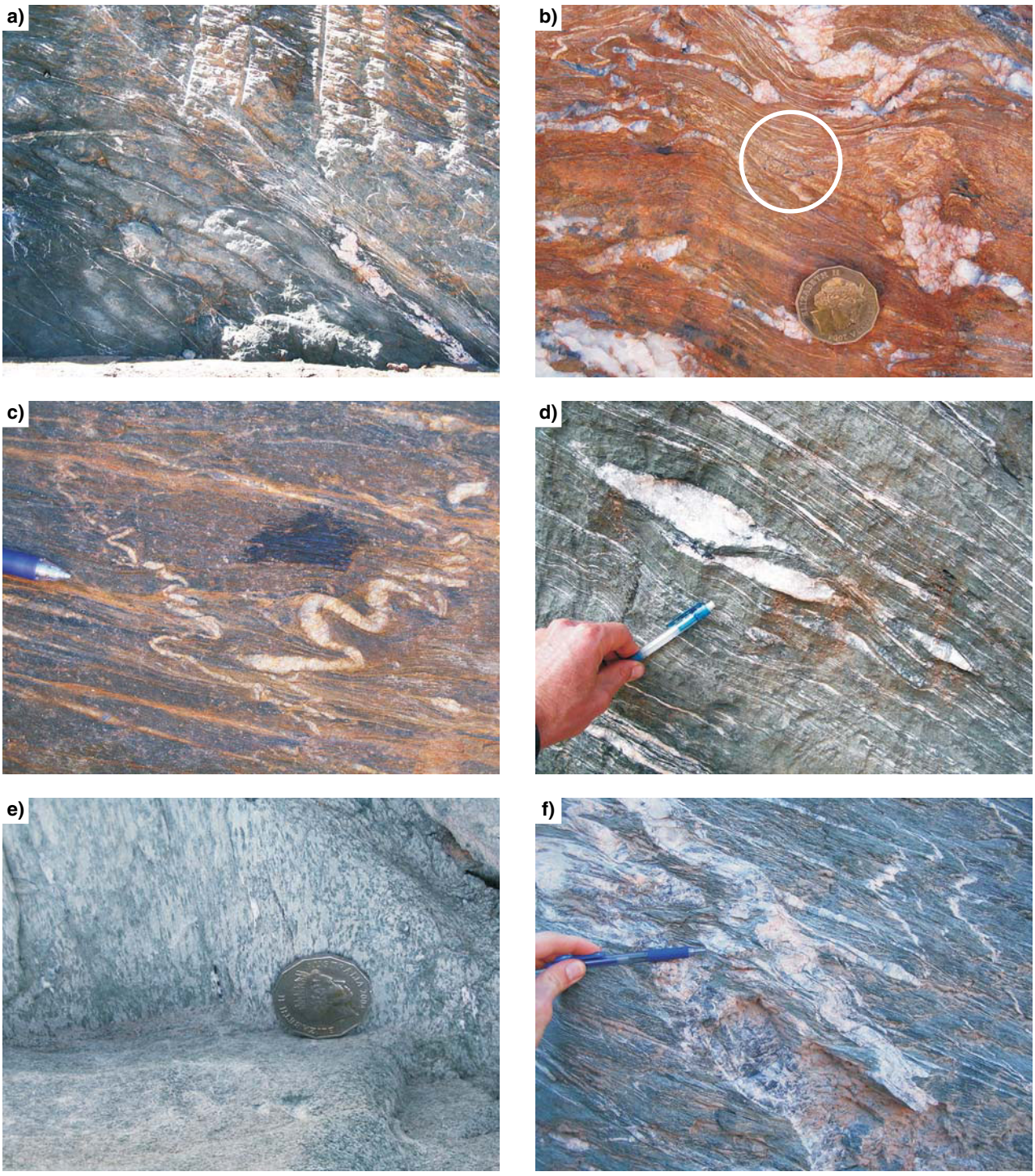

Figure 22. Compilation of photographs from Gwalia openpit: a) Relict pillow lavas showing the basalt stratigraphy is upward facing to the east (view north); b) complex crenulations of early foliation (?$S_{1/2}$ shown in the circle) overprinted by the main S_3 extensional fabric (view north onto wall); c) conjugate veins flattened by a steeply inclined σ_1 (developed during extension) and developing gently dipping axial planes to F_3 folds (view north onto wall); d) S–C–C' extensional fabric elements all showing down-to-the-east and southeast extension (view north onto wall); e) amphibole defining a down-dip stretching lineation (view west); and f) D_3 extensional overprint on earlier veins that may be originally developed during D_2 contraction (e.g. Tarmoola; view north onto wall)

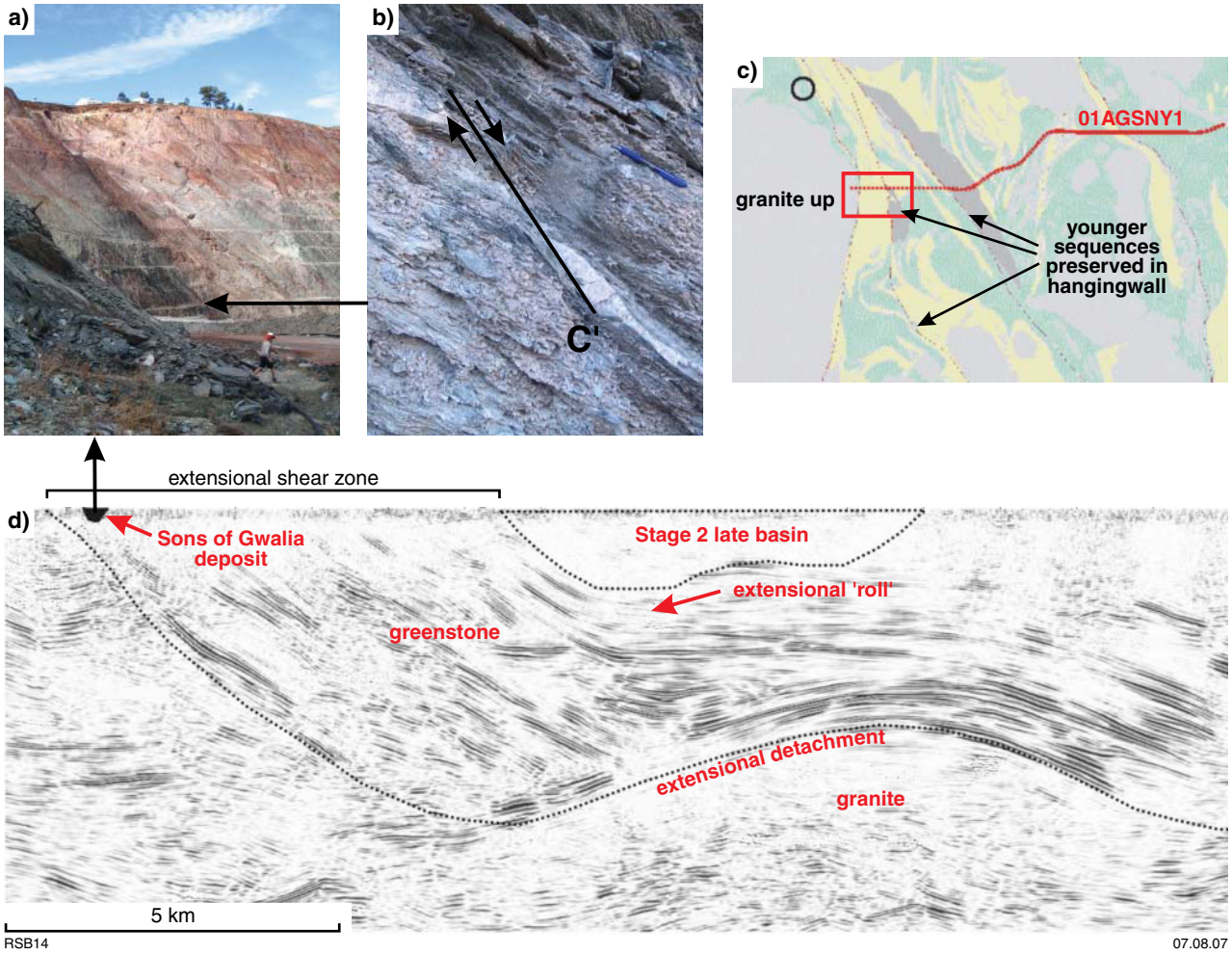

Figure 23. Compilation of extension recorded on a range of scales in the Leonora area: a) note parallelism of the layering (foliation) in the pit (view north) with the seismic events imaged in the section (d); b) extensional C' plane at the mesoscale; c) map of the seismic line crossing major faults with the youngest sequences (late basins) in the hangingwall; d) east–west seismic line through the Gwalia pit vicinity to around 6 km depth shows extensional S–C and C' planes in the events at this scale. These intense bands of reflectivity (shearing) are up to 5 km wide and roll onto a granite dome at depth. This rolling of the fabric onto a detachment is consistent with extension (see Fig. 8 for an analogue)

fabric-forming event. These veins are less deformed and cut the foliation, but have asymmetric folds with axial planes parallel to the main foliation, consistent with down-to-the-east normal kinematics (Fig. 24b).

Across the pit, the L_3 boudins and fold axes rotate towards the stretching lineation, suggesting a tendency towards sheath-like folding related to normal down-to-the-southeast shearing along high-strain zones (Fig. 21a). While the spread of fold-axis orientations may be a function of the original vein orientation, the spread of boudin neck lineations suggests strong transposition into the 'a' or shear direction (Fig. 21a).

Consistent S–C and C' planes at a range of scales and most asymmetric folds indicate extensional tectonics. A large-scale extensional C' plane is evident in the northwest corner of the pit, west of the portal entry (Fig. 24a). In rare outcrops the main shearing fabric (S_3) also hosts a crenulation in the microlithons between the phyllosilicate domains, implying a likely earlier phase of deformation (Fig. 22b).

Sets of white carbonate veins, many conjugate with northwest and southeast dips, are locally cut by related brittle sinistral-reverse faults that dip steeply to the northwest (Fig. 24c). These structures are assigned to D_{4b} and the resolved shortening direction (σ_1) associated with this event is approximately east–west (east-southeast – west-northwest) compression. An example of this set of veins is evident at the northern end of the western wall. The last event observed in the pit are east-northeasterly striking sinistral faults associated with carbonate veining. These are brittle faults associated with D_5 approximate northeast–southwest compression (Figs 24c and 25).

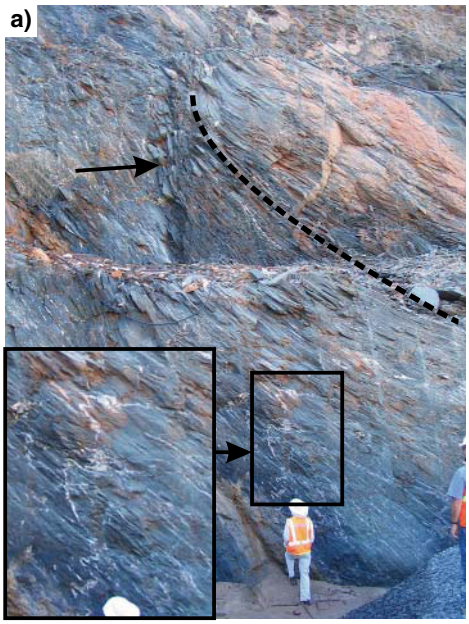

Figure 24. Compilation of photographs from Gwalia openpit: a) steep C' extensional shear planes developed over a limited vertical height (see arrow). Their depth extent may be related to the rheology contrast and thickness of layers being extended and boudinaged (view north); b) quartz veins overprint the main S_3 extension foliation and are dragged and offset by ongoing progressive D_3 extension (view north); and c) S_3 foliation cut by later D_4 veins which are cut by a D_{4b} sinistral reverse fault. View west-southwest of a moderately inclined surface

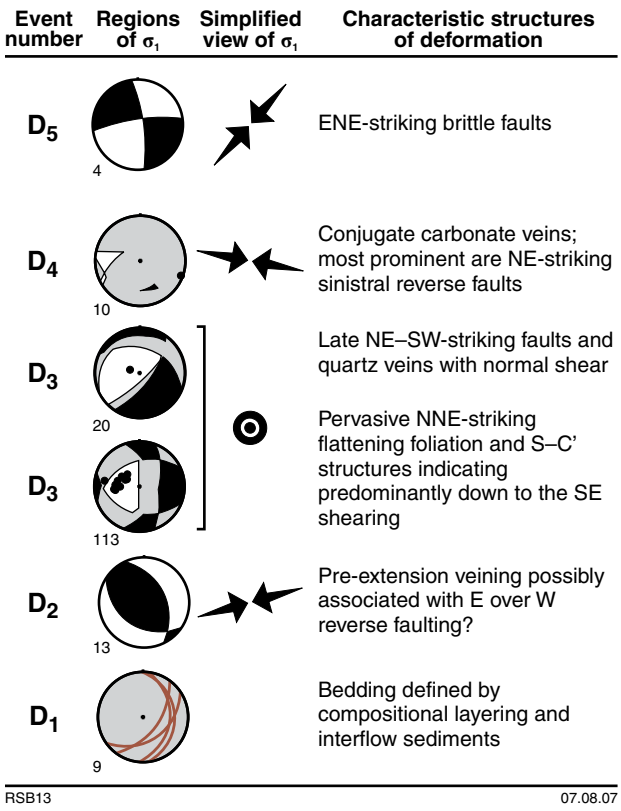

Figure 25. Stereographic compilation of structural elements in the Gwalia pit. Note the dominant fabric elements developed during D_3 extension

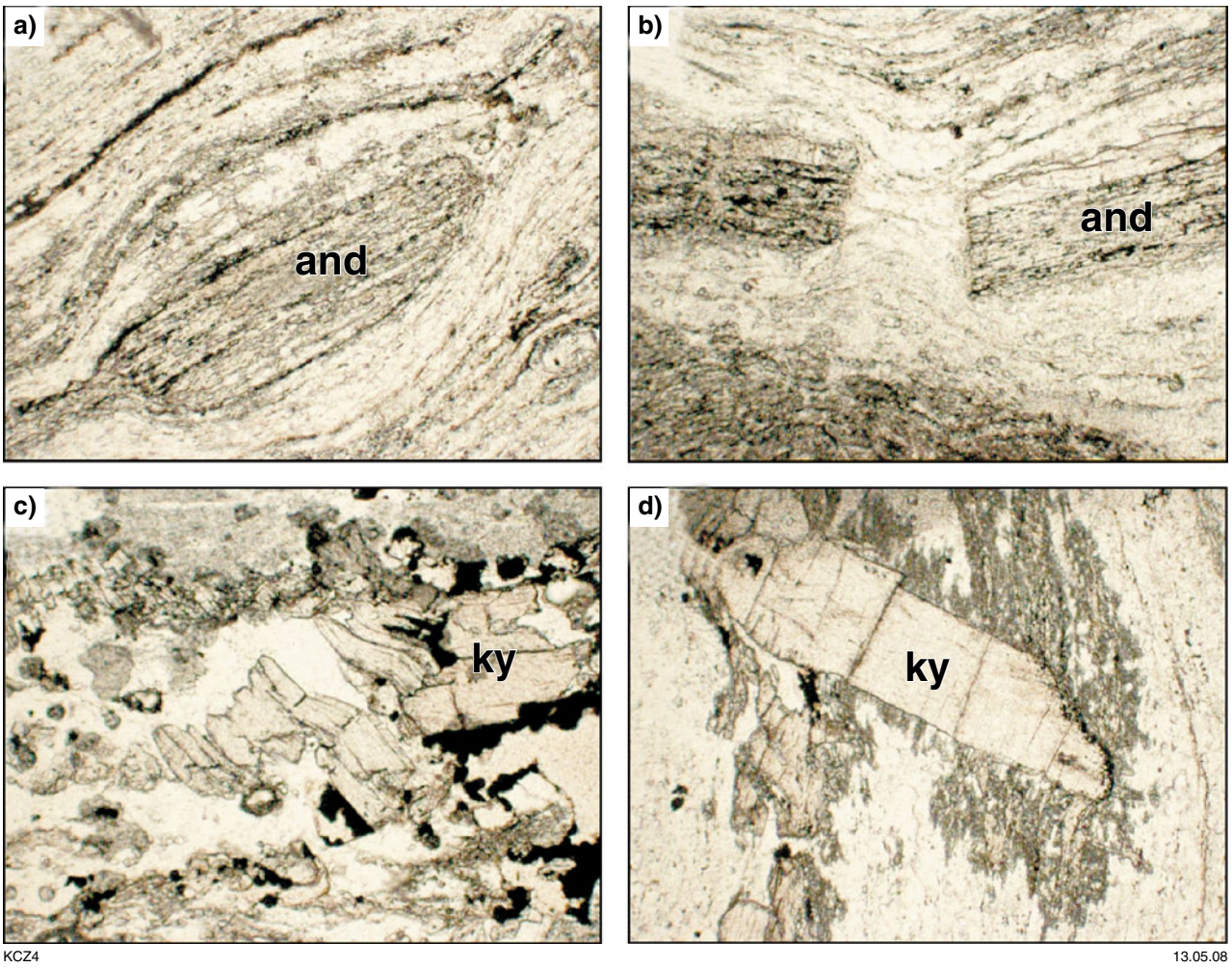

Figure 26. Sample Y242: a) early enveloped andalusite (×2.5 ppl); b) boudinaged andalusite (×2.5 ppl); c) kinked kyanite (×6.3 ppl); d) early skeletal andalusite over-printed by kyanite, or alternatively late skeletal andalusite growth on post-kinematic kyanite (×6.3 ppl)

Locality 4: Kyanite Hill — extensional M_{3a} metamorphism (MGA 338070E 6801592N)

Travel back to the highway from the Gwalia deposit and head about 2 km south of Leonora. The field locality is on the edge of the hill on the west side of the highway.

Kyanite Hill petrology

Kyanite–andalusite aluminous schist from the Gindalbie Domain has a strongly foliated matrix assemblage consisting of quartz aggregate ribbons – graphite – skeletal andalusite–skeletal kyanite(–muscovite). Andalusite occurs as synkinematic poikiloblastic and as skeletal masses containing inclusion trails aligned with the foliation (Fig. 26a). The early andalusite poikiloblasts are boudinaged and flattened leading to being enveloped by the foliation as a result of ongoing progressive deformation (Fig. 26b). Late-stage ?sillimanite forms within the foliation. In sample Y242b, post-kinematic kyanite laths grow across the foliation at high angles (Fig. 26d). Some kyanite grains are kinked during late-stage flattening across the foliation (Fig. 26c). Retrogressive muscovite forms on kyanite margins. Skeletal andalusite grows out from kyanite margins, growing preferentially along foliation planes (Fig. 26d). Sequence of mineral growth is from quartz–graphite–muscovite1 matrix foliation parageneses to rare sillimanite growth followed by kyanite growth and finally late-stage muscovite2 and andalusite2 growth. These relations indicate an anticlockwise turn around the alumino-silicate triple junction (Fig. 27). The main foliation also contains later stage sillimanite growth and is overprinted by post-kinematic kyanite laths, indicating burial with heating through the peak of metamorphism. Kyanite laths are partially enveloped by late-stage andalusite beards, indicating post-peak decompression with cooling back into the andalusite field.

M_{3a} metamorphic conditions

Post-volcanic turbiditic basins (PVTB), such as the Mount Belches Formation, are diagnostic of extensional rift settings and offer constraints on the thermo-barometric evolution at 2665–2650 Ma (Fig. 28). Peak metamorphism was at 500–

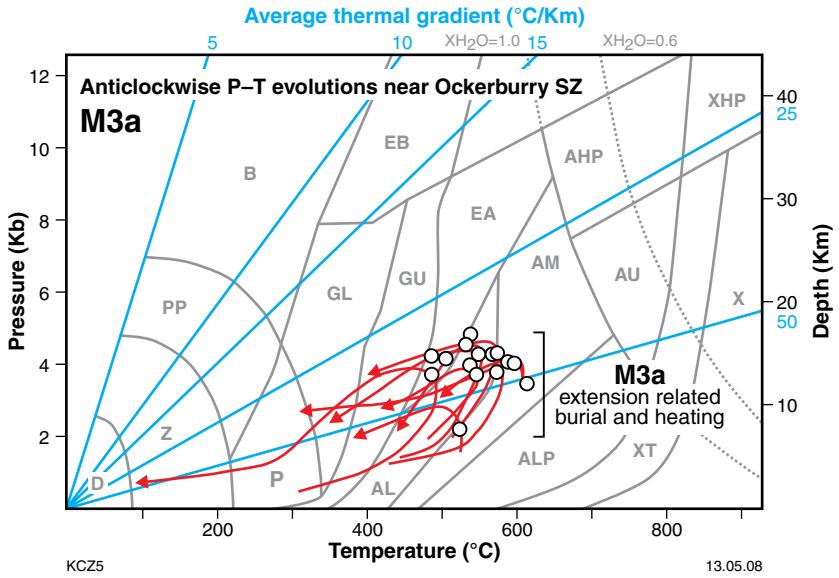

Figure 27. Peak pressure–temperature (P–T) loci and P–T evolutions from samples with anticlockwise P–T evolutions in the vicinity of the Ockerburry Shear Zone

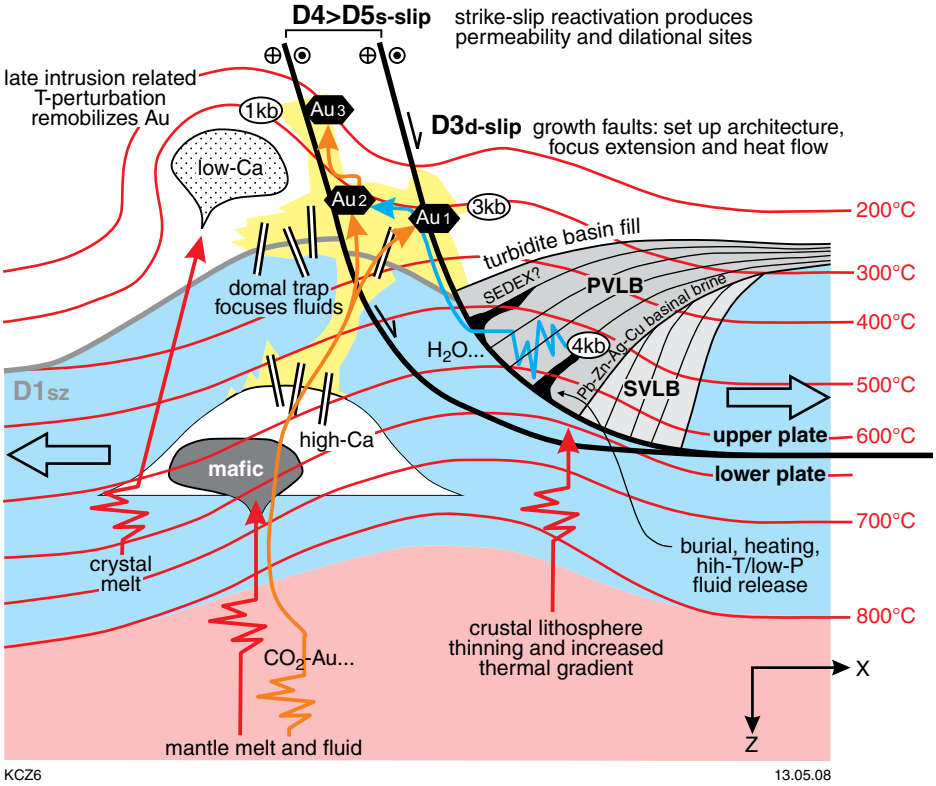

Figure 28. Model for M_{3a} lithospheric extension at c. 2665–2650 Ma, and the consequent outcomes of: post-volcanic late basin rifts; listric growth fault architecture; input of mantle components into the shallow crust such as mafic granites and CO_2-metal-rich fluid; M_{3a} post-kinematic thermal perturbation resulting in low-Ca crustal melting; H_2O-rich fluid release and fluid driving and ultimately resulting in fluid mixing and primary gold mineralization. A lagging effect is later phases of Au-mineralization, by remobilization during successive M_{3b} thermal perturbations associated with low-Ca crustal melts and suitable mineralization sites by strike-slip reactivation of structures. Green circle is relative site of Kyanite Hill

580°C and 4 ± 1 kb, indicating a high temperature:depth ratio of 40–50°C/km. Post-kinematic porphyroblasts indicate that peak metamorphism accompanied a static stress regime, subsequent to formation of an early burial, bedding-parallel mica foliation. P–T paths follow anticlockwise loops of heating with burial, followed by near-isobaric cooling paths (Fig. 29). Recognition of a post-2665 Ma high-heat flow thermal anomaly accompanying turbiditic basinal infill has implications for driving basinal brine circulation and release of large volumes of hydrous fluid by both dewatering and dehydration reactions (Fig. 28). Anticlockwise P–T paths though peak conditions of about 570°C and 3.2 – 4.0 kb are also documented from a number of sites outside the PVTB's, within the underlying stratigraphy (Fig. 29). All are distributed along a narrow zone within and close (<5 km) to the Ockerburry shear zone (Fig. 29). The main sites are Kyanite Hill at Leonora, New Celebration Mine (Hodge, 2007), Gordon Mine and Mount Martin, linking with the Mount Belches basin and defining a linear domain of 360 km length. At present, all correlated M_{3a} parageneses have only been identified in association with the Ockerburry shear zone, indicating that this structure was the dominant crustal structure accommodating M_{3a} lithospheric extension in the east Yilgarn Craton. Other M_{3a} high heat flow domains of rifted upper-plate settings are inferred (Fig. 30).

M_{3a} tectonic setting

A model for the crustal architecture during M_{3a} lithospheric extension and metamorphism is presented in Figure 3 that summarizes all barometric, thermal, magmatic, and fluid consequences of lithospheric extension. The structural architecture developed by lithospheric extension produces upward transport by domal culminations in the lower plate and downward transport by depositional basins in the upper plate, separated by low-angle extensional shear zones or growth faults (Fig. 28). The flanks of lower-plate domes may be recognized by exhumed high-P M_1 parageneses and old stratigraphy (>2750 Ma). The domal cores may be recognized by high proportions of late low-Ca granites triggered in part by decompressional melting of an exhuming lowerplate, in association with the M_{3a} thermal anomaly (Fig. 28). The upper-plate domain accommodated lithospheric extension and subsidence and focused the high-heat flow, and will be recognized by post-volcanic turbiditic rift basins, mantle-sourced syenite and mafic granites and rifts bound by growth faults (Fig. 28). Deep seismic profiles indicate that most crustal structures have listric form and are inclined to the east (Goleby et al., 1993, 2002). These pre-existing structures include growth faults associated with synvolcanic clastic basins, and their reactivation lead to development of PVTB depositional troughs (Fig. 1). The PVTB troughs are sited at zones of maximum lithospheric extension during M_{3a} and will approximately coincide with the zone of highest geothermal gradients and heat flow. The form of the domains of high heat flow and rifting is anticipated to be relatively narrow and elongate, arcuate to curvi-linear zones interspersed by wide lower-plate domains of doming (Fig. 30). M_{3a} extension started after cessation of downgoing subduction and, consequently, it is possible that gravity-driven slab rollback induced lithospheric extension of the east Yilgarn Craton during M_{3a}.

Locality 5: Mertondale — gold in sinistral transpression (MGA 357972E 6828340N)

Travel back north to Leonora. Leave Leonora at the north end of town and drive 31 km along the Nambi road. As you approach the Mertondale area there is an old chimney on the right. Turn right onto the mine's access road and take the left fork at 400 m. This road swings south and then east around the Mertondale 3 and 4 pit. The main decline into the Mertondale 3 and 4 pit is from the northeast.

The purpose of visiting the Mertondale pit is to demonstrate the regional superposition pattern of north-northwesterly striking reverse and sinistral transpressional shear zones overprinted by north-striking dextral transtensional faults. Gold at Mertondale is associated with sinistral transpression localized on the edges of the central porphyry intrusion.

The Mertondale group of gold deposits is located 30 km northeast of Leonora (Fig. 31). Mineralization is localized along high-strain shears at basalt–porphyry contacts in the north–south-striking Mertondale 3 and 4 pit and along low-strain shear zones within the east–west-striking Mertondale 2 pit (Nisbet and Williams, 1990). The deposits are located along the Mertondale shear zone, a large north–south splay of the north-northwesterly trending Keith–Kilkenny shear zone to the south.

Gold is associated with quartz, carbonate, and silicic alteration. Nisbet and Hammond (1989) and Nisbet (1991) recognized that the area has been affected by two major deformations, each related to gold. They described an early sinistral shearing event followed by a dextral shearing event on north-northwesterly striking faults. This study supports this result while demonstrating a greater level of complexity in the structural history.

The structural stratigraphy of the Mertondale group of pits comprises up to five events (Fig. 32). The earliest structural element preserved is an upright foliation within low-strain microlithons of the pervasive north–south-striking foliation. It is unclear as to whether this remnant fabric represents an early deformation or if it is part of the progressive deformation history associated with the development of the penetrative foliation.

The second structural element at Mertondale is expressed as foliation-parallel quartz veins, which are boudinaged within the pervasive foliation. The timing of these veins is restricted to pre- to syn-main S_{4a} fabric formation (Fig. 32).

The dominant structural feature of the Mertondale deposit is the D_{4a} north–south-striking pervasive foliation. This foliation is associated with reverse-shear sense kinematic indicators (Fig. 33a,b) and rare downdip stretching lineations. The inferred stress vector for the formation of this foliation is east–west contraction (Fig. 32).

The pervasive reverse-sense shear fabric is overprinted by a sinistral strike-slip shear zone localized on the edge of the central porphyry (Fig. 33c). The porphyry

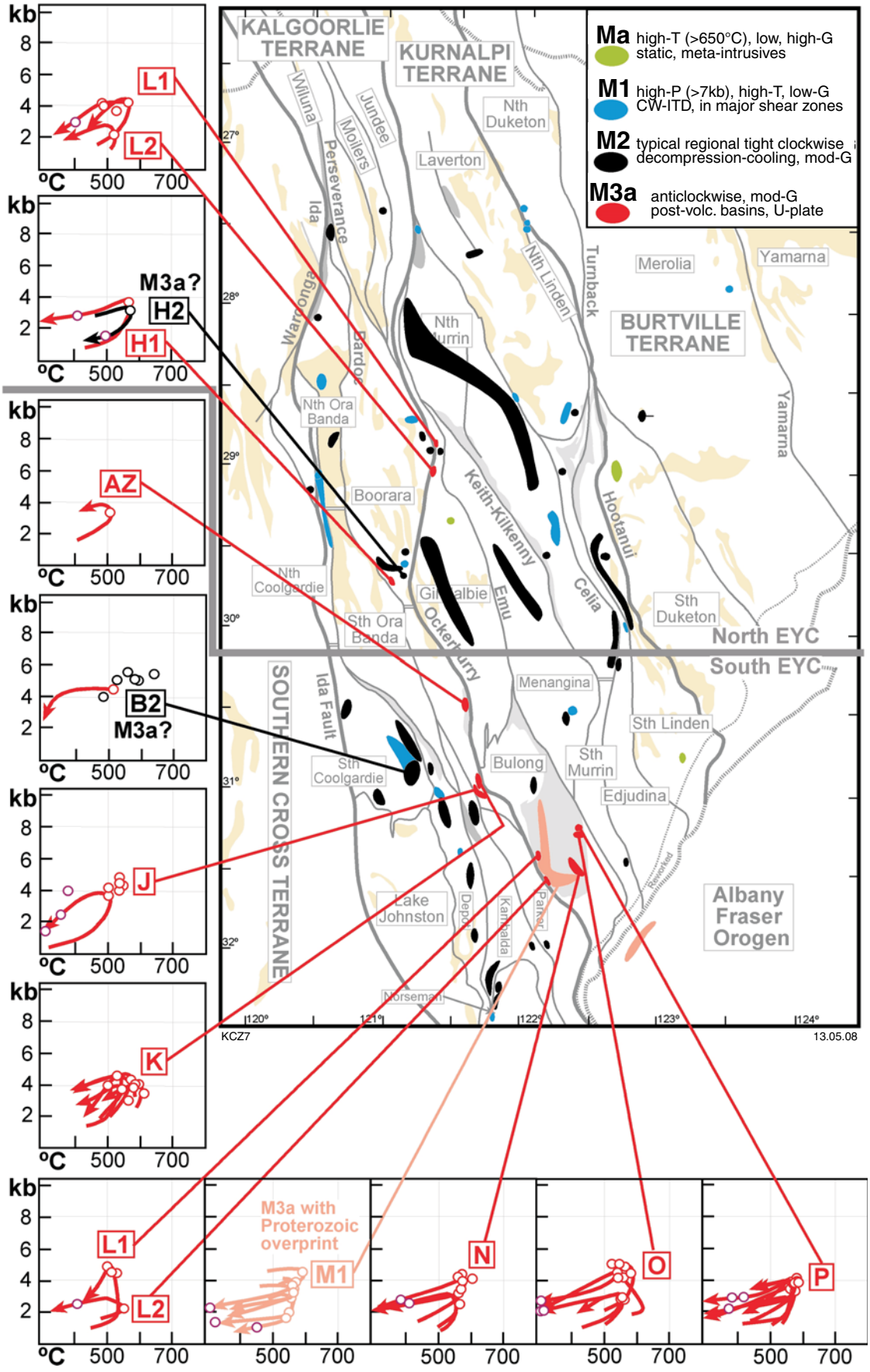

Figure 29. Integration of the interpreted M_{3a} P–T evolutions with the results of metamorphic domain analysis outlining regions that experienced common metamorphic histories. Green circle is site of Kyanite Hill

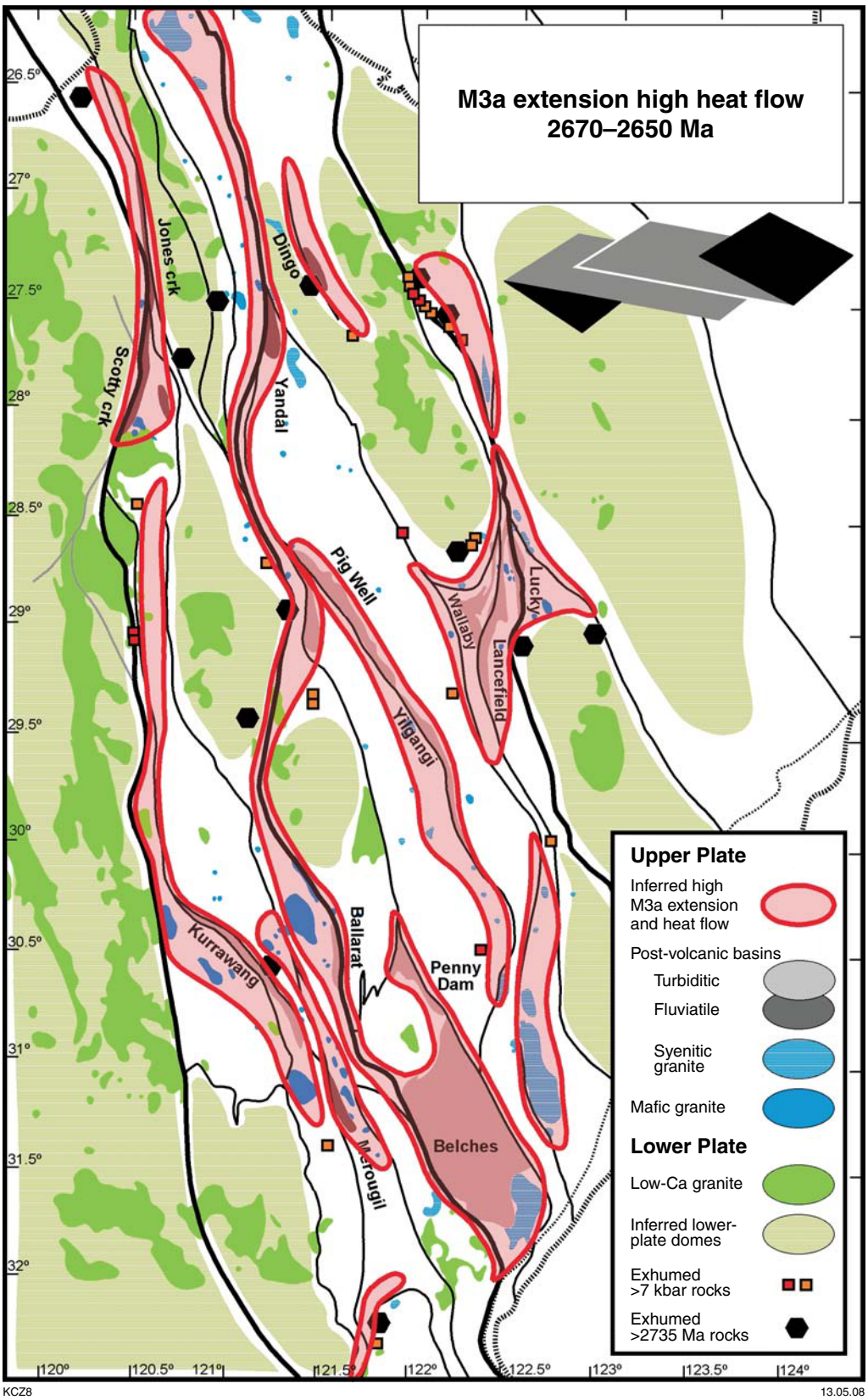

Figure 30. Inferred distribution of the effects of M_3 lithospheric extension and distribution of possible lower-plate domes (blue) versus upper-plate highly extended and high-heat flow domains (red). Flanks of lower-plate domes are indicated by exhumed old stratigraphy (hexagons) and high-P M_1 parageneses (squares). Cores of lower-plate domes loosely coincide with low-Ca granites (green). Upper-plate domains of high extension coincide with post-volcanic late basins (grey) and mafic and syenitic granites (dark blue) and define hypothetical zones of high M_3 heat flow (red outline)

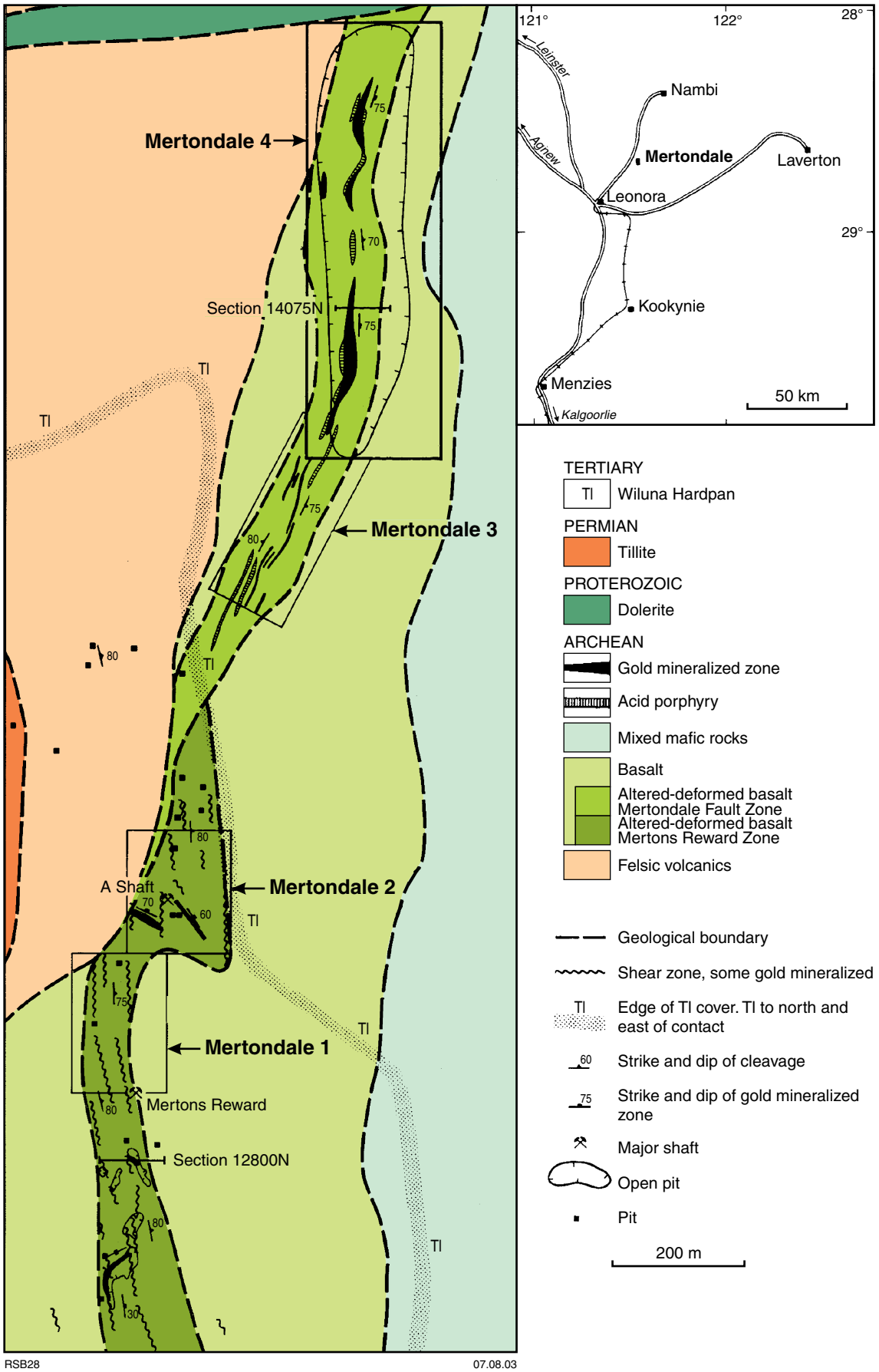

Figure 31. Location map and geology of the Mertondale line of deposits (after Nisbet and Williams, 1990)

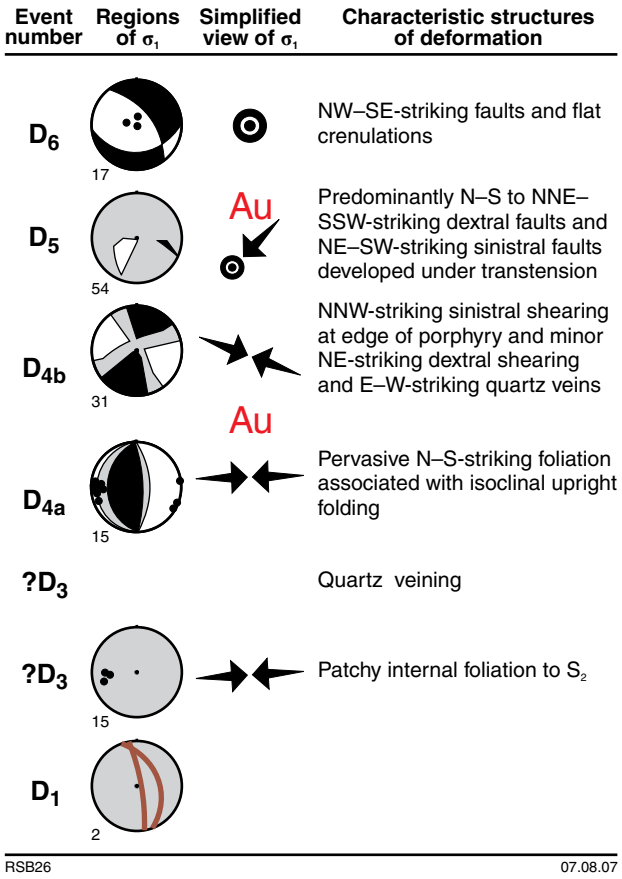

Figure 32. Compilation of structural elements from Mertondale

is inferred to have intruded parallel to the S_{4a} pervasive foliation. Sinistral strike-slip shearing during the D_{4b} phase was the result of a clockwise rotation of σ_1 from east-northeast – west-southwest to east-southeast – west-northwesterly directed shortening and a switch in the other principal stresses σ_2 and σ_3, (similar to the history at Yunndaga at Locality 1). An example of the sinistral strike-slip shear zone can be observed in the pavement halfway down the decline.

Overprinting the reverse-sense shear pervasive foliation and the sinistral strike-slip shear zone are brittle, predominantly north–south-striking, dextral strike-slip (transtensional) faults. These faults are associated with quartz–carbonate veining along the fault planes (Fig. 33d,f) and northwest–southeasterly striking crenulations of the S_4 fabric (Fig. 33e). P–T dihedra analysis of the brittle dextral strike-slip faults indicates σ_1 was inclined to the southwest during this event (Fig. 32), indicating a transtensional mode of deformation. Excellent examples of the dextral strike-slip faults can be observed along the western wall of the pit. This dextral D_5 event in the Mertondale group of pits probably correlates with the main gold events and dextral shearing in the Nambi and Mount Redcliffe pits along strike to the north (Blewett and Czarnota, 2007b).

The dextral strike-slip faults are overprinted by D_6 normal faults and horizontal foliations associated with extension (Fig. 32).

Locality 6: Victor Well — dextral shear and gold (MGA 331455E 6811653N)

From Leonora travel north until you reach a large Y intersection. Take the right fork and travel 800 m north and turn left (west) onto a dirt track for 400 m. At the crossroads of two tracks turn left (south) for 1 km and turn left (east) for 300 m to the locality.

Danger: OPEN SHAFTS are present in the immediate vicinity.

Victor Well is an example of north-northeasterly trending, ductile, dextral strike-slip shear zones that host gold and overprints and earlier west-northwest striking extensional shear fabric. The exposure demonstrates the highly partitioned nature of the dextral event as it is only developed over a few metres in width and is absent at the margins of this pit. The foliation could be interpreted as a typical 'S_2' fabric, but kinematically is different to that seen at Yunndaga (sinistral) and Gwalia (normal).

Victor Well is a small pit 3–4 m deep and 25 m long, located 17 km north-northwest of Leonora (Fig. 15). Gold is hosted in a pyritic quartz vein within a north–northeast-striking dextral shear zone that crosscuts the regional east–west-trending fabric and lithology (basalt and porphyry) observed in the walls of the pit. The first penetrative fabric is extensional and overprints the porphyry and basaltic host rock. It is interpreted that this north-dipping fabric represents the regional D_3 extensional foliation that wraps around the Raeside Batholith and is exposed at the nearby Sons of Gwalia and Tarmoola mines (Fig. 34).

The west–southwest S_3-trending fabric has been rotated into the central D_5 dextral shear zone, which is characterized by a pervasive shear fabric with well-developed S–C foliations (Fig. 34). Crosscutting C' dextral shear bands are also common (see Fig. 34). The stretching lineation plunges gently to the south-southeast. This dextral shearing stage is associated with quartz veins and the gold event, and is interpreted to be related to northeast–southwest regional D_5 contraction (Fig. 34).

The last stage of deformation is recorded by sparsely developed steeply dipping north–south-trending D_5 crenulations.

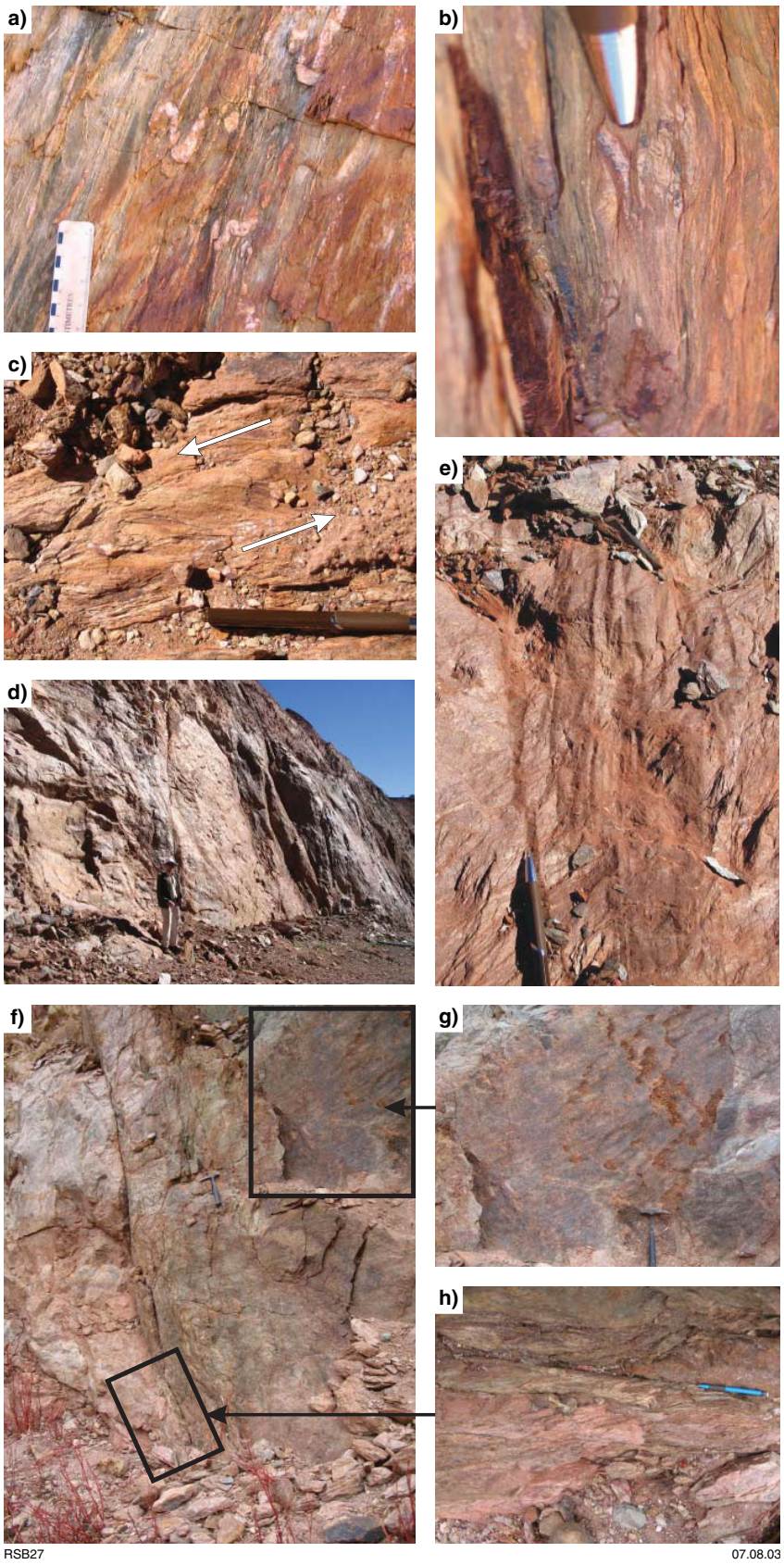

Figure 33. Compilation of photographs from Mertondale:a) view south (onto wall) of down plunge of asymmetric F_{4a} folds consistent with east-over-west reverse faulting and shear; b) view east-northeast (onto pavement) of dextral strike-slip sigma structures associated with D_{4a} approximately east–west shortening; c) view southwest (onto pavement) of D_{4b} sinistral S–C shear zones developed on edge of the porphyry dyke; d) view northwest of D_5 dextral transtensional faults that are common throughout Mertondale; e) D_5 crenulations (view northwest onto wall); and f) D_5 dextral fault dragging a D_{4b} sinistral fault; (g) which cuts the S_{4a} foliation (h), view west of wall

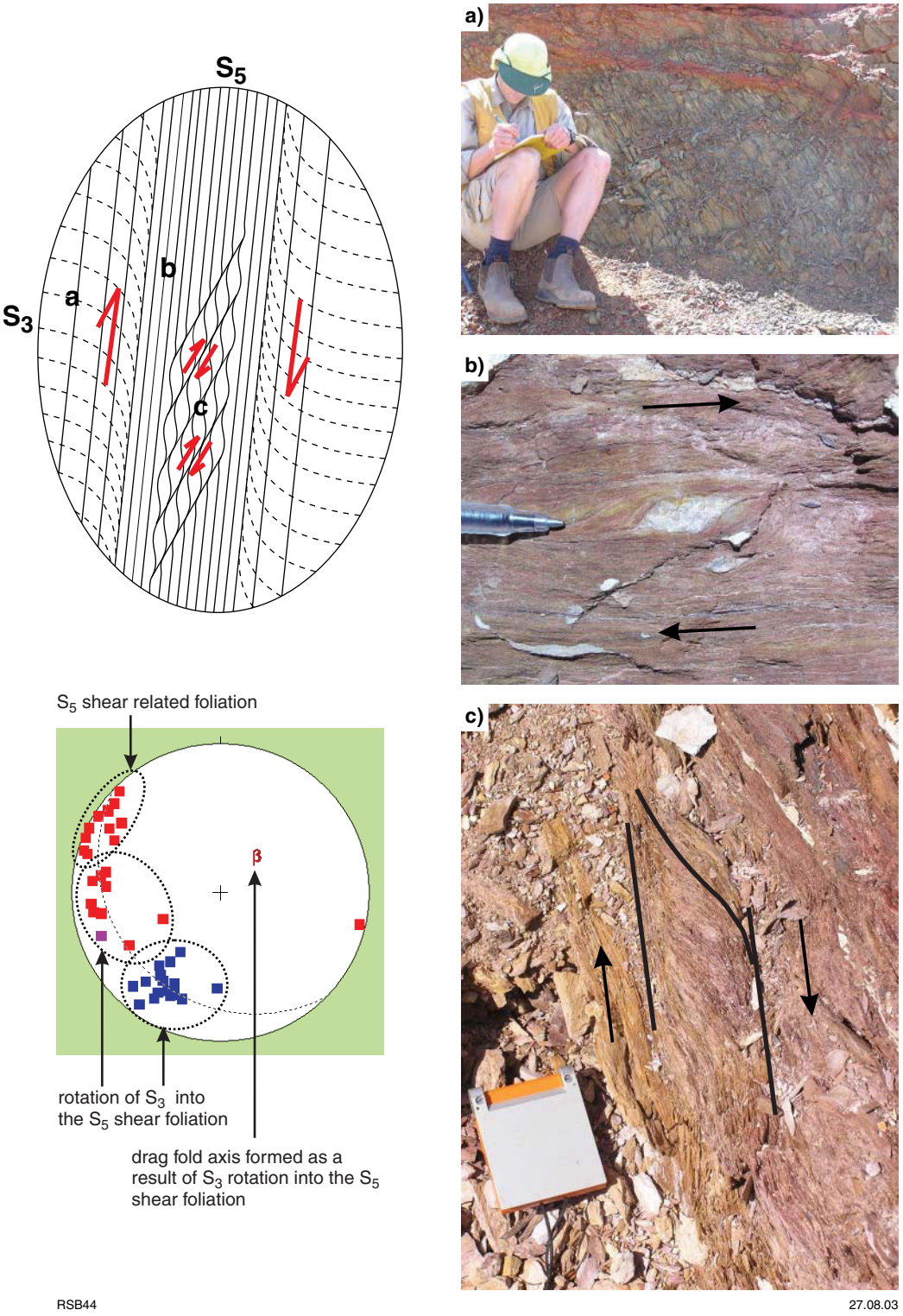

Figure 34. Schematic diagram of Victor Well pit illustrating the rotation of S_3 into the D_5 dextral shear zone and the development of C' planes in the central part of the shear zone. Letters indicate photo locations. Stereographic representation of the schematic diagram showing the rotation of the S_3 fabric into the D_5 dextral shear zone: a) view west of pencil intersection lineation of S_3 and S_5 dextral shear-related foliation; b) view east of dextral stair stepping indicating that S_5 is a shear plane; and c) view south-southwest of dextral C' plane in central dextral shear zone

Excursion localities — Mount Margaret Dome area

Day 3

Locality 7: Westralia — gold in reverse shear zones associated with banded iron-formation (WGS84 409393E 6816838N)

From Leonora travel 66 km along the highway to Laverton and turn right (south) at the sign to the Mount Margaret community. Travel south for 4.5 km and turn left (east) at the T-intersection at Garden Well. Drive along this road for 17 km and follow the signs to the Mount Morgan group of deposits and Westralia.

The purpose of visiting Westralia is to examine the contractional and extensional nature of the steeply dipping dominant foliation as well as the presence of later shallow easterly dipping thrust faults developed during D_2 through to D_5 deformation.

The Westralia pit is the largest in the Mount Morgans district, with a total gold produced of nearly 1 million ounces (Vielricher et al., 1998). The deposit provides a good example of a banded iron-formation (BIF)-related gold deposit, within mineralization occurring within reverse faults localized along reverse-sheared edges of thin steeply northeast-dipping units of BIF and porphyry dykes, in a mainly tholeiitic basaltic sequence (Figs 35 and 36a). Talc–chlorite schists after komatiite occur in the west and lamprophyre dykes are also common in the pit (Beardsmore, 1999). Westralia is close to the Celia Shear Zone (Fig. 2) and it provides a likely proxy for its kinematics. The numerous porphyry and lamprophyre dykes along with units of BIF act as good structural markers for structural analysis.

The structural event history appears complex (Fig. 10). The earliest structural features are preserved as refolded folds and foliations in units of BIF intruded by porphyry dykes (Fig. 36b). This early complex history is attributed to D_2 contraction. The northern part of the pit shows porphyries intruding along a pre-existing foliation and overprinted by D_3 extensional deformation expressed as extensional boudinage of the porphyry dykes (Fig. 36c).

This period of extension is overprinted by renewed east-over-west shearing (D_4) and subsequent normal faults. In turn the reverse faults are overprinted by D_5 north–south-striking dextral strike-slip faults and northeast-over-southwest thrusts (Fig. 36d,e). Late brittle D_6 normal faults occur in more competent units (Fig. 36f), whereas a horizontal crenulation is developed within highly foliated rocks.

Locality 8: Jupiter — syenite-hosted gold (a Wallaby analogue; MGA 423669E 6813053N)

Back out onto the large dirt road and drive east along it until you come to an intersection (signposted Mount Margaret). Turn right towards Mount Margaret and follow this road for 8.5 km and take another right and drive 3.3 km through the Mount Margaret community and turn right onto a small track. Follow this track for 1.1 km and turn right and drive 1.5 km towards the Jupiter mullock heaps. Walk south across the breached causeway towards the lookout at the northwestern side of the deposit.

Jupiter is a spectacular syenite-hosted gold deposit. It is an analogue for the Wallaby deposit and shows the interaction of magmatic and hydrothermal fluids. The central syenite body is comprised of multiple radiating dykes and sills of varying magma composition. The geometry of the syenite dykes illustrates how magma can establish a local stress field (σ_1 vertical) during magma emplacement.

Locality 8a: View southeast of the Jupiter pit

The view to the southeast of the main features of the colourful Jupiter pit (Fig. 37) reveals a radial distribution of syenite dykes into pillow basalt. This radial distribution illustrates how magma over pressure can establish a local stress field during magma emplacement with vertical $\sigma 1$ and equal σ_2 and σ_3. The syenite is also intruded by a quartz–feldspar porphyry dyke. Despite best attempts this syenite has not yielded sufficient zircon to be dated. Regionally these syenites are about 2665 Ma (e.g. Wallaby and Hanns Camp), and it is inferred that the Jupiter Syenite is of equivalent age and was emplaced during the D_3 extension and late basin formation in the region.

The D_3 syenite is cut by northeast-over-southwest D_{4a} shear zones and associated quartz veins. An example of a ductile east-over-west shear is also exposed in the southern wall of the pit. Duuring et al. (2000) identified two such shear zones in the pit, with greatest gold grades centred around these shear zones (Fig. 37).

Locality 8b: Syenite dykes, faults, and alteration up close and personal

Walk to the bottom of the pit.

The greenstones at Jupiter are comprised almost entirely of pillow basalts. The pillow basalts face south and are folded about the Mount Margaret Anticline, although no upright foliation associated with this F_2 folding is observed at Jupiter. Here is a good example of the development of major regional folds (F_2) without foliation development (Fig. 38a). This is despite the site's location at the hinge of the major structure and a region where such a foliation would be expected (see

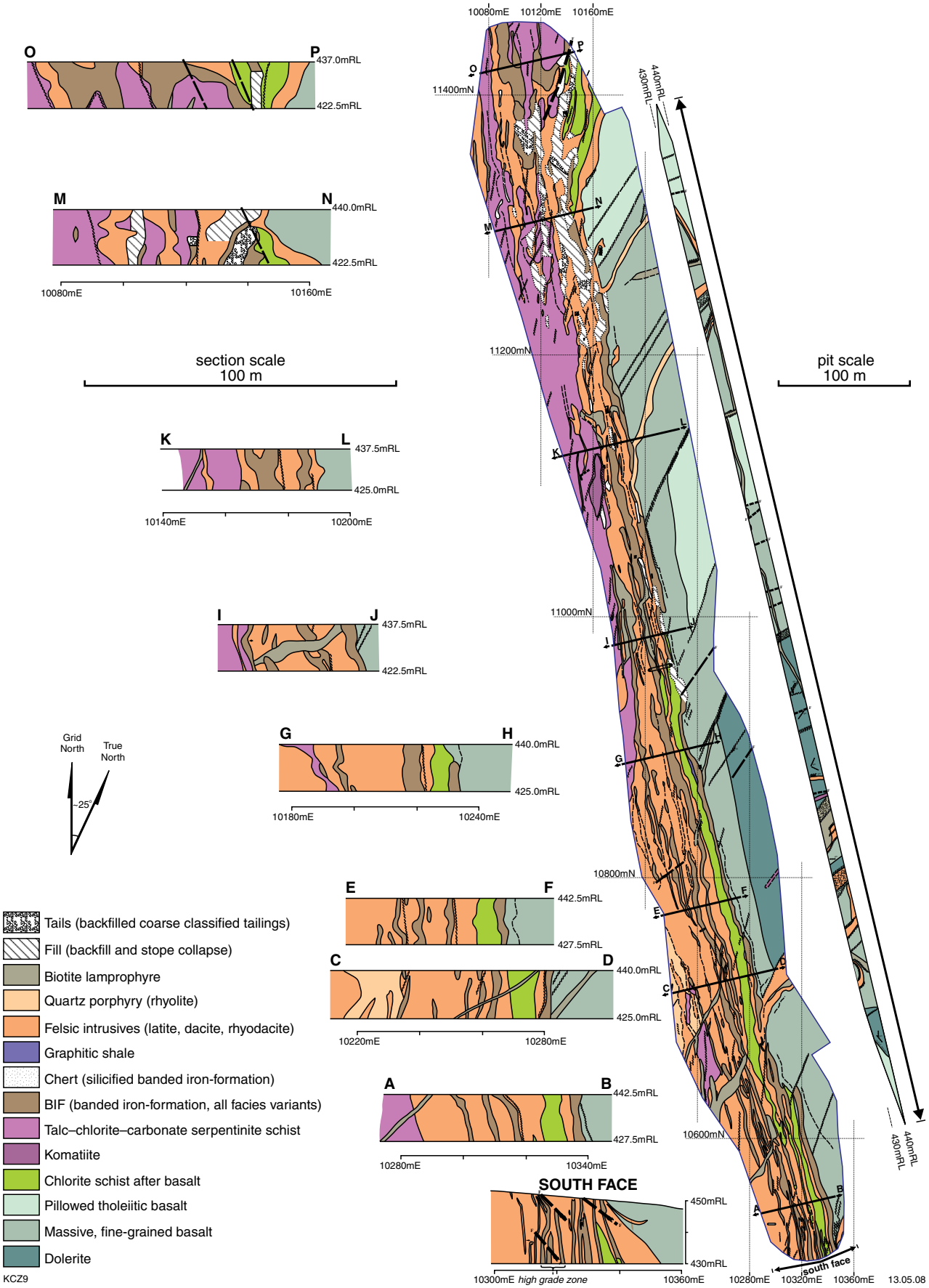

Figure 35. Map and cross sections of the Westralia pit. Interpreted geology simplified from plan28B-Gb3 by Beardsmore (1999) for Homestake Gold of Australia. Map provided courtesy Placer Dome Asia Pacific Ltd

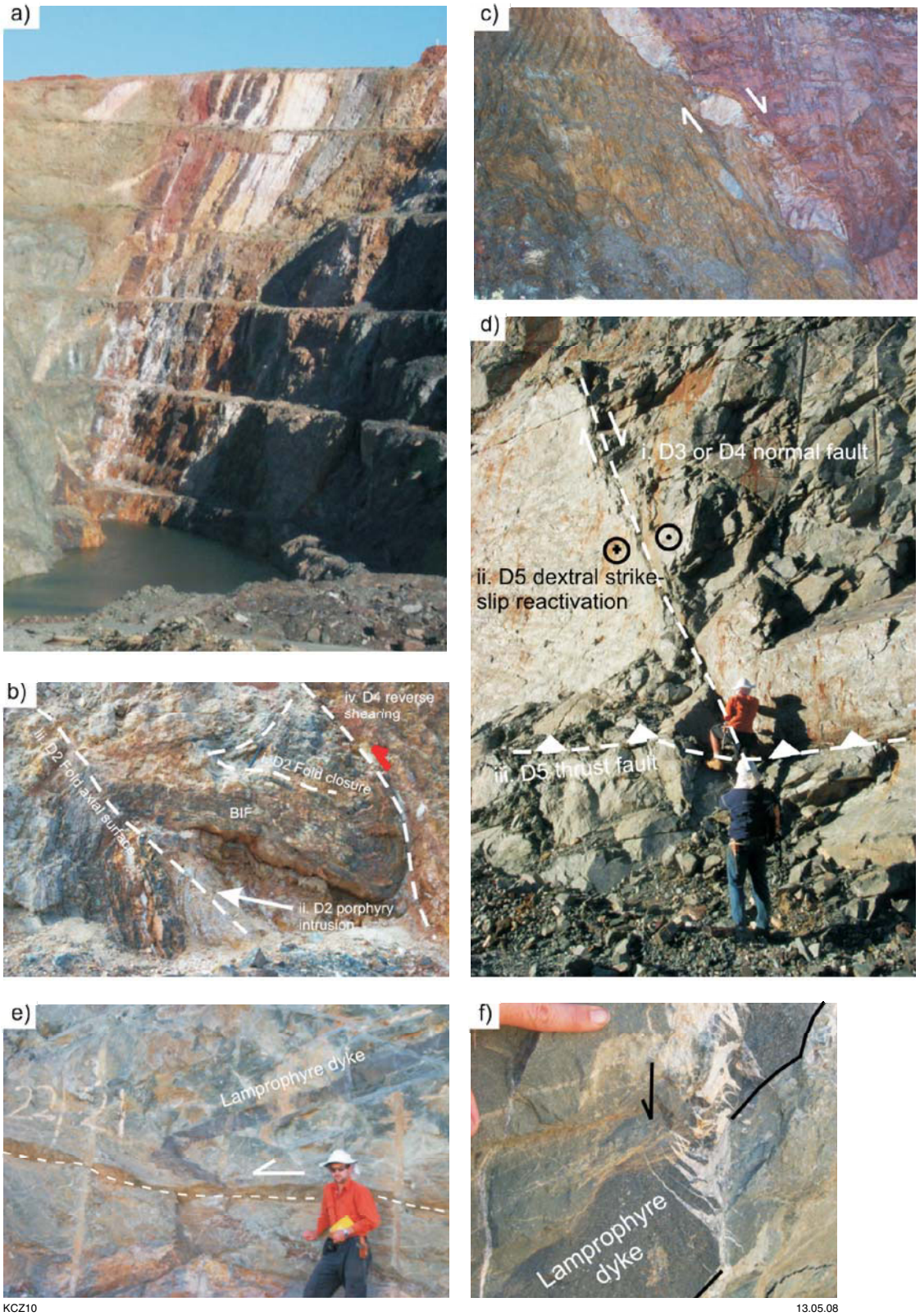

Figure 36. Compilation of photographs from the Westralia pit: a) view south-southeast of steeply east-northeast dipping BIF with bedding-parallel porphyry intrusion at the centre of the Westralia mine; b) view north of D_2 folds intruded by a D_2 porphyry and refolded by a continuation of upright D_2 folding, followed by D_4 reverse east-over-west shearing; c) view north of D_3 normal shearing and porphyry intrusion; d) view north of a steep D_3/D_4 normal fault reactivated during D_5 as a dextral strike slip fault and cut by a later D_5 low-angle northeast-over-southwest reverse shear zone; e) view towards the northeast of a D_5 thrust displacing a lamprophyre dyke; f) view northeast of a late northeast-striking sinistral fault offsetting a lamprophyre dyke

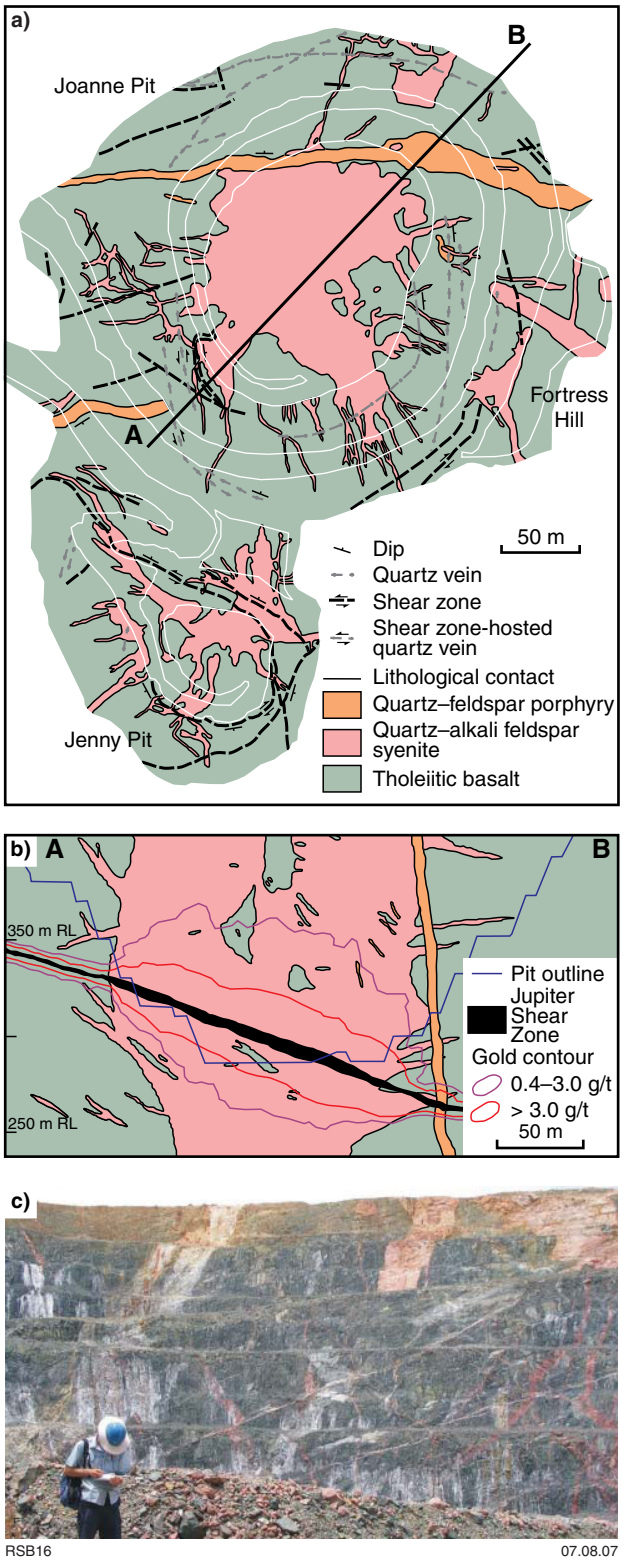

Figure 37. a) Geological map and (b) cross section of the Jupiter deposit, showing zonation of ore grade at the intersection of an east-southeasterly dipping D_4 shear zone with the Jupiter Syenite (after Duuring et al., 2000); and c) photograph of the syenite dykes cutting the basalt stratigraphy and being cut by D_4 thrusts

D_2: termination of an arc and east-northeast – west-southwest contraction).

The pillow basalts are cut by a large variety of syenite and pink, magmatic calcite dykes and minor sills (Fig. 38b,c). Minor quartz and pyrite are associated with the calcite dykes and these are inferred to host gold (as at Wallaby).

D_{4a} quartz veins with reverse-sense kinematics and associated carbonate alteration of the wallrock cut the syenite dykes. The carbonate alteration associated with these veins blows out at intersections with syenite dykes. This relationship implies that the syenite dykes were less permeable than the surrounding basalts during D_4 contraction and shearing. In the western wall of the pit, there is a similar relationship between a vertical zone of alteration and the quartz veins. However in this case, the quartz veins appear to act as a seal to a vertical fluid pathway (Fig. 38d).

Ductile east(to northeast)-over-west(to southwest) D_{4a} shear zones are associated with the quartz veining event. These structures record amazing strain localization (Fig. 38e) and the development of S–C structures. The best examples of this can be seen in the western wall of the saddle between the north and south pit, and along the southern wall at the bottom of the pit. High-grade mineralization (>3.0 g/t) was centred around these two ductile shear zones.

The reverse-sense quartz veins and syenite dykes are cut by D_5 predominantly steeply dipping and north-northeasterly striking, carbonate, dextral normal faults (Fig. 38f). Associated with these faults are northeast-striking sinistral faults. The resultant P–T dihedra analysis of this event indicates that these faults developed under transtension, with $\sigma 1$ plunging to the southwest (Fig. 39).

D_6 normal faults, quartz veins and crenulations record late extension of the system. The relationship of these structures to the D_5 dextral transtensional event is unclear at Jupiter due to a lack of overprinting relationships.

Leave the Jupiter access roads and once at the T-junction with the Mount Margaret road turn right and follow the road east and north to the main bitumen highway. Turn right to Laverton.

Locality 9: Lancefield — extensional gold with a dextral strike-slip overprint (MGA 439046E 6840781N)

Follow the signs out of Laverton marked Kalgoorlie and Leonora. Follow the bitumen 5 km out of town and turn right onto the Erlistoun road for 200 m and left into Lancefield (Metex Exploration office).

The purpose of visiting Lancefield is to demonstrate the significant down-to-the-southeast extensional shear system developed on the southeastern end of a major granitoid batholith. This contrasts with east-down extension at

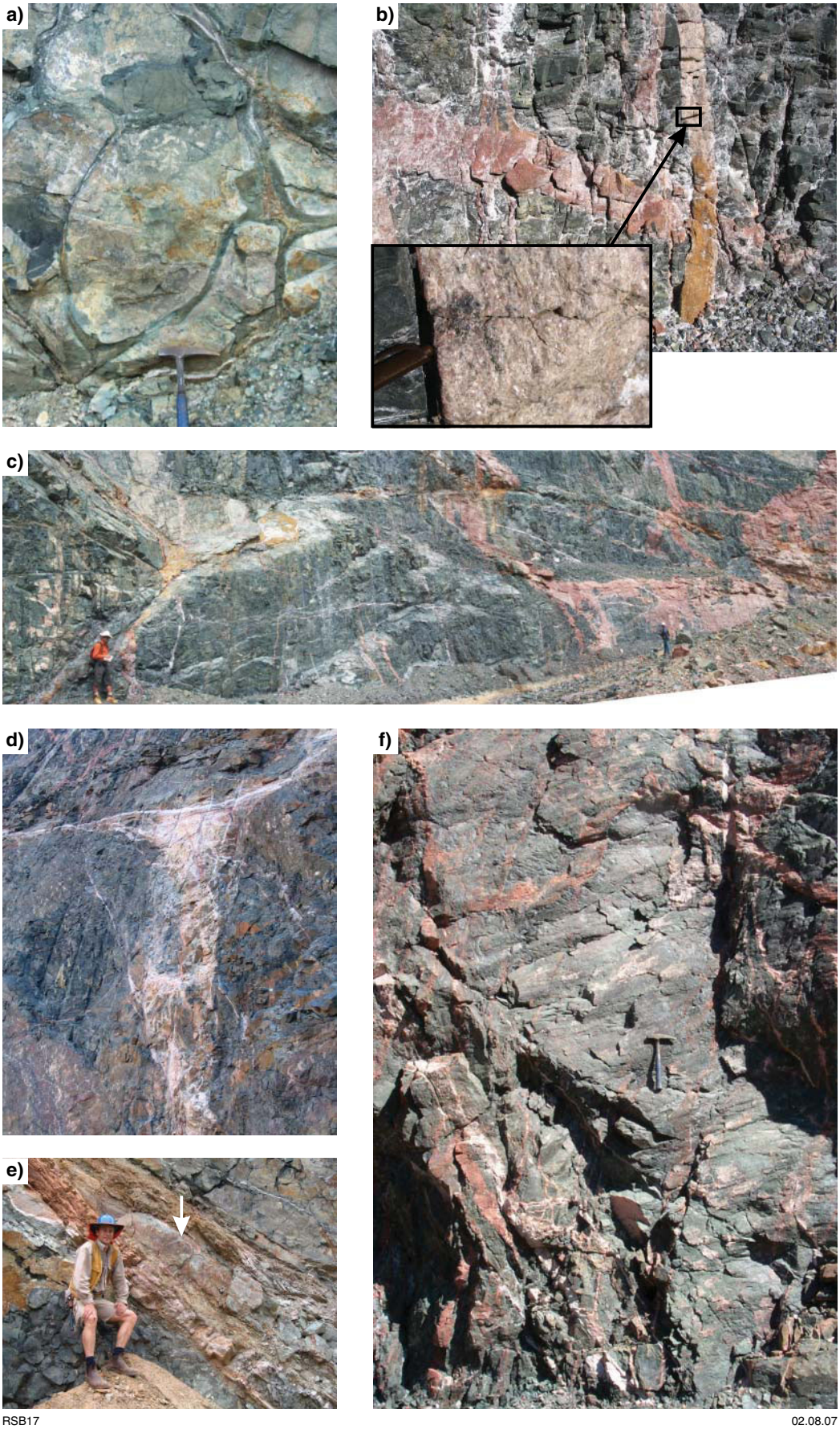
a)
b)
c)
d)
e)
f)
RSB17
02.08.07

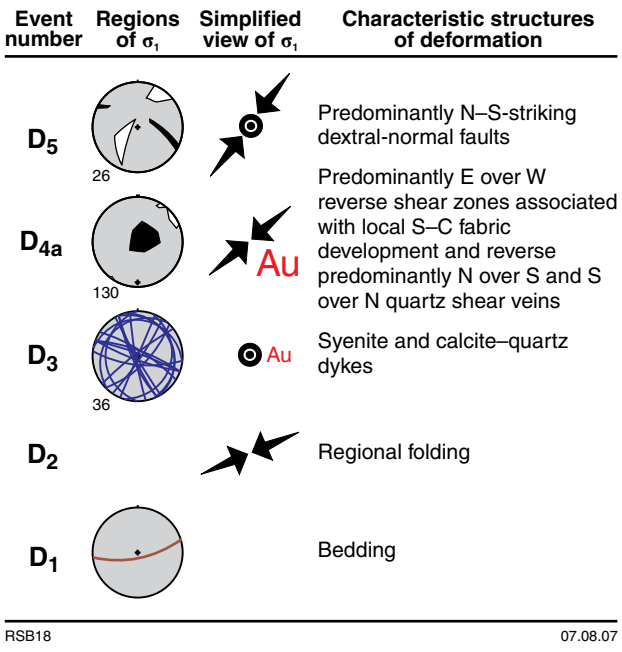

Figure 39. Stereographic compilation of structural elements into discrete events at the Jupiter deposit. Note the D_3 extension event defined by the radial array of syenite dykes. These intersect at the centre of the hemispherical projection illustrating a vertical σ_1. It is likely that σ_1 was driven from below by a magma chamber at depth. Gold (and sulfides) was likely introduced into the upper crust during the emplacement of the syenite and calcite veins (see Fig. 38b inset) and was remobilized during the D_4 contraction. Note also the switch in σ_3 (black sectors) between D_4 and D_5 from vertical with reverse-sense tectonic mode (D_4) to horizontal with strike-slip tectonic mode (D_5). This pattern illustrates the power of the P–T dihedra method for understanding and unravelling the subtleties of the complex evolution of this system

Figure 38. (opposite) Compilation of structural events and features at the Jupiter pit: a) view west of undeformed steeply dipping pillow basalts without a foliation. These pillow basalts were folded during D_2 about the Mount Margaret Anticline (without axial planar foliation) prior to D_3 extension and emplacement of the syenite and carbonate dykes; b) D_3 (pink) syenite dykes and sills cut by a D_3 calcite (–quartz–pyrite) dyke parallel to the earlier syenite dykes. Inset shows sulfides hosted by steep calcite dykes; c) collage of photos showing the main Jupiter reverse-sense ductile shear zone offsetting syenite dykes (view north-northeast); d) vertical fluid pathways and damage zone (bleached alteration) restricted or cut by D_4 shears and associated quartz veins (view west); e) D_4 east-northeast over west-southwest reverse-sense shear zones cutting intact pillow basalt. Photo illustrates the extreme strain partioning over narrow zones and is an analogue for the strain partitioning across the EGST as a whole (view northwest); f) D_5 dextral-normal brittle faults with well-developed oblique-slip carbonate slicken lines defining the movement sense (view west)

Leonora and north-down extension on the north end of Lawlers Anticline. Furthermore, Lancefield illustrates a significant dextral-shearing overprint that is characteristic of the Laverton Tectonic Zone and was particularly well developed at King of Creation to the north.

Danger: OPEN SHAFTS are present in the immediate vicinity; please watch your step and do not approach the shafts.

The Lancefield gold deposit is located in the Laverton area, 8 km north-northwest of the town of Laverton (Fig. 2). It is situated at the southeast edge of the amphibolite-grade granites of the Mount Margaret Anticline within amphibolite-grade greenstones (ultramafic schist) with an underlying domal-granitoid intrusion (Hronsky, 1993). Gold is hosted within two low-angle east- to southeast-dipping shear zones that are defined by so-called 'shale' or 'chert'.

Williams and Whitaker (1993) described significant extension around the southern margin of the Mount Margaret Anticline, with an overall granite to the north-northwest and greenstone to the south-southeast sense of shear. This extensional event formed the main fabric elements at Lancefield, and these are used as a deformation 'pin' for other events. This event is regionally linked to the D_3 late basin-forming event (Blewett and Czarnota, 2007b) and this location was likely the footwall to the Wallaby Basin at about 2665 Ma (see also McIntyre and Martyn, 2005). The main extensional fabric is a composite S–C foliation (Fig. 40b,f) at a range of scales (millimetre to decimetre). The fabric and shear zones overprint and show flattened early quartz veins and a locally fine 'early' foliation is preserved as crenulations (Fig. 40a,b).

East–west striking crenulations and folds (Fig. 41a) overprint the main S–C extensional fabric (Fig. 42) and are linked with the regional sinistral event known as D_{4b} (Blewett and Czarnota, 2007b). However, these crenulations could be interpreted as late-stage D_3 south-directed extension. A more significant reworking occurred during D_5 dextral shearing (Fig. 42), and these are well developed along the north-trending sections of the pit. S–C fabrics and crenulations are developed in this event and the outcrop breaks with a distinctive rhomboid geometry (Fig. 41b–e). The last stage, D_6, was the development of low-angle crenulations and normal faults during extension or vertical flattening (Figs 41f and 42).

The timing of gold is not easy to reconcile. Hronsky (1993) suggested that gold was deposited during a retrogressive stage, with temperatures of 325°C (±50) compared to the peak metamorphic temperatures of 450°C and pressures of 1.5 (±0.5) kb. This would place the gold in the D_{4b} sinistral or D_5 dextral times. However, Hronsky (1993) showed that gold was deposited in low-strain domains about boudin necks — these boudins developed during the extension (D_3). Lancefield may be a location of more than one gold event. Wallaby and Sunrise Dam are examples in the region where this has also been demonstrated (Miller, 2006).

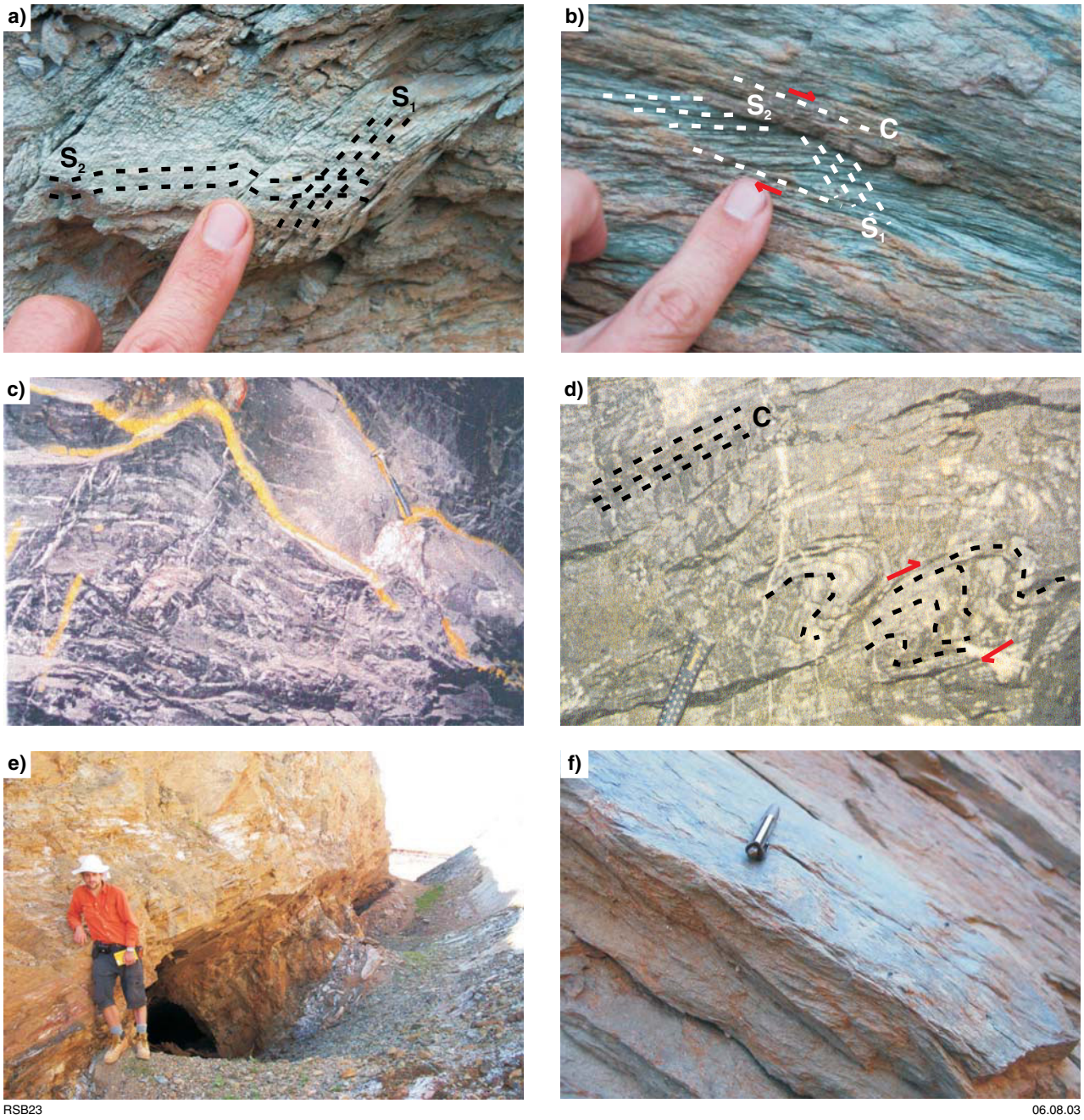

Figure 40. Compilation of photos of extension-related ore zones at the Lancefield mine: a) an early S_1 fabric within S_3 S-plane (view north); b) down-to-east extensional S–C shear fabric (S_3) and earlier internal fabric within shear planes (view northeast); c) underground photograph (after Hronsky, 1993) looking east of boudin necks (right-hand side) hosting gold; d) folding resulting from the inversion of D_3 extensional shear zones as a result of $D_{?4/5}$ reverse up-to-west shearing (photo from Hronsky, 1993); e) view southwest of main line of lode in down-to-east D_3 extensional shear zone; and f) extensional S–C fabric with undulations in main D_3 S-plane due to the intersection with S_3 C' planes (view north). Sense of shear is down to the east

Locality 9a: View north over the openpit

The main features of this stop are to show the convex-curved outline of the pit that mirrors the shape of the granite in the footwall beneath (Figs 43 and 44). The old mill and headframe base are preserved on a narrow septum transecting the pit. Note the active extension on pre-existing normal faults (down to the east) caused by the underground collapse of the lower workings.

Locality 9b: Extensional shear zone via the northern access ramp of openpit

The access ramp provides a dip and strike section through the extensional shear zone at Lancefield. On the dip section, note the two fabrics (S–C) indicative of east-down D_3 extensional shearing. On the strike section these down-to-the-east shears are best seen by viewing northwards onto joint faces. Also along the strike section, a series

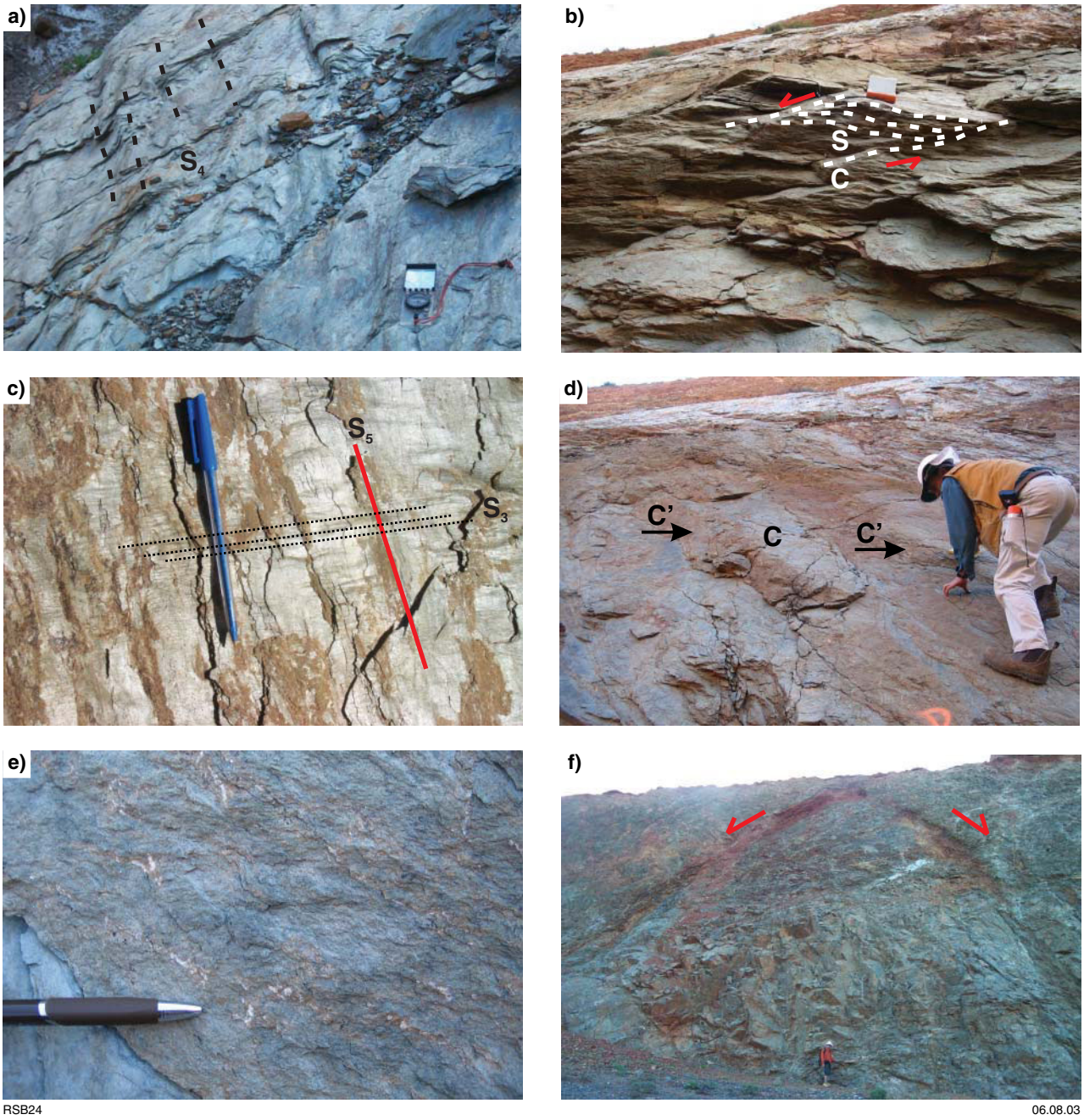

Figure 41. Compilation of photographs from post-D_3 extensional events in the Lancefield pit: a) well-developed S_4 crenulations overprint the main extensional S_3 S–C fabric (view west). Inferred contraction was oriented approximately north-northwest. These crenulations could be interpreted as related to D_3 C' planes and late-stage D_3 south-directed extension; b) view west up-dip of dextral D_5 S–C shear zone (which appear as sinistral shear because the view is from below). The intersection of the S–C planes promotes a rhomboid geometry to the outcrop when viewed from below; c) view west onto the main composite foliation that dips moderately to the east (towards the viewer). Here, the earlier S_3 (subhorizontal) crenulations are likely S_3 C' planes of down-to-the east extension and are overprinted by north–south dextral slicken lines and crenulation cleavage. Slicken fibres are concentrated on the downward-stepping C' plane sections (S_5) of the S_3 crenulated main-foliation plane. Here is an example of foliation reuse from down-to-the-east extension to north–south dextral shear about gentle east-dipping foliations; d) view west looking up of D_5 dextral reactivation of S_3 extensional main foliation. Stair stepping of long section C plane (dip right in this view) with shorter section S_5 C' plane (dip left in this view). Note that carbonate mineral fibres are located on the short C' extensional step overs (arrows); e) view west onto oblique fault plane showing detail of dextral strike-slip slicken line fibres defined by carbonate; and f) D_6 extensional faults are the last event to deform the Lancefield pit (view northwest)

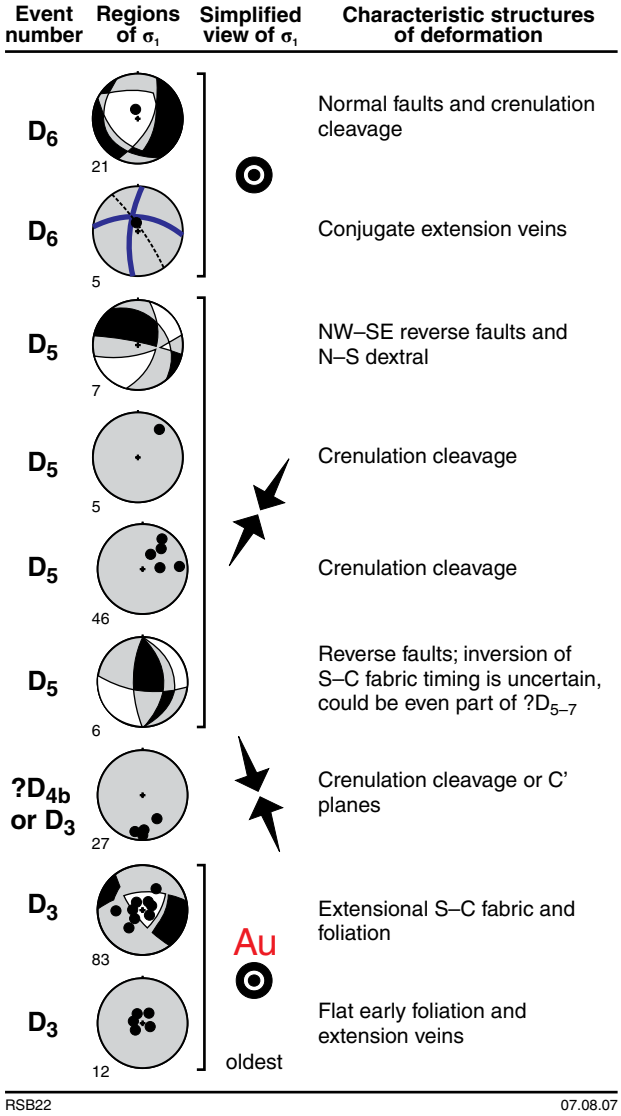

Figure 42. Compilation of structural elements at the Lancefield pit

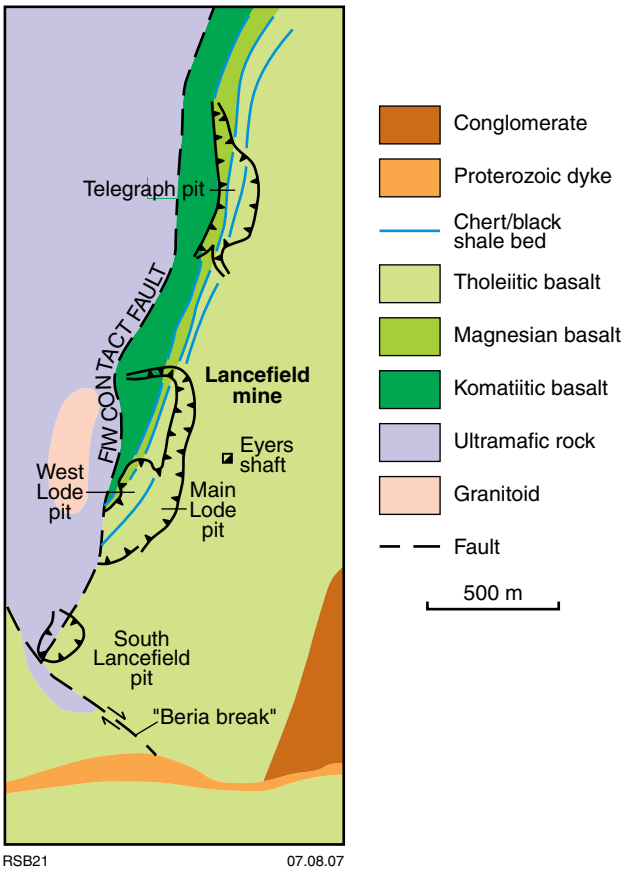

Figure 43. Simplified geological map of the Lancefield deposit and region (after Hronsky, 1993). Note the proximity of the granitoid intruding the footwall ultramafic rock and the location and geometry of the Lancefield pit

Figure 44. Panorama of the Lancefield deposit highlighting the convex nature of the pit and the Lancefield shear zone

of C' planes intersect the exposed C planes and they are revealed as centimetre-wide monoclines (with east-down vergence).

From the strike section look upwards and note that the foliation and outcrop also break out into pronounced S–C fabric at decimetre scales (Fig. 41b). The view is from below and appears sinistral, but geometrically and regionally it should be viewed from above and is therefore dextral. The D_5 dextral shear is also apparent on the faces at the pit floor. When viewed onto the moderately east-dipping rock face (towards you), the S planes dip to the right and the C planes dip to the left. Note also that carbonate slickenlines (D_4) are only developed on these left-dipping C-planes, which cut and smear-out the C' planes of the earlier D_3 extension.

Excursion localities — Laverton area

Day 4

After an overnight at Laverton Downs Homestead (north of Laverton) return to the main road and turn right (north) for 33 km until the first graded track (abandoned haul road) on the right. Take this track for approximately 3 km straight to the mine.

Locality 10: King of Creation — transpressional, dextral shear-zone gold (MGA 440615E 6885202N)

This pit is a fine example of extreme partitioning of deformation into a dextral strike-slip shear zone. It is noteworthy as it demonstrates that the penetrative foliation is not developed only by flattening, but has a significant component of shear. This dextral foliation contrasts with sinistral, reverse, and extensional (normal) shearing seen elsewhere on this trip and illustrates why a penetrative foliation striking north–south to north-northwest – south-southeast (the old 'S_2') can not be used as a marker fabric for structural correlations.

The King of Creation deposit is located 53 km north of Laverton (Fig. 2), on the eastern limb of the Mount Margaret Anticline in greenschist-facies greenstones. Strain increases dramatically towards a major dextral shear zone within the centre of the pit, which is assumed to have hosted gold mineralization. Here is another example of where mineralization and regions of intense strain are coupled. It is likely that deformation is required to create 'damage zones' and hence permeability for enhanced fluid flow (Cox, 1999), although in this case permeability formation is dynamic and related to active shearing, rather than brittle faulting.

Kinematically the pit is simple, with one progressive period of northeast–southwest contraction responsible for the development of:

- foliations (flattening and shear fabrics);
- veining and porphyry dyke intrusion;
- boudinage of porphyry and veins;
- asymmetric folds;
- S–C–C' in less competent units;
- box folds and sheath folds (Fig. 45).

Walk from the east ramp into the central high-strain zone and notice this transition from foliation and veins (which are conjugate) to transposed veins, and finally complex folds (Fig. 45). The central shear zone has spectacular refolded folds. The asymmetry of these is generally Z-shaped, consistent with the D_5 dextral shear couple (Fig. 46c).

Strain is highly partitioned into a narrow north-northwesterly trending mineralized corridor, some 50 m wide. This zone records multiple phases of deformation and transposition under a significant dextral regime, whereas the margins of the pit are strained only by a single, dextral strike-slip penetrative foliation (Fig. 45).

A feature of transpressional shear zones is the separation of the stretch and vorticity within a shear zone (Fossen and Tickoff, 1998) into a vertical component, whereas the overall kinematics of the shear zone is strike-slip. The vertical stretching at King of Creation is evident by the development of a patchy vertical stretching lineation and gently plunging folds, with curvilinear hinge lines (Fig. 46b,c) that tend towards sheath-like development. The dextral strike-slip vorticity or kinematics in the shear zone are evidenced by the boudinage of quartz veins, the development of box-shaped folds, and the anticlockwise transection of the foliation across gently plunging fold hinges (Fig. 46a; Blewett and Pickering, 1988).

Late carbonate north–southwesterly ($D_{\gamma 7}$) striking dextral faults and extensional normal faults and crenulations ($D_{\gamma 6}$), with unclear timing with respect to one another, complete the sequence of events (Fig. 46d).

Locality 11: Hanns Camp Syenite (MGA 445094E 6837519N)

Travel through the town of Laverton and drive straight on to the east on the Yamarna White Cliffs road for 11 km. The Hanns Camp Syenite outcrops on both sides of the road.

The purpose of visiting this site is to see a regional exposure of granite, although an area this large of syenite is unusual. The pronounced gently dipping foliation likely developed during extension, provides an age constraint on this event and links it to the development of the coeval Wallaby Basin to the west (which is intruded also by syenite).

The Hanns Camp Syenite is located around 5 km east of Laverton. It was emplaced at 2664 ± 2 Ma (Cassidy et al., 2002a), probably during regional extension. Details of the structural history of this site may be found in Blewett et al. (2004b). The syenite has a pronounced gently east-dipping

Figure 45. Strain partitioning across the King of Creation shear zone under dextral transpression. All fabric elements (including the main S_5 foliation) are consistent with development under dextral transpression. The increase in strain into the centre of the pit again demonstrates the importance of deformation intensity in focusing fluid flow into the most highly damaged zones (and therefore mineralization). For detailed P–T dihedra see Figure 10. From east to west (over a 50 m distance) into the shear zone centre (all photos view north-northwest): a) S_5 penetrative fabric with minor superimposed dextral strike-slip shearing of boudinaged porphyry; b) asymmetric folding of conjugate quartz veins; c) tight to isoclinal folding and boudinage of conjugate quartz veins; d) S–C–C' dextral strike-slip fabric elements; and e) F_5 box folds related to dextral strike-slip shearing in the high-strain centre of the pit

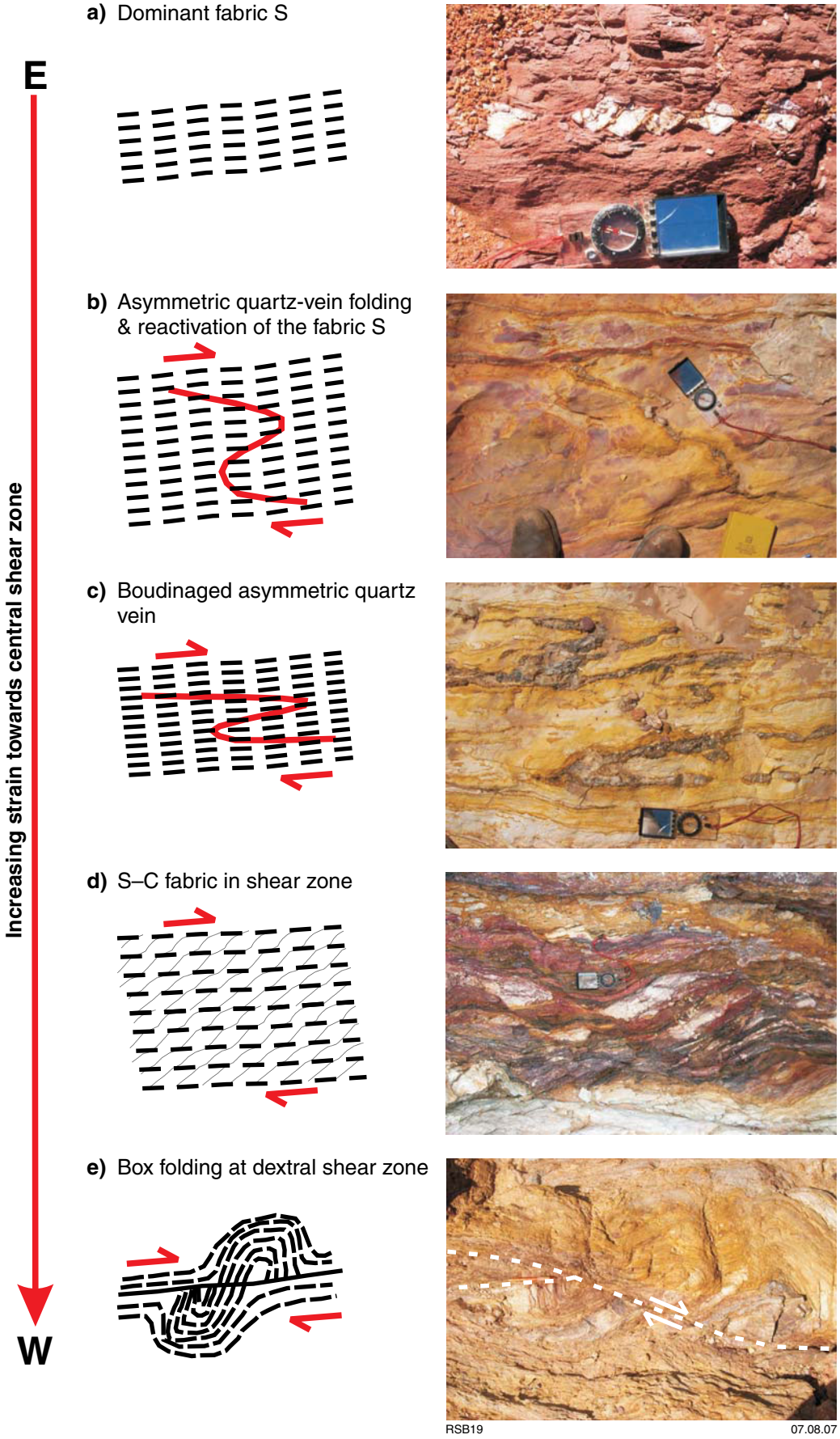
a) Dominant fabric S
b) Asymmetric quartz-vein folding & reactivation of the fabric S
c) Boudinaged asymmetric quartz vein
d) S–C fabric in shear zone
e) Box folding at dextral shear zone
E
W
Increasing strain towards central shear zone
RSB19
07.08.07

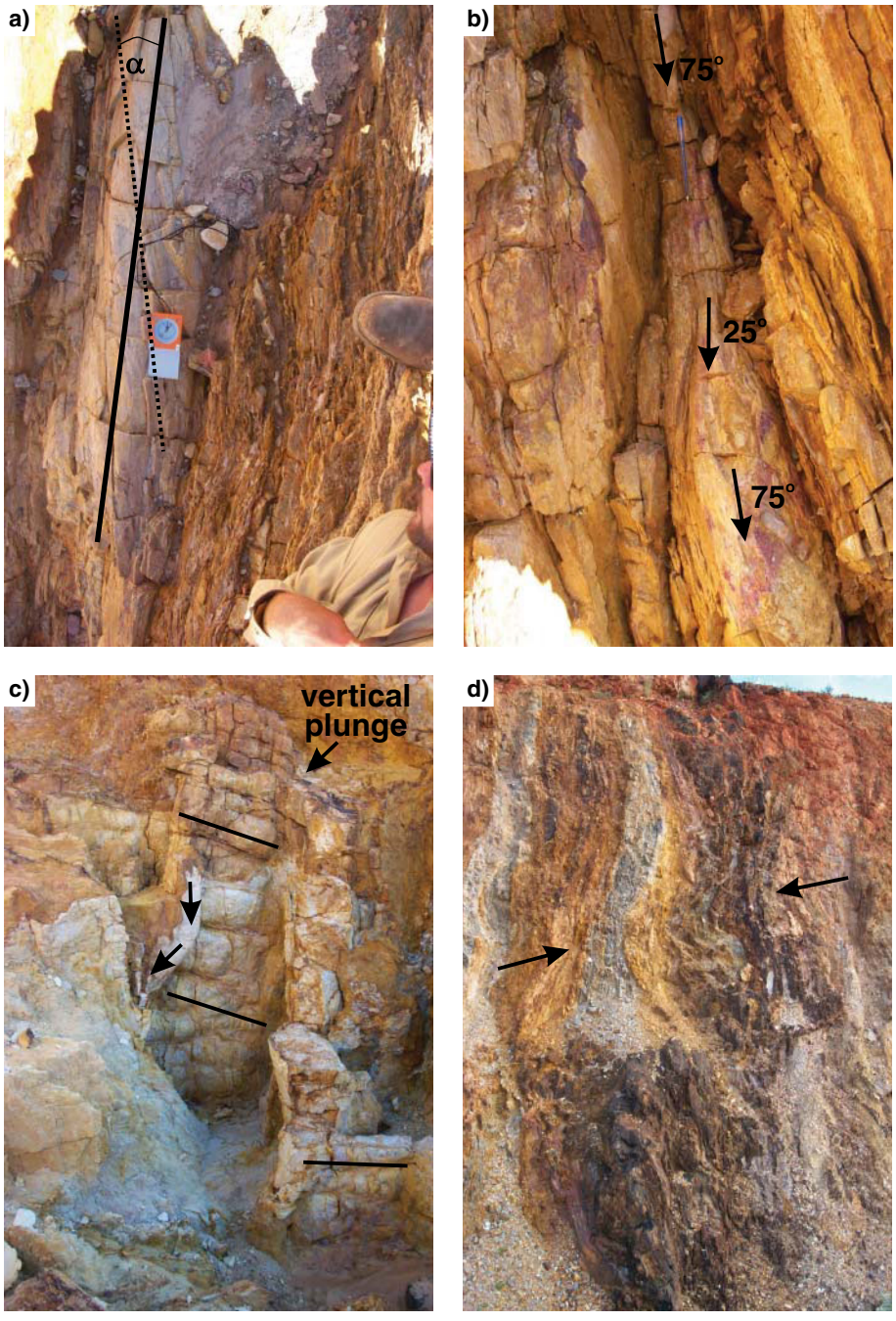

Figure 46. Collage of folds and associated foliation at King of Creation: a) view north-northwest of anticlockwise transection α of S_5 cleavage (pecked line) gently plunging F_5 fold hinges (solid line) in competent quartzite bed, consistent with dextral transpression (see Blewett and Pickering, 1988); b) view south of steep wall with periclinal plunge of F_5 fold axis pitching from 75 to 25° through the F_5 axial surface; c) view west onto a wall with complex F_5 drag fold, with changes in fold plunge (see arrows). Main folds plunge subvertically and have Z-asymmetry consistent with dextral shear. A component of vertical stretch is apparent on the bedding planes (as gently plunging mullions highlighted by black bars); d) view south onto rear wall of King of Creation with late extensional structures defined by gently dipping axial surfaces of F_6 folds in walls of the pit. These are common in the Laverton region (see also Davis and Maidens, 2003), and may reflect a link between high strains during D_5 and subsequent relaxation during D_6

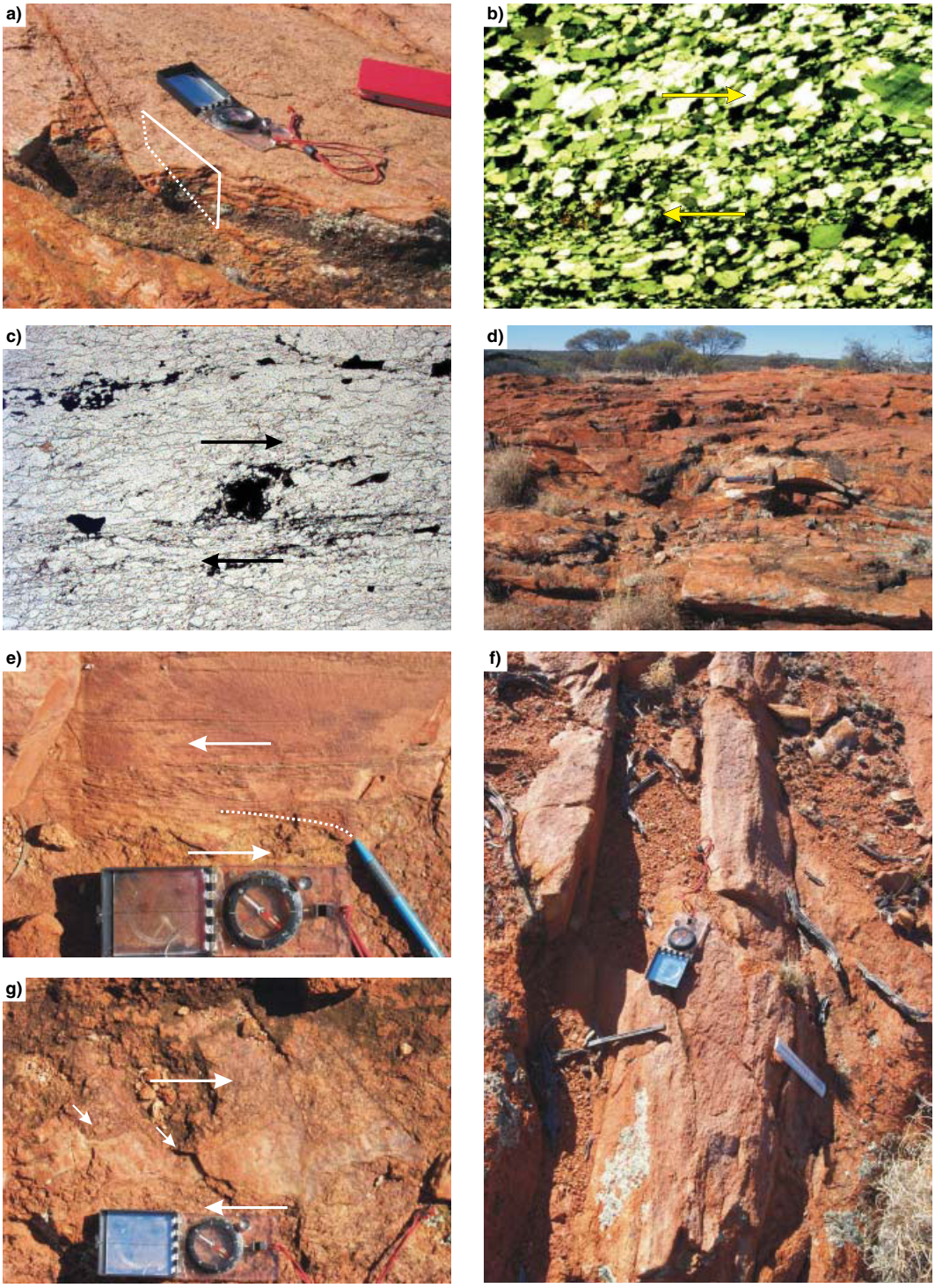

Figure 47. Compilation of structural events of the c. 2665 Ma Hanns Camp Syenite: a) view north-northeast of gently dipping high-strain foliation (extensional) with well-developed southeast-plunging lineation. Box is thin section planes in (b) and (c); b) microphotograph (perpendicular to foliation and parallel to lineation) of down-to-the southeast extensional kinematics (preferred fabric orientation) from within the high-strain foliation in a siliceous phase of the Hanns Camp Syenite; c) microphotograph (perpendicular to foliation and parallel to lineation) of down-to-the-southeast extensional kinematics (S–C) from within the high-strain foliation in a siliceous phase of the Hanns Camp Syenite; d) view north-northwest of open upright F_{4a} folds with a gentle north-northwesterly plunge; e) north-northwesterly trending, steeply dipping S_{4b} sinistral shear. Inferred σ_1 was likely oriented northwest–southeast to west-northwest – east-southeast during this event; f) view north-northwest of tight upright F_{4a} folds. Note ruler and chisel defining the folded S_3 surface over the F_{4a} hinge; f) bookshelf boudinage of quartz vein associated with north-trending D_5 dextral shear

mylonitic foliation (Fig. 47a) with a north-northwest to south-southeast movement direction. Kinematic indicators observed in several thin sections of a fine-grained siliceous phase suggest that movement was extensional, with down-to-the-east and southeast kinematics (Fig. 47b,c). This mylonitic fabric is overprinted by spaced north- and north-northwest-trending D_{4b} sinistral shear zones (Fig. 47e) and open to tight upright folds that developed during ~northwest–southeast contraction (Fig. 47d,f). Later minor D_5 dextral shears reflect a switch to northeast–southwest transtension, with the final event northeast-trending kink bands of the main penetrative foliation (Fig. 47g).

We hope that you enjoyed the trip and that it met with your expectations.

Return to Laverton and the highway back to Leonora and Kalgoorlie, this trip is about a four-hour drive.

Acknowledgements

We would like to acknowledge the following companies for access to their ground and their support of this field trip:

A1 Minerals: King of Creation
Barrick: Jupiter and Westralia
Metex: Lancefield
Navigator Resources: Mertondale
Regal Resources: Yunndaga.
St Barbara: Tarmoola, Gwalia and Victor Well

This project has been a rewarding and challenging experience for both of us. We would like to thank the sponsors for their ongoing commitment to the Y1-P763 and Y4 pmd*CRC projects . Special mention to:

- Trevor Beardsmore (Barrick) who provided his excellent reports on Mount Morgans and Lawlers, and was a constant source of encouragement for our work.
- John Beeson (ex-Placer) who accompanied us in the field in the Laverton district and we welcomed his contributions.
- Simon Apps (Barrick) who provided support at Lawlers and smoothed our way underground at New Holland. Barrick also provided field support while we were based at Lawlers.
- Cees Swager (ex-AngloGold Ashanti) who provided advice on the direction of our research and was always receptive to novel ideas.
- Phung Nguyen (Goldfields Agnew) who provided permission and access to the Agnew pits.
- Bob Love (SOG now St Barbara) who provided access to the Leonora deposits, especially Tarmoola and Gwalia openpits.
- Bruce Groenewald, Sarah Jones and Charlotte Hall (GSWA) who were always available for discussion.
- The GSWA are gratefully acknowledged for providing their 4WD vehicle and fuel support for our field work, and also their safety back up systems (especially Brain Moore at Carlisle base, and Wayne Hitchcock at Kalgoorlie). Without their help this work could not have been accomplished.

References

Angelier, J, 1984, Tectonic analysis of fault slip data sets: Journal of Geophysical Research, 89, p. 5835–5848.

Archibald, NJ, Bettenay, LF, Binns, RA, Groves, DI, and Gunthorpe, RJ, 1978, The evolution of Archaean greenstone terrains, Eastern Goldfields Province, Western Australia: Precambrian Research, 6, p. 103–131.

Barley ME, Brown, SJA, Cas, RAF, Cassidy, KF, Champion, DC, Gardoll, SJ, and Krapez, B, 2003, An integrated geological and metallogenic framework for the eastern Yilgarn Craton: developing geodynamic models of highly mineralised Archaean granite–greenstone terranes. AMIRA Project P624, Final Report.

Barley, ME, Brown, SJA, Krapez, B, and Cas, RAF, 2002, Tectonostratigraphic analysis of the Eastern Yilgarn Craton: an improved geological framework for exploration in Archaean Terranes: AMIRA Project P437A, Final Report.

Barley, ME, Eisenlohr, BN, Groves, DI, Perring, CS, and Vearncombe, JR, 1989, Late Archean convergent margin tectonics and gold mineralization; a new look at the Norseman–Wiluna Belt, Western Australia: Geology, 17, p. 826–829.

Bayasgalan, A, Jackson, J, Ritz, JF, and Carretier, S, 1999, Field examples of strike-slip fault terminations in Mongolia and their tectonic significance: Tectonics, 18, p. 394–411.

Beakhouse, GP, 2007, Structurally controlled, magmatic hydrothermal model for Archaean lode gold deposits: a working hypothesis: Ontario Geological Survey, Open File Report 6193, 133p.

Beardsmore, TJ, 1999, The geology, tectonic evolution and gold mineralisation of the Mount Morgan's region: results of structural geological mapping: Technical Report No 893, Homestake Gold Australia Ltd, p. 124.

Beardsmore, TJ, 2002, The geology, tectonic evolution and gold mineralisation of the Lawlers region: a synopsis of present knowledge: Barrick Gold of Australia, Technical Report 1026, 279p.

Binns, RA, Gunthorpe, RJ, and Groves, DI, 1976, Metamorphic patterns and development of greenstone belts in eastern Yilgarn Block, Western Australia: John Wiley & Sons, New York, USA, p. 303–313.

Blewett, RS, 2006, Chapter 6: An assessment of the utility of the new 3D data versus 2D data at a regional scale: geodynamic insights, *in* Final Report Y2 pmd*CRC project 3D geological models of the eastern Yilgarn Craton *edited by* RS Blewett and AP Hitchman: p. 139–161 [DVD-ROM]

Blewett, RS, Cassidy, KF, Champion, DC, and Whitaker, AJ, 2004a, The characterisation of granite deformation events in time across the Eastern Goldfields Province, Western Australia: Geoscience Australia, Record 2004/10 [CDROM].

Blewett, RS, Cassidy, KF, Champion, DC, Henson, PA, Goleby, BR, and Kalinowski, AA, 2004b, An orogenic surge model for the eastern Yilgarn Craton: implications for gold mineralising systems, *in* SEG 2004, Predictive Mineral Discovery Under Cover *edited by* J Muhling: Centre for Global Metallogeny, The University of Western Australia, Publication 33, p. 321–324.

Blewett, RS, Cassidy, KF, Champion, DC, Henson, PA, Goleby, BR, Jones, L, and Groenewald, PB, 2004c, The Wangkathaa Orogeny: an example of episodic regional 'D_2' in the late Archaean Eastern Goldfields Province, Western Australia: Precambrian Research, 130, p. 139–159.

Blewett, RS, Champion, DC, Whitaker, AJ, Bell, B, Nicoll, M, Goleby, BR, Cassidy, KF, and Groenewald, PB, 2002a, A new 3D model of the Leonora–Laverton transect: implications for the tectonic evolution of the eastern Yilgarn Craton: Australian Institute of Geoscientists Bulletin, 36, p. 18–21.

Blewett, RS, Champion, DC, Whitaker, AJ, Bell, B, Nicoll, M, Goleby, BR, Cassidy, KF, and Groenewald, PB, 2002b, Three dimensional (3D) model of the Leonora–Laverton transect area: implications for Eastern Goldfields tectonics and mineralisation, *in* Geology, geochronology and geophysics of the north eastern Yilgarn Craton, with an emphasis on the Leonora–Laverton transect area *edited by* KF Cassidy: Geoscience Australia, Record 2002/18, p. 83–100.

Blewett, RS, and Czarnota, K, 2007a, Diversity of structurally controlled gold through time and space of the central Eastern Goldfields Superterrane — a field guide: Geological Survey of Western Australia, Record 2007/19, 65p.

Blewett, RS, and Czarnota, K, 2007b, The Y1-P763 project final report November 2005. Module 3 — Terrane Structure: Tectonostratigraphic architecture and uplift history of the Eastern Yilgarn Craton: Geoscience Australia, Record 2007/15.

Blewett, RS, and Czarnota, K, 2007c, A new integrated tectonic framework of the Eastern Goldfields Superterrane, *in* Kalgoorlie 2007 *edited by* F Bierlien and C Knox-Johnson: Geoscience Australia, Record 2007/14.

Blewett, RS, and Pickering, KT, 1988, Sinistral shear during the Acadian deformation in north-central Newfoundland, based on transecting cleavage: Journal of Structural Geology, 10, p. 125–127.

Brown, SJA, Barley, ME, Krapez, B, and Cas, RAF, 2002, The Late Archaean Melita Complex, Western Australia: shallow submarine bimodal volcanism in a rifted arc environment: Journal of Volcanology and Geothermal Research, v. 115, p. 303–327.

Campbell, IH, and Hill, RI, 1988, A two-stage model for the formation of the granite–greenstone terrains of the Kalgoorlie–Norseman area, Western Australia: Earth and Planetary Science Letters, 90, p. 11–25.

Cassidy, KF, 2006, Geological evolution of the Eastern Yilgarn Craton (EYC), and terrane, domain and fault nomenclature, *in* 3D Geological Models of the Eastern Yilgarn Craton – Y2 Final Report pmd*CRC *edited by* RS Blewett and AP Hitchman: Geoscience Australia, Record 2006/04, p. 1–19 [DVD-ROM].

Cassidy, KF, and Champion, DC, 2004, Crustal evolution of the Yilgarn Craton from Nd isotopes and granite geochronology: implications for metallogeny, *in* SEG 2004, Predictive Mineral Discovery Under Cover *edited by* J Muhling: Centre for Global Metallogeny, The University of Western Australia, Publication 33, p. 317–320.

Cassidy, KF, Champion, DC, Fletcher, IR, Dunphy, JM, Black, LP, and Claoué-Long, JC, 2002a, Geochronological constraints on the Leonora–Laverton transect area, north-eastern Yilgarn Craton: Geoscience Australia, Record 2002/18, p. 37–58.

Cassidy, KF, Champion, DC, Krapez, B, Barley, ME, Brown, SJA, Blewett, RS, Groenewald, PB, and Tyler, IM, 2006, A revised geological framework for the Yilgarn Craton, Western Australia: Geological Survey of Western Australia, Record 2006/8, 8p.

Cassidy, KF, Champion, DC, McNaughton, NJ, Fletcher, IR, Whitaker, AJ, Bastrakova, IV, and Budd, AR, 2002b, Characterisation and metallogenic significance of Archaean granitoids of the Yilgarn Craton, Western Australia: Minerals and Energy Research Institute of Western Australia (MERIWA), Report No. 222, 514p.

Champion, DC, 2006, Terrane, domain and fault system nomenclature, *in* 3D Geological Models of the Eastern Yilgarn Craton–Y2 Final Report pmd*CRC *edited by* RS Blewett and AP Hitchman: Geoscience Australia, Record 2006/4, p. 19–38 [DVD-ROM].

Champion, DC, Cassidy, KF, and Budd, A, 2002, Chapter 8, Overview of the Yilgarn magmatism: implications for crustal development, *in* Characterisation and metallogenic significance of Archaean granitoids of the Yilgarn Craton, Western Australia *edited by* KF Cassidy, DC Champion, NJ McNaughton, IR Fletcher, AJ Whitaker, IV Bastrakova, and AR Budd: Minerals and Energy Research Institute of Western Australia (MERIWA), Report No. 222, 514p.

Champion, DC, and Sheraton, JW, 1997, Geochemistry and Nd isotope systematics of Archaean granites of the Eastern Goldfields, Yilgarn Craton, Australia; implications for crustal growth processes: Precambrian Research, 83, p. 109–132.

Chen, SF, Witt, W, and Liu, SF, 2001, Transpressional and restraining jogs in the northeastern Yilgarn Craton, Western Australia: Precambrian Research 106, p. 309–328.

Claoué-Long, JC, Compston, W, and Cowden, A, 1988, The age of the Kambalda greenstones resolved by ion microprobe — implications for Archaean dating methods: Earth and Planetary Science Letters, 89, p. 239–259.

Coates, SP 1993, Geology and grade control at the Sons of Gwalia Mine Leonora, Western Australia, *in* Proceedings of the international mining geology conference *edited by* I Robertson, W Shaw, C Arnold, and L Kevin: Australian Institute of Mining and Metallurgy 5/93, Publication Series, p. 125–132.

Cox, SF, 1999, Deformational controls on the dynamics of fluid flow in mesothermal gold systems, *in* Fractures, fluid flow and mineralization *edited by* KJF McCaffrey, L Lonergan, and J Wilkinson: Geological Society, Special Publications 155, p. 123–140.

Czarnota, K, and Blewett, RS, 2005, A modified PT-dihedra method in brittle ductile lode Au systems — establishing a regional deformation framework in areas of limited outcrop. STOMP conference: James Cook University, Economic Geology Research Unit, 64, p. 34.

Czarnota, K, and Blewett, RS, 2007, Don't hang it on a foliation to unravel a structural event sequence: an example from the Eastern Goldfields Superterrane: Geological Society of Australia, Specialist Group, Tectonics and Structural Geology, Abstracts, Deformation I the Desert, Alice Springs, 9–13 July 2007, p. 75.

Davis, BK, and Maidens, E, 2003, Archaean orogen-parallel extension; evidence from the northern Eastern Goldfields Province, Yilgarn Craton: Precambrian Research, 127, p. 229–248.

DeCelles, PG, and Giles, KA, 1996, Foreland basin systems: Basin Research, 8, p. 105–123.

Drummond, BJ, Goleby, BR, and Swager, CP, 2000, Crustal signature of Late Archaean tectonic episodes in the Yilgarn Craton, Western Australia: evidence from deep seismic sounding: Tectonophysics, 329, p. 193–221.

Dunphy, JM, Fletcher, IR, Cassidy, KF, and Champion, DC, 2003, Compilation of SHRIMP U–Pb geochronological data, Yilgarn Craton, Western Australia, 2001–2002: Geoscience Australia, Record 2003/15, 139p.

Duuring, P, Hagemann, SG, and Groves, DI, 2000, Structural setting, hydrothermal alteration, and gold mineralisation at the Archaean syenite-hosted Jupiter Deposit, Yilgarn Craton, Western Australia: Mineralium Deposita, 35, p. 402–421.

Duuring, P, Hagemann, SG, and Love, RJ, 2001, A thrust ramp model for gold mineralization at the Archaean trondhjemite-hosted Tarmoola Deposit; the importance of heterogeneous stress distributions around granitoid contacts: Economic Geology, 96, p. 1379–1396.

Eisenlohr, BN, Groves, D, and Partington, GA, 1989, Crustal-scale shear zones and their significance to Archaean gold mineralization in Western Australia: Mineralium Deposita, 24, p. 1–8.

Evans, W, 2003, Yunndaga Review: Placer Dome Asia Pacific, Internal Memorandum (unpublished).

Fletcher, IR, Dunphy, JM, Cassidy, KF, and Champion, DC, 2001, Compilation of SHRIMP U–Pb geochronological data, Yilgarn Craton, Western Australia, 2000–2001: Geoscience Australia, Record 2001/47, 111p.

Fossen, H, and Tickoff, B, 1998, Extended models of transpression and transtension, and application to tectonic settings, *in* Continental transpressional and transtensional tectonics *edited by* RE Holdsworth, RA Strachan, and JF Dewey: Geological Society of London, Special Publications 135, p. 15–33.

Gee, RD, 1979, Structure and tectonic style of the Western Australian Shield: Tectonophysics, 58, p. 327–369.

Gee, RD, Baxter, JL, Wilde, SA, and Williams, IR, 1981, Crustal development in the Archaean Yilgarn Block, Western Australia: Geological Society of Australia, Special Publication 7, p. 43–56.

Geological Survey of Western Australia, 2007, Compilation of geochronology data, June 2007 update: Geological Survey of Western Australia.

Goleby, B, Blewett, RS, Champion, DC, Korsch, RJ, Bell, B, Groenewald, PB, Jones, LEA, Whitaker, AJ, Cassidy, KF, and Carlsen, GM, 2002, Deep seismic profiling in the NE Yilgarn: insights into its crustal architecture: Australian Institute of Geoscientists, Bulletin 36, p. 63–66.

Goleby, BR, Rattenbury, MS, Swager, CP, Drummond, BJ, Williams, PR, Sheraton, JE, and Heinrich, CA, 1993, Archaean crustal structure from seismic reflection profiling, Eastern Goldfields, Western Australia: Australian Geological Survey Organisation, Record 1993/15, 54p.

Goscombe, B, Blewett, RS, Czarnota, K, Maas, R, and Groenewald, BA, 2007, Broad thermo-barometric evolution of the Eastern Goldfields Superterrane, *in* Kalgoorlie 2007 *edited by* F Bierlien and C Knox-Johnson: Geoscience Australia Record, 2007/14, p. 33–38.

Goscombe, B, Gray, D, Carson, C, Groenewald, PB, Scrimgeour, I, 2005, Classification of metamorphic gradients and their utilisation as indicators of tectonic regime: James Cook University, Economic Geology Research Unit, Contribution 64, 175.

Gower, CF, 1976, Laverton, Western Australia, 1:250 000 Geological Series–Explanatory Notes. Australian Government Publishing Service, Canberra, 30p.

Hall, G, 2007, Exploration success in the Yilgarn Craton insights from the Placer Dome experience, the need for integrated research, *in* Kalgoorlie 2007 *edited by* F Bierlien and C Knox-Johnson: Geoscience Australia, Record 2007/14.

Hallberg, JA, 1985, Geology and mineral deposits of the Leonora–Laverton area, northeastern Yilgarn Block, Western Australia: Hesperian Press, Perth, Western Australia, 140p.

Hammond, RL, and Nisbet, BW, 1992, Towards a structural and tectonic framework for the Norseman–Wiluna Greenstone Belt, Western Australia, *in* The Archaean — Terrains, Processes and Metallogeny *edited by* JE Glover and SE Ho: Geology Department and University Extension, The University of Western Australia, Publication 22, p. 39–50.

Hammond, RL, and Nisbet, BW, 1993. Archaean crustal processes as indicated by the structural geology, Eastern Goldfields Province of Western Australia, *in* Kalgoorlie 93 — an international conference on crustal evolution, metallogeny, and exploration of the Eastern Goldfields *edited by* PR Williams and JA Haldane: Australian Geological Survey Organisation, Record 1993/54, p. 105–114.

Henson, PA, 2006, Chapter 2: An integrated geological and geophysical 3D map for the EYC, *in* 3D Geological Models of the Eastern Yilgarn Craton — Y2 Final Report pmd*CRC *edited by* RS Blewett and AP Hitchman: Geoscience Australia, Record 2006/04, p. 32–85 [DVD-ROM].

Henson, PA, and Blewett, RS, 2006, 3D interpretation of the Eastern Yilgarn: new architectural insights from construction of the 3D map, *in* 3D Geological Models of the Eastern Yilgarn Craton — Y2

Final Report pmd*CRC *edited by* RS Blewett and AP Hitchman: Geoscience Australia, Record 2006/04, p. 207–216 [DVD-ROM].

Henson, PA, Blewett, RS, Champion, DC, Goleby, BR, and Cassidy, KF, 2004a, Using 3D 'map patterns' to elucidate the tectonic history of the Eastern Yilgarn, *in* Predictive Mineral Discovery Cooperative Research Centre; Extended Abstracts from the June 2004 Conference *edited by* AC Barnicoat and RJ Korsch: Geoscience Australia, Record 2004/9, p. 87–90.

Henson, PA, Blewett, RS, Champion, DC, Goleby, BR, and Cassidy, KF, 2004b, A dynamic view of orogenesis and the development of the Eastern Yilgarn, *in* Predictive Mineral Discovery Cooperative Research Centre; Extended Abstracts from April 2004 conference *edited by* AJ Barnicoat, and RJ Korsch: Geoscience Australia, Record 2004/9, p. 91–94.

Henson, PA, Blewett, RS, Champion, DC, Goleby, BR, Cassidy, KF, Drummond, BJ, Korsch, RJ, Brennan, T, and Nicoll, M, 2005, Domes: the characteristic 3D architecture of the world-class lode-Au deposits of the Eastern Yilgarn: Economic Geology, Research Unit Contribution 64, p. 60.

Henson, PA, Blewett, RS, Champion, DC, Goleby, BR, and Czarnota, K, 2007, How does the 3D architecture of the Yilgarn control hydrothermal fluid focussing, *in* Kalgoorlie 2007 *edited by* F Bierlien and C Knox-Johnson: Geoscience Australia, Record 2007/14.

Hill, RI, Chappell, BW, and Campbell, IH, 1992, Late Archaean granites of the southeastern Yilgarn Block, Western Australia: age, geochemistry and origin: Transactions Royal Society of Edinburgh, Earth Sciences, 83, p. 211–226.

Hodge, JL, 2007, PhD thesis, University of Western Australia (unpublished).

Hronsky, JMA, 1993, The role of physical and chemical processes in the formation of ore-shoots at the Lancefield gold deposit, Western Australia: Western Australia, PhD thesis (unpublished).

Kent, AJR, and Hagemann, SG, 1996, Constraints on the timing of lode-gold mineralisation in the Wiluna greenstone belt, Yilgarn Craton, Western Australia: Australian Journal of Earth Sciences, v. 43, p. 573–588.

Kositcin, N, Brown, SJA, Barley, ME, Krapez, B, Cassidy, KF, and Champion, DC, 2008, SHRIMP U–Pb zircon age constraints on the Late Archaean tectonostratigraphic architecture of the Eastern Goldfields Superterrane, Yilgarn Craton, Western Australia: Precambrian Research, v. 161, p. 5–33.

Krapez, B, Brown, SJA, Hand, J, Barley, ME, and Cas, RAF, 2000, Age constraints on recycled crustal and supracrustal sources of Archaean metasedimentary sequences, Eastern Goldfields Province, Western Australia: Evidence from SHRIMP zircon dating: Tectonophysics, 322, p. 89–133.

Liu, S, and Chen, S, 1998, Structural framework of the northeastern Yilgarn Craton and implications for hydrothermal gold mineralisation: Australian Geological Survey Organisation, Research Newsletter, 29, p. 21–23.

Liu, SF, Stewart, AJ, Farrell, T, Whitaker, AJ, and Chen, SF, 2000, Solid geology of the north Eastern Goldfields, Western Australia: Geoscience Australia, 1:500 000-scale print-on-demand map (Catalogue No 53233).

McIntyre, JR, and Martyn, JE, 2005. Early extension in the Late Archaean northeastern Eastern Goldfields Province, Yilgarn Craton, Western Australia: Australian Journal of Earth Sciences, 52, p. 975–992.

Mikucki, EJ, and Roberts, FI, 2003, Metamorphic petrography of the Kalgoorlie region, Eastern Goldfields Granite–Greenstone Terrane: METPET database: Geological Survey of Western Australia, Record 2003/12.

Miller, JM, 2006, Linking structure and mineralisation in Laverton, with specific reference to Sunrise Dam and Wallaby, *in* Predictive Mineral Discovery CRC; Extended Abstracts for the April 2006 Conference *edited by* AC Barnicoat and RJ Korsch: Geoscience Australia, Record 2006/7, p. 62–67.

Morey, A, 2007, Controls on gold endowment within the Bardoc Tectonic Zone, Eastern Goldfields Province, Western Australia: Monash University, PhD thesis (unpublished).

Mueller, AG, Harris, LB, and Lungan, A, 1988, Structural control of greenstone-hosted gold mineralisation by transcurrent shearing: a new interpretation of the Kalgoorlie mining district, Western Australia: Ore Geology Reviews, 3, p. 359–387.

Myers, JS, 1995, The generation and assembly of an Archaean supercontinent — evidence from the Yilgarn Craton, Western Australia, *in* Early Precambrian Processes *edited by* MP Coward, and AC Ries: Geological Society London, Special Publication 95, p. 143–154.

Myers, JS, 1997, Preface; Archaean geology of the Eastern Goldfields of Western Australia; regional overview: Precambrian Research, 83, p. 1–10.

Nelson, DR, 1996, Compilation of SHRIMP U–Pb zircon geochronology data, 1995: Geological Survey of Western Australia, Record 1996/5, 168p.

Nelson, DR, 1997, Compilation of SHRIMP U–Pb zircon geochronology data, 1996. Geological Survey of Western Australia, Record 1997/2, 189p.

Nguyen, TP, 1997, Structural controls on gold mineralisation at the Revenge Mine and its tectonic setting in the Lake Lefroy area, Kambalda, Western Australia: University of Western Australia**,** PhD thesis (unpublished), 205p.

Nisbet, BW, 1991, Timing of structure and mineralisation at Mertondale and its relationship to structure and mineralisation in the Leonora region, *in* Structural geology in mining and exploration; abstracts to accompany conference: University of Western Australia, Geology Department and University Extension, Publication 25, p. 132–134.

Nisbet, BW, and Hammond, RL, 1989, Structure of the Mertondale Mine area and implications for regional geology and mineralisation, *in* Australasian Tectonics: Geological Society of Australia, Abstracts 24, p. 101–103.

Nisbet, BW, and Williams, CR, 1990, Mertondale gold deposits, Leonora, *in* Geology of the Mineral Deposits of Australia and Papua New Guinea *edited by* FE Hughes: The Australian Institute of Mining and Metallurgy, Melbourne, p. 337–342.

Ojala, VJ, McNaughton, NJ, Ridley, JR, Groves, DI, and Fanning, CM, 1997, The Archaean Granny Smith gold deposit, Western Australia: age and Pb-isotope tracer studies: Chronique de la Recherche Miniere, 529, p. 75–89.

Passchier, CW, 1994, Structural geology across a proposed Archaean terrane boundary in the eastern Yilgarn Craton, Western Australia: Precambrian Research, 68, p. 43–64.

Platt, JP, Allchurch, PD, and Rutland, RWR, 1978, Archaean tectonics in the Agnew supracrustal belt, Western Australia: Precambrian Research, 7, p. 3–30.

Potma, WA, Schaubs, PM, Robinson, JA, Sheldon, HA, Roberts, PA, Zhang, Y, Zhao, C, Ord, A, and Hobbs, BE, 2007, Regional geology of the Archaean nuclei of the Western Shield, *in* Procceeedings of Geoconferences (WA) Inc. Kalgoorlie '07 Conference *edited by* FP Bierlein and CM Knox-Robinson: Geoscience Australia, Record 2007/14, p. 214–217.

Robert, F, Poulsen KH, Cassidy KF, Hodgson CJ, 2005, Gold metallogeny of the Superior and Yilgarn Cratons: Economic Geology, 100th Anniversary Volume, p. 1001–1033.

Rodgers, J, 1995, Lines of basement uplifts with external parts of orogenic belts: American Journal of Science, 295, p. 455–487.

Ross, AA, Barley, ME, Brown, SJA, McNaughton, NJ, Ridley, JR, and Fletcher, IR, 2004, Young porphyries, old zircons; new constraints

on the timing of deformation and gold mineralisation in the Eastern Goldfields from SHRIMP U–Pb zircon dating at the Kanowna Belle gold mine, Western Australia: Precambrian Research, 128, p. 105–142.

Sheldon, HA, Barnicoat, AC, Zhang Y, and Ord, A, 2007, Metamorphism in the Eastern Yilgarn Craton: implications for fluid flow and mineralisation, *in* Kalgoorlie 2007 *edited by* F Bierlien and C Knox-Johnson: Geoscience Australia, Record 2007/14.

Smithies, RH, and Champion, DC, 1999, Geochemistry of felsic igneous alkaline rocks in the Eastern Goldfields, Yilgarn Craton, Western Australia: a result of lower crustal delamination? — implications for Late Archaean tectonic evolution: Journal of the Geological Society of London, 156, p. 561–576.

SRK Consulting, 2000, Global Archaean synthesis—Yilgarn module: consultants report, 88p (unpublished).

Standing, JG, 2008, Terrane amalgamation in the Eastern Goldfields Superterrane, Yilgarn Craton: Evidence from tectonostratigraphic studies of the Laverton Greenstone Belt: Precambrian Research, v. 161, p. 114–134.

Stewart, AJ, 1998, Recognition, structural significance, and prospectivity of early F_1 folds in the Minerie 1:100,000 sheet area, Eastern Goldfields, Western Australia: Australian Geological Survey Organisation, Research Newsletter, 29, p. 4–6.

Swager, CP, 1989, Structure of the Kalgoorlie greenstones—regional deformation history and implications for the structural setting of gold deposits within the Golden Mile: Geological Survey of Western Australia, Professional Papers, Report 25, p. 59–84.

Swager CP, 1997, Tectono-stratigraphy of late Archaean greenstone terranes in the southern Eastern Goldfields, Western Australia: Precambrian Research, 83, p. 11–42.

Swager, CP, and Griffin, TJ, 1990, An early thrust duplex in the Kalgoorlie–Kambalda greenstone belt, Eastern Goldfields Province, Western Australia: Precambrian Research, 48, p. 63–73.

Swager, CP, and Nelson, DR, 1997, Extensional emplacement of a high-grade granite gneiss complex into low-grade granite greenstones, Eastern Goldfields, Western Australia: Precambrian Research, 83, p. 203–209.

Swager, CP, Witt, WK, Griffin, TJ, Ahmat, AL, Hunter, WM, McGoldrick, PJ, and Wyche, S, 1992, Late Archaean granite–greenstones of the Kalgoorlie Terrane, Yilgarn Craton, Western Australia, *in* The Archaean — Terrains, Processes and Metallogeny *edited by* JE Glover and SE Ho: University of Western Australia, Geology Department and Extension Service, Publication 22, p. 107–122.

Swarnecki, MS, 1988, Alteration and deformation in a shear zone hosting gold mineralisation at Harbour Lights, Leonora, WA, *in* Archaean gold mineralisation in a normal-motion shear zone at Harbour Lights, Leonora, Western Australia *edited by* SE Ho and DI Groves: University of Western Australia, Geology Department and University Extension, Abstracts, 12, p. 111–129.

Tripp, GI, Cassidy, KF, Rogers, J, Sircombe, K, and Wilson, M, 2007, Stratigraphy and structural geology of the Kalgoorlie greenstones: Key Criteria for gold exploration, *in* Kalgoorlie 2007 *edited by* F Bierlien and C Knox-Johnson: Geoscience Australia, Record 2007/14, p. 203–208.

Vearncombe, JR, 1992, Archaean gold mineralization in a normal-motion shear zone at Harbour Lights, Leonora, Western Australia: Mineralium Deposita, 27, p. 182–191.

Vearncombe, JR, 1998, Shear zones, fault networks, and Archaean gold: Geology, 26, p. 855–858.

Vielricher, RM, Burton, D, and Vanderhor, F, 1998, Mount Morgans (Westralia), *in* Vanderhor, F and Groves, DI, 1995, Systematic documentation of Archaean gold deposits of the Yilgarn Block. Report on results of MERIWA project M195: Part II Mine data Sheets: p. II-85–II-89.

Weinberg, RF, Moresi, L, and van der Borgh, P, 2003, Timing of deformation in the Norseman–Wiluna Belt, Yilgarn Craton, Western Australia: Precambrian Research, 120, p. 219–239.

Wilde, SA, Valley, JW, Peck, WH, and Graham, CM, 2001, Evidence from detrital zircons for the existence of continental crust and oceans on Earth 4.4 Gyr ago: Nature, v. 409, p. 175–178.

Williams, PR, 1993, A new hypothesis for the evolution of the Eastern Goldfields Province, *in* Kalgoorlie '93—An International Conference on Crustal Evolution, Metallogeny, and Exploration of the Eastern Goldfields *edited by* PR Williams and JA Haldane: Australian Geological Survey Organisation, Record 1993/54, p. 73–83.

Williams, PR, and Currie, KL, 1993, Character and regional implications of the sheared Archaean granite–greenstone contact near Leonora, Western Australia: Precambrian Research, 62, p. 343–365.

Williams, PR, Nisbet, BW, and Etheridge, MA, 1989, Shear zones, gold mineralization and structural history in the Leonora district, Eastern Goldfields Province, Western Australia: Australian Journal of Earth Sciences, 36, p. 383–403.

Williams, PR, and Whitaker, AJ, 1993, Gneiss domes and extensional deformation in the highly mineralised Archaean Eastern Goldfields Province, Western Australia: Ore Geology Reviews, 8, p. 141–162.

Witt, WK, 1992, Porphyry intrusions and albitites in the Bardoc–Kalgoorlie area, Western Australia, and their role in Archaean epigenetic gold mineralization: Canadian Journal of Earth Sciences, 29, p. 1609–1622.

Witt, WK, 1994, Geology of the Bardoc 1:100 000 sheet: Geological Survey of Western Australia, 1:100 000 Geological Series Explanatory Notes, 50p.

Witt, WK, 2001, Tower Hill gold deposit, Western Australia; an atypical, multiply deformed Archaean gold–quartz vein deposit: Australian Journal of Earth Sciences, 48, p. 81–99.

Wyche, S, and Farrell, T, 2000, Regional geological setting of the Yandal greenstone belt, northeast Yilgarn Craton, *in* Yandal Greenstone Belt *edited by* N Phillips and R Anand: Australian Institute of Geoscientists, Bulletin, 32, p. 41–54.

Yeats, CJ, McNaughton, NJ, Ruettgar, D, Bateman, R, Groves, DI, Harris, JL, and Kohler, E, 1999, Evidence for diachronous Archaean lode gold mineralization in the Yilgarn Craton, Western Australia: a SHRIMP U–Pb study of intrusive rocks: Economic Geology, v. 94, p. 1259–1276.

Yeats, CJ, Kohler, EA, McNaughton, NJ, and Tkatchyk, LJ, 2001, Geological setting and SHRIMP U–Pb geochronological evidence for ca. 2680–2660 Ma lode-gold mineralization at Jundee–Nimary in the Yilgarn Craton, Western Australia: Mineralium Deposita, v. 36, p. 125–136.

CZARNOTA et al.

Structural and metamorphic controls on gold through time and space in the central Eastern Goldfields Superterrane — a field guide

RECORD 2008/9

This Record is published in digital format (PDF) and is available online at: www.doir.wa.gov.au/GSWApublications. Laser-printed copies can be ordered from the Information Centre for the cost of printing and binding.

Further details of geological publications and maps produced by the Geological Survey of Western Australia can be obtained by contacting:

Information Centre
Department of Industry and Resources
100 Plain Street
East Perth WA 6004
Phone: (08) 9222 3459 Fax: (08) 9222 3444

www.doir.wa.gov.au/GSWApublications